MOLECULAR CLONING, FUNCTIONAL ANALYSIS, AND RNA EXPRESSION ANALYSIS OF ZFCX45.6: A ZEBRAFISH CARDIOVASCULAR CONNEXIN.

by

Tara L. Christie

A Thesis
Submitted to the Faculty of Graduate Studies
In Partial Fulfilment of the Requirements for the Degree of

MASTER OF SCIENCE

Department of Zoology
University of Manitoba
Winnipeg, Manitoba

THE UNIVERSITY OF MANITOBA

FACULTY OF GRADUATE STUDIES

*****

COPYRIGHT PERMISSION PAGE

MOLECULAR CLONING, FUNCTIONAL ANALYSIS, AND RNA EXPRESSION ANALYSIS OF ZFCX45.6: A ZEBRAFISH CARDIOVASCULAR CONNEXIN

BY

TARA L. CHRISTIE

A Thesis/Practicum submitted to the Faculty of Graduate Studies of The University of Manitoba in partial fulfillment of the requirements of the degree of

Master of Science

ABSTRACT

Gap junctions are intercellular channels that allow the direct exchange of molecules up to about 1200 Daltons in size. Six connexins join together to form a hemichannel termed a connexon, and two connexons from different cells dock to form an aqueous channel. A gap junction is formed by the aggregation of hundreds of these channels into plaques. Gap junctions function in a variety of biological processes such as tissue homeostasis, embryonic development, and tumorigenesis. In the vertebrate cardiovascular system, gap junctions function in intercellular communication essential for the co-ordinated propagation of the heartbeat, and the control of vasomotor responses in the vascular system.

In this study, a connexin gene encoding a polypeptide of 400 amino acids, with a molecular weight of 45.6 kDa, was cloned from zebrafish genomic DNA. Accordingly, the connexin was named zfCx45.6. ZfCx45.6 exhibits 53% amino acid identity to chick Cx42 which is expressed in the cardiovascular system. With the use of the LN54 radiation hybrid panel, zfCx45.6 was mapped to zebrafish linkage group 9. Northern blots and RT-PCR revealed the presence of zfCx45.6 mRNA in the embryo before 2 hours post fertilization (hpf), and then again beginning at about 12 hpf, after which time no major changes in expression levels were detected. In the adult, zfCx45.6 mRNA continued to be detected in the heart, as well as the brain, liver and ovary, but not the lens. Whole mount *in-situ* hybridization revealed zfCx45.6 mRNA was highly expressed in the major vasculature of the entire embryo, and to a lesser extent in the heart.

The zebrafish (*Danio rerio*) is an excellent model system to study cardiovascular development, in part due to its large, externally developing, optically transparent

embryos, and the fact that early development can occur in the absence of functional circulation. With the previous isolation of zebrafish Cx43 and Cx43.4, zebrafish orthologues have now been isolated for three of the four connexins expressed in the mammalian cardiovascular system. With the advent of antisense technologies and methods allowing for the measurement of many cardiovascular functions in minute animals and embryos, these studies lay the groundwork for future studies on the role of connexins in the developing and mature vertebrate cardiovascular system using the zebrafish model system.

ACKNOWLEDGEMENTS

I would like to thank my thesis supervisor Gunnar Valdimarsson for taking me on as a student in his lab. With his advice and support I have learned a great deal over the last few years. I would also like to thank the other members of my thesis committee, Elissavet Kardami and Ross McGowan, for their insight and suggestions.

Thanks to all the students who have been in (and through) the lab, especially Shaohong and Liz. Their comments and discussions, whether related to lab material or not, made working in the lab a thoroughly enjoyable experience. Special thanks to Roxane for the weekly meetings.

Most of all, I would like to thank my friends, family and loved ones. Your support through the hard times, and celebration in the good times were much appreciated.

TABLE OF CONTENTS

LIST OF FIGURES

ABBREVIATIONS

Amp	ampicillin
AS	antisense
bp	base pairs
BCIP	5-bromo-4-chloro-3-indolyl phosphate
BLAST	basic local alignment tool
BSA	bovine serum albumin
CIAP	calf intestinal alkaline phosphatase
CPM	counts per minute
Cx	connexin
dpf	days post fertilization
DEPC	diethylpyrocarbonate
DIG	digoxygenin
DNA	deoxyribonucleic acid
DNP	dinotrophenol
DTT	dithiothreitol
EDTA	ethylenediaminetetraacetic acid
EtBr	ethidium bromide
hpf	hours post fertilization
HYB	hybridization buffer
ISH	*in situ* hybridization
kb	kilobases
LB	Luria-Bertani
M	molar
mRNA	messenger RNA
NBT	nitroblue tetrazolium
NGS	normal goat serum
OD	optical density
PAC	P1 artificial chromosome
PCR	polymerase chain reaction
PK	protein kinase
PTU	1-phenyl-2-thiourea
RH	radiation hybrid
RNA	ribonucleic acid
rRNA	ribosomal RNA
RT-PCR	reverse transcriptase PCR
tRNA	transfere RNA
S	sense
UTR	untranslated region
UV	ultraviolet
X-gal	5-bromo-4-chloro-3-inodyl-β-D-galactosidase
°C	degrees Celsius
EC	endothelial cells
SMC	smooth muscle cells

CHAPTER 1. INTRODUCTION:

1. 1. Gap Junctions: Structure and Function

Gap junctions are collections of intercellular channels that allow the direct exchange of molecules up to about 1200 Daltons in size, such as ions, second messengers, and small metabolites (White *et al.*, 1995; Bruzzone *et al.*, 1996a). The structural units of gap junctions are connexins (Cx). Six connexin units join together on the cell membrane to form a hemichannel termed a connexon, and two connexons from different cells dock to form an aqueous channel (Figure 1). A gap junction is formed by the aggregation of hundreds of these dodecameric channels into plaques 1-2 μm in diameter (Yeager *et al.*, 1998).

The connexin genes belong to a multi-gene family with representatives in all vertebrate groups investigated (Yeager *et al.*, 1998; Bruzzone *et al.*, 1996a). Gap junctions in invertebrates such as *C. elegans* (Starich *et al.*, 2001) and *Drosophila* (Curtin *et al.*, 1999) are morphologically and functionally similar to vertebrate gap junctions, but the constituent proteins do not posses sequence similarity to vertebrate connexins and therefore are termed innexins (invertebrate connexins)(for a review see Phelan and Starich, 2001). Connexins are identified according to their species of origin and molecular mass predicted from cloned DNA sequences. For example, the rat connexin with a molecular mass of 46kDa is termed rCx46. This naming system was adopted at the Gap Junction meeting held in Asilomar in 1987 (Beyer *et al.*, 1987). Though this is the most widely used naming method, confusion can often arise when dealing with orthologous connexins, since they often have very different molecular mass, thus

Figure 1. Gap Junction Structure.

The structural units of gap junctions are connexins. **A.** The coding sequence of all connexins consists of four transmembrane domains (M1 to M4) and cytoplasmic NH_2- and COOH- termini. The resulting extracellular loops (E1 and E2) contain three cysteines in conserved positions. **B.** Six connexin units join together to form a hemichannel termed a connexon, and two connexons from different cells dock to form an aqueous intercellular channel. Hundreds of these intercellular channels aggregate into plaques to form a gap junction. (EC: extracellular, IC: intracellular, PM: plasma membrane).

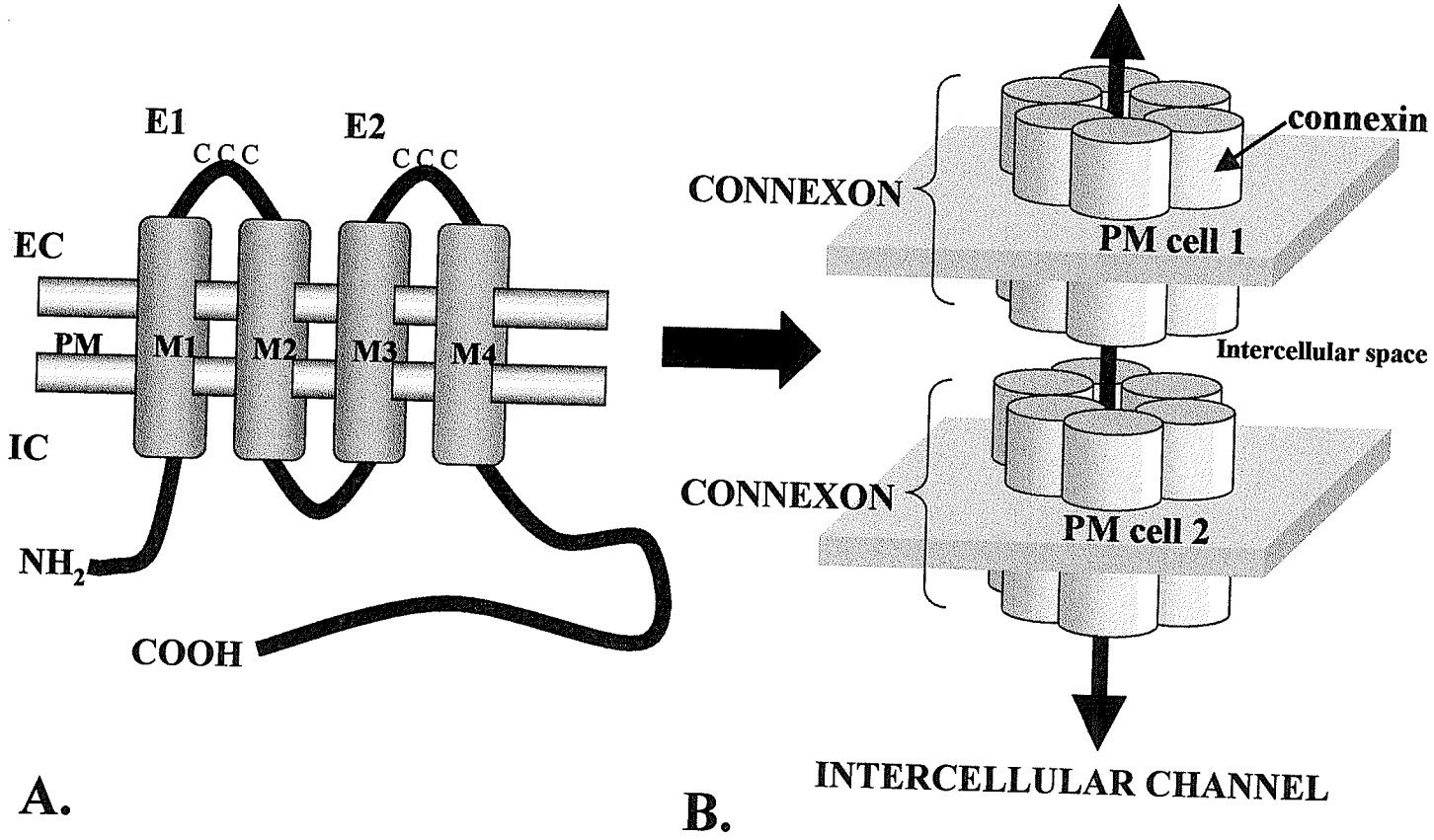
E1
E2
C C C
C C C
EC
PM
M1
M2
M3
M4
IC
NH2
COOH
A.
connexin
CONNEXON
PM cell 1
Intercellular space
CONNEXON
PM cell 2
INTERCELLULAR CHANNEL
B.

resulting in different names. An alternate method of naming has been adopted by some researchers based on the identification of structural subfamilies of connexins and division into the alpha, beta, or gamma class (Willicke *et al.*, 2002). At this point in time, one uniform classification scheme has not been adopted.

Generally, the entire coding region of a connexin is contained within one exon, with an additional one or two exons located in the 5' untranslated region (UTR) (White and Paul, 1999). The exceptions to this rule are the Cx35/Cx36 orthologues as they contain an intron within the coding region (White and Paul, 1999). The coding sequence of all connexins predicts a common topological model with respect to the plasma membrane (Figure 1). This structure consists of four transmembrane domains (M1 to M4) and cytoplasmic NH_2- and COOH- termini, resulting in a cytoplasmic loop, and two extracellular loops (E1, E2) (Yeager *et al.*, 1998). The extracellular loops of all connexins contain three conserved cysteines in a characteristically conserved sequence: CX_6CX_3C in the first extracellular loop, and CX_4CX_5C in the second extracellular loop. The exception to this conserved cysteine sequence is found in rCx31 (Hoh *et al.*, 1991). The conserved cysteines in the extracellular loops are involved in the formation of intramolecular disulfide bonds that are essential for normal folding and/or channel function. The transmembrane domains and extracellular loops are also highly conserved among different connexins (White *et al.*, 1995). The third transmembrane domain and two extracellular domains are thought to contribute to the pore wall (Bruzzone *et al.*, 1996a; Skerrett *et al.*, 2002).

As all connexins share the same overall structure, theoretically, many different possible combinations of connexins joining to form connexons, or different connexons

aggregating to form intracellular channels, could arise. Connexins can form homotypic channels where only one type of connexin makes the pore, heterotypic channels where each connexon contributing to the intracellular channel is created from different connexins, or heteromeric channels where two or more types of connexins make the hemichannel (Bruzzone *et al.*, 1996a). For example, Cx40 and Cx43 are expressed in various locations in the heart, and have been shown to form current carrying heterotypic channels in transfected HeLa cells (Valiunas *et al.*, 2000).

Almost all cell types possess gap junctions at some point in their development, but they are absent in skeletal myocytes, some neurons, most circulating blood cells, and spermatozoa (Bruzzone *et al.*, 1996a). Many connexins can be expressed in more than one tissue, and a single cell type can express more than one connexin. For example, the rodent atrial myocytes expresses multiple connexins including Cx40 and Cx43, whereas Cx43 is also expressed in the brain, gonads, skin and lens.

Gap junctions allow the direct and rapid exchange of small molecules between cells, and therefore provide a simple, yet critical method for coordinating a wide range of cellular behaviors in multicellular organisms (White and Paul, 1999). The widespread expression and molecular diversity of connexins can make the role of gap junctions difficult to discern, but some of the critical functions of gap junctions have been elucidated by the discovery of disease causing mutations (Bruzzone *et al.*, 1996a). The association of connexin mutations with human pathologies such as X-linked Charcot-Marie-Tooth disease (Cx32) (Bergoffen *et al.*, 1993), nonsyndromic deafness (Cx26) (Kelsell *et al.*, 1997), and "zonular pulverulent"cataracts (Cx50) (Shiels *et al.*, 1998) demonstrate the importance of gap junctions in growth and development. It has also been

proposed that because action potential propagation in the heart is gap junction dependant, irregular gap junction distribution in the heart contributes to discontinuous propagation, thus predisposing the heart to arrhythmias (Severs, 1994). Targeted disruptions of connexin genes by homologous recombination in embryonic stem cells of rodents have been used to study specific connexins already implied in disease, and to determine the roles of connexins not previously linked to a disease (White and Paul, 1999). Interestingly enough, it should be noted that in the majority of cases, mutations in one connexin tend to result in specific abnormalities, and not all the organ systems expressing the mutated connexin are affected. For example, mouse Cx37 is detected in many locations including lung and between the oocytes and granulosa cells (Simon, 1997). The knockout mouse is infertile, but appears not to have any problems in the lungs, or other locations of Cx37 expression. This could possibly arise from compensation by other connexins expressed in the lungs and other locations, whereas Cx37 may be the only connexin expressed between the oocyte and granulosa cells.

Gap junctions have also been found to play a role in tumorigenesis. In certain carcinoma cell lines connexin genes are transcriptionally down regulated (Rose *et al.*, 1993; Hirschi *et al.*, 1996). Incorporation of exogenous connexin genes into the genomes of these cell lines results in decreased tumorigenicity. These findings suggest that the reexpression of gap junctions in tumor cell lines may play an important role in normalizing tumor cell behavior. How connexins function as tumor suppressors has not yet been determined.

Another function of gap junctions is to rapidly coordinate the activity of groups of cells. For example, gap junctions are important in the contraction of cardiac and smooth

muscle cells. Studies of pregnant rats have shown that Cx43 expression increases in the uterine myometrium the day before parturition (Risek *et al.*, 1990). It is thought that the increased expression of Cx43 leads to the formation of gap junctions that are needed to synchronize the contractivity of the myometrial cells during parturition. It has also been found that the expression of three connexins, Cx43, Cx32 and Cx26, is restricted to specific cell types within the rodent mammary gland, and to specific times during the activity of the gland (Pozzi *et al.*, 1995). Studies have determined that in the luminal cells of both the mouse (Locke *et al.*, 2000) and rat (Yamanaka *et al.*, 2001) Cx26 levels start to increase early in pregnancy, and both Cx26 and Cx32 reached their maximum expression levels during lactation. These results suggest a possible role for gap junctions in the coordination of the secretory epithelium of the mammary gland during pregnancy and lactation.

1. 2. Connexins in the Cardiovascular System

1. 2. a. Connexins in the heart

In the heart, contractions are controlled by the coordinated spread of electrical excitation through the cardiac muscle (Gourdie, 1995). A high degree of cell-cell communication is not only important for conduction of the action potentials, but it is also essential to achieve the coordinated and rhythmic impulses that are generated by the pacemaker cells of the sinoatrial node in the right atrium (Bleeker *et al.*, 1980). These impulses are prevented from immediately passing to the ventricles by an insulating connective tissue layer, but are thought to quickly conduct through the Purkinji fibers, in part due to the high density of gap junctions present in the fibers (Kupperman *et al.*,

2000). Also, the strength and efficiency of the atrial and ventricular muscles depends on the synchronized contraction of the working myocytes of which they are composed (Gros and Jongsma, 1996). Gap junctions ensure the propagation of action potentials between myocytes and are therefore responsible for the coordinated contractions of the atria and ventricles.

The number of gap junctions in the heart varies with the developmental stage and location within the heart (i.e. atria versus ventricles, etc.) (Gros and Jongsma, 1996). In the fetal, neonatal, and infant mammalian heart, numerous small gap junctions are found evenly distributed throughout the myocyte cell surface (Severs, 1994). Before adulthood gap junctions are distributed along zones of lateral contact between myocytes (Gourdie *et al.*, 1990). In the adult mammalian heart, gap junction plaques are primarily found in the proximity of cell adhesion junctions at intercalated disks (Gourdie, 1995; Angst *et al.*, 1997), with the largest accumulation at the periphery of the disks, thus forming zones of end-to-end electrical and mechanical attachment between myocytes. It has been proposed that this developmental change in the electrical contact between myocytes determines maturational changes in the degree and type of propagation signal, in that the conduction becomes preferential in the direction of the myocyte long axis (Gourdie *et al.*, 1995).

The main connexins found in heart myocytes are Cx37, Cx40, Cx43, and Cx45, with Cx43 being the most predominant (Davis *et al.*, 1994) (Figure 2.A.). Connexin43 has been cloned and sequenced from many mammals including humans (Bruzzone *et al.*, 1996b). It is associated with the gap junctions of most myocytes (Gros and Jongsma, 1996). In most species Cx43 is not detected in the conducting system of the heart, but it

Figure 2. Connexin Expression in the Cardiovascular System.

The main connexins found in the cardiovascular system are Cx37, Cx40, Cx43, and Cx45. **A.** In the mammalian heart, Cx43 is the predominant connexin, detected in the myocardium of both the atria and ventricles. Connexin40 is also found in the atrial myocardium, and is the predominant connexin of the His bundle and bundle branches. Connexin45 is detected in the AV node, His bundle, and the peripheral portion of the ventricular conduction system. Cx37 is detected widely in multiple compartments of the heart. **B.** Endothelial cells (EC) of blood vessels express Cx37, Cx40, and Cx43, while the smooth muscle cells (SMC) primarily express Cx43 and sometimes Cx40 and Cx45. (SA node: Sino-atrial node, AV node: Atrio-ventricular node, RA: right atrium, LA: left atrium, RV: right ventricle, LV: left ventricle, HB: Bundle of His, BB: bundle branches)

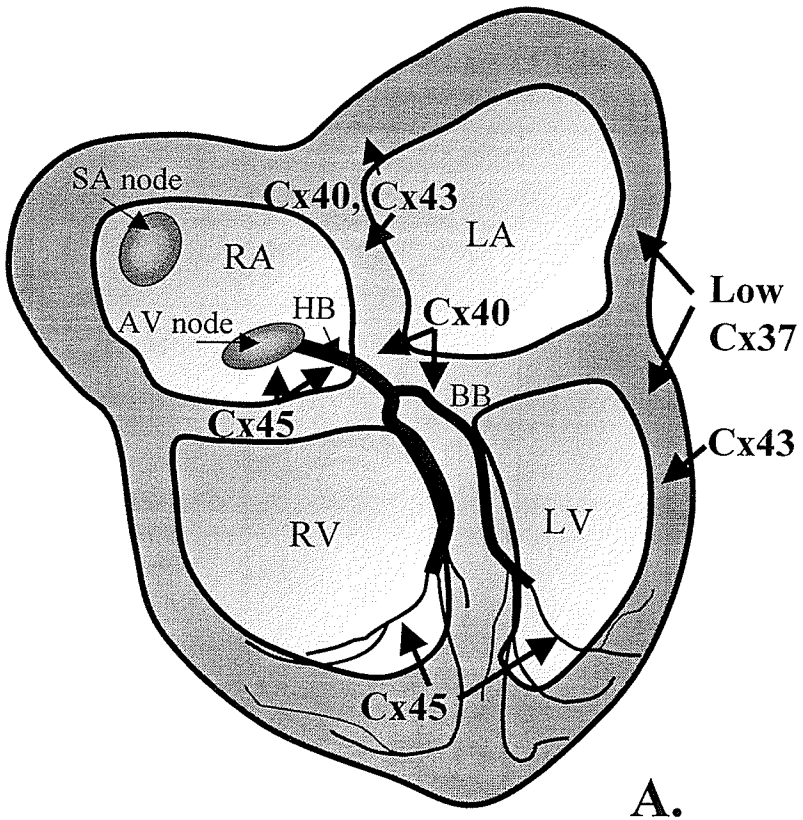
SA node
Cx40, Cx43
RA
LA
AV node
HB
Cx40
Low
Cx37
BB
Cx45
Cx43
RV
LV
Cx45

A.


EC: Cx37,
Cx40, Cx43
SMC: Cx43,
Cx40, Cx37,
Cx45

B.

is co-expressed with Cx40 in the atrium, and is the only connexin expressed in the ventricular myocardium (Jongsma, 2000). Connexin45 has also been cloned and sequenced from many organisms (Bruzzone *et al.*, 1996b). In the mouse and rat, Cx45 is undetectable in the major portion of working ventricular myocardium (Coppen *et al.*, 1998). Connexin45 is prominently expressed in the AV node and His bundle, and detected in very low levels in the peripheral portion of the ventricular conduction system, thus being the connexin most widely expressed by the conduction tissue (Coppen *et al.*, 1999; Kruger *et al.*, 2000). Connexin40 has also been cloned and sequenced from several organisms, including humans (Bruzzone *et al.*, 1996b). Connexin40 is abundant in the atrial myocardium of almost all species studied (Jongsma, 2000). It is also the predominant connexin found in the His bundle and bundle branches of the heart. Connexin37 has been cloned and characterized in the mouse, rat, and human (Reed *et al.*, 1993; Haefliger *et al.*, 1992; Willecke *et al.*, 1991). The distribution of Cx37 in the heart has been controversial as to the extent and location of expression, but a recent study has found that Cx37 is widely distributed in multiple compartments of the cardiovascular system (Haefliger *et al.*, 2000). In prenatal development, Cx37 is found predominantly in the endothelial and endocardial cells, but is also visible in small amounts in the trabeculated and compact layers of the myocardium, and mesenchyme of the conotruncal ridges and atrioventricular cushions.

1. 2. b. Connexins in the vascular system

The cardiovascular system is not only comprised of the heart, but also a closed system of blood vessels whose main function is to deliver blood carrying nutrients, water and metabolites to the tissues, and metabolic wastes away from the tissues. The basic

structure of the vascular system consists of hollow tubes of squamous endothelial cells (EC) in direct contact with the blood, surrounded by one to many sheets of smooth muscle cells (SMC). Thus, EC form a continuous monolayer lining the luminal surface of the entire cardiovascular system (Nilius and Droogmans, 2001) (Figure 2.B.). Many fundamental processes in the vascular system are regulated by EC, such as control of blood flow and blood pressure, coagulation, platelet aggregation, vessel permeability, wound healing and angiogenesis (Nilius and Droogmans, 2001). Endothelial cells also provide a structural and metabolic interface between the blood and underlying tissue (Yeh *et al.*, 1997). Gap junctions therefore can be considered to have a complicated role in the vascular system as they mediate the direct electrical and metabolic intercellular communication between EC, EC and SMC, and EC and lymphocytes and monocytes (Nilius and Droogmans, 2001). For example, it is believed that intercellular communication through gap junctions between SMC and/or EC mediates vasodilation and vasoconstriction (for a review see Christ *et al.*, 1996).

Not surprisingly, the connexins expressed in the vascular system are similar to those expressed in the heart. Generally, EC have been found to express Cx40, Cx43 and Cx37, while the SMC primarily express Cx43 and sometimes Cx40, Cx45, and/or Cx37 (Christ *et al.*, 1996; Rummery *et al.*, 2002; Kruger *et al.*, 2000)(Figure 2.B.). Multiple studies have shown the expression of gap junctions in the endothelium and smooth muscle layer is not uniform, but varies in different segments of the vasculature. For example, Cx40 is the most predominant connexin detected in the murine kidney vasculature, but its expression is regulated (Seul and Beyer, 2000). Connexin40 is abundant in the EC of the large blood vessels of the kidney, and in the EC of the smaller

interlobular arteries and proximal portion of the afferent arterioles. Expression of Cx40 decreases as the afferent arterioles reach the glomerulus, and is not detected in the glomerular isthmus where the afferent and efferent arterioles join the glomeruli. Expression is patchy but intense in the EC of the glomeruli, and also in the SMC of the juxtaglomerular apparatus. Connexin40 is not detected in the SMC elsewhere in the vascular system. These results suggest the importance in coordinating the function of cells within individual blood vessels, and the absence in the juxtaglomerular region possibly prevents the conduction of signal between the glomerulus and afferent or efferent arterioles. This differential expression of connexins may contribute to the modulation of gap junction function in different segments of the arterial wall (Yeh *et al.*, 1997).

1. 3. The Role of Gap Junctions in Cardiovascular Development

The question of the importance of different connexins for cardiac excitation, vascular integrity, and cardiovascular development are not easy to answer due to the wide distribution of connexins and their complex properties (Jongsma, 2000). Little was known about the specific functional roles of individual connexins in normal and abnormal cardiovascular function and development, but with the creation of connexin knockout mice, some of their roles are being elucidated (Jalife *et al.*, 1999). Knockout mice have been generated for the four major connexins expressed in the cardiovascular system. With the exception of the Cx37-null mouse, the other knockout mice demonstrate specific defects related to cardiovascular development and/or function (see Appendix I). For example, Cx40 knockout mice ($Cx40^{-/-}$) have been generated

independently by two labs (Simon *et al.*, 1998; Kirchoff *et al.*, 1998), and both groups found the knockout mice demonstrated partial but not complete conduction block. Action potentials still passed from the atria to the ventricles, through the His-Purkinji system, but the time for the excitation to travel this distance was longer than it was in wild type mice. It was also noted that intraventricular conduction was slower, most likely due to slow conduction in the Purkinji fibers. This blockage in the His-Purkinji system resulted in uncoordinated ventricular excitation and spatially altered propagation of electrical activity throughout the working myocardium (Simon *et al.*, 1998). Further studies (Vanderbrink *et al.*, 1999) demonstrated the $Cx40^{-/-}$ mice not only possessed functional abnormalities in the His-Purkinji system (an expected result as this is the predominant site of Cx40 expression), but also in the AV node (Vanderbrink *et al.*, 2000). These abnormalities were greater than expected given the trace amounts of Cx40 expressed in this region. This data suggests a significant role for Cx40 in atrionodal conduction and/or proximal His-bundle conduction. More studies are needed to localize the exact site of conduction delay. While it was a surprise that $Cx40^{-/-}$ mice did not demonstrate a complete conduction block, this may be explained by the compensatory expression of alternative connexins in the region such as Cx45 (Coppen *et al.*, 1998).

1. 4. The Role of Gap Junctions in Heart Disease

As demonstrated by the above studies on knockout mice, connexins are required for proper heart development and conduction. It is believed that due to this requirement, mutations in human heart connexins contribute to the initial pathogenesis and eventual clinical manifestation of some human cardiovascular diseases (Severs *et al.*, 2001). For

example, in humans, electrocardiograms similar to those of the $Cx40^{-/-}$ mice would be characteristic of first degree AV block, associated with bundle branch block (Simon *et al.*, 1998). As well, abnormalities in Cx43 have been detected in human ischaemic heart disease (Severs *et al.*, 1995). In heart tissue, the border zones adjacent to infarct scars show a disruption of the usual ordered distribution of gap junctions. There is also a widespread down regulation of Cx43 in the myocardium near the infarct. Connexin43 expression is also decreased both at the mRNA and protein level in the left ventricle in end stage congestive heart failure (Dupont *et al.*, 2001). As well, Cx40 expression is increased in a location consistent with Purkinji fibers in ischemic cardiomyopathy.

Chagas heart disease, caused by a protozoan parasite *Trypansoma cruzi*, is one of the leading causes of sudden death in Latin America after coronary heart disease (for a review see http://caibco.ucv.ve/ARTICULO/Implicat.htm). In acutely affected rat heart cells, beating is less synchronous and regular, and cell coupling is reduced (deCarvalho *et al.*, 1994). The basis of this decrease in coupling is apparently a mislocalization of Cx43 in the infected cells where the total amounts of Cx43 protein are normal, but the protein is not found at the membrane. It is believed that the conduction disturbances characterised by this disease occur as a result of this modification of channels in the diseased heart.

Over the last 50 years, major advances have been made in the diagnosis and treatment of heart disease, yet the incidence of disease is the same or greater than in the past (Lohr and Yost, 2000). This is due to technological advances allowing for increased detection rates, and the extended survival time of affected patients. Despite our increased ability to diagnose and treat heart conditions, we still have a limited understanding of

heart development. It has become of great importance to understand these processes to help develop methods to prevent heart disease. When studying cardiovascular development and disease, one must have a good model system to provide insight into the genetic, molecular and cellular processes that are critical to normal cardiovascular development.

1. 5. Zebrafish as a Model System for Cardiovascular Development Studies

From the above studies it would appear that the mouse is an ideal vertebrate system to use for cardiovascular studies, but it does have drawbacks. The major drawback being that the opacity of the mother and uterus make access to early developmental stages difficult (Driever and Fishman, 1996). Another difficulty is that mouse embryos with severe cardiac deformations die very early in development thus making detection of the defects difficult (Warren and Fishman, 1998). Large-scale murine mutagenic screens, used to rapidly determine candidate genes important in heart and other organ development, are also expensive due to the cost of maintaining the large number of animals needed to perform these screens (Driever and Fishman, 1996). Development of the vertebrate heart is a complex process remarkably similar among all vertebrates, especially in the early stages (Opitz and Clark, 2000). Thus, an alternative strategy for studying cardiovascular development is to use a model system, such as the zebrafish (*Danio rerio*), that can overcome the above difficulties.

George Streisinger (University of Oregon) was the first to recognize the many benefits of using the small freshwater tropical zebrafish as a model system for development studies over 20 years ago. Such benefits of the zebrafish as a model for

vertebrate development include: relatively short generation time, large clutch size, large optically transparent embryos, and easy access to all developmental stages (Driever and Fishman, 1996). A benefit specific to cardiovascular studies is that early development can continue for a period of time in the absence of functional circulation (Lohr and Yost, 2000). Even though the cardiovascular system of the zebrafish is functional by 24 hours post fertilization (hpf), it is not essential in the early stages, as the embryo is small enough to obtain the oxygen it requires through simple diffusion (Warren and Fishman, 1998). Zebrafish cardiovascular mutants can develop normally for a few days, and thus allow for a more thorough evaluation of altered cardiovascular development, and other organ systems (Lohr and Yost, 2000).

Another benefit over the mouse as a model system is that large-scale mutagenesis screens of the zebrafish genome are relatively inexpensive (Driever *et al.*, 1996). The large and transparent zebrafish embryos also facilitate the identification of mutants. Large-scale screens in zebrafish, conducted by two independent groups, have resulted in the identification of 6447 mutations (Dreiver *et al.*, 1996; Haffter *et al.*, 1996). About 2000 of these mutations were deemed interesting, and over 50 mutations affected the formation and function of the cardiovascular system (Chen *et al.*, 1996; Stanier *et al.*, 1996). It is likely that most of the genes involved in zebrafish cardiac development have human homologues, and therefore are candidates for genes that contribute to clinical disorders such as arrhythmias and heart failure (Warren and Fishman, 1998). Over time, analysis of these mutant fish may also provide information as to the genetic pathways that are critical to the establishment of normal cardiovascular development and function.

These mutants could also serve as targets for the development of new, more effective pharmaceuticals.

1. 6. Zebrafish Cardiovascular Development

The heart is the first organ to develop and become functional, and generally appears when the need for oxygen and nutrition cannot be met by diffusion alone due to increased volume, or metabolic rate (Hu *et al.*, 2000). The zebrafish heart is a prototypic vertebrate heart consisting of four chambers connected in a series: sinus venosus, atrium, ventricle, and bulbous arteriosus (Hu *et al.*, 2000). It is a tubular structure with no septa dividing the atrium and ventricle (Lohr and Yost, 2000). Though the adult zebrafish heart bears significant dissimilarities anatomically to the adult human heart, embryonic fish hearts are similar to the embryonic hearts of other vertebrates, including mammals (Lohr and Yost, 2000). The zebrafish embryonic heart actually resembles that of a three-week post implantation human embryo (Harvey, 1999). Only later in cardiac development does the mammalian heart structure diverge from the fish as mammals generate atrial and ventricular septae (Hu *et al.*, 2000). Despite the anatomic differences between adult zebrafish and mammalian hearts, many processes involved in early heart formation appear to be conserved among vertebrates (Lohr and Yost, 2000). It is the absolutely essential nature of the heart in both the embryo and adult that results in its unique and highly constrained characteristics (Opitz and Clark, 2000). The conservation of the processes involved in heart development among vertebrates are becoming better defined as more cellular and molecular markers are discovered (Lohr and Yost, 2000).

A closer look at the morphological and physiological descriptions of the developing zebrafish heart demonstrates the similarity between fish and mammalian hearts (Hu *et al.*, 2000). In all vertebrates, myocardial progenitors involute early during gastrulation and come to occupy bilateral positions in the anterior lateral plate mesoderm, ventral to the anterior foregut (Yelon *et al.*, 2000; Opitz and Clark, 2000; Kupperman *et al.*, 2000). This process is known as *precardial cell migration* (Lohr and Yost, 2000). In zebrafish these cells migrate to the level of the hindbrain by 18 hpf (Lohr and Yost, 2000). These cells then form two bilateral myocardial tubes. During somitogenesis, a second phase of migration occurs as the precardial cells move towards the ventral midline where they surround endothelial precursor cells and fuse to form a definitive heart tube with an outer myocardial layer and an inner endocardial sinus (Lohr and Yost, 2000; Kupperman *et al.*, 2000; Yelon *et al.*, 2000). This process is known as *cardiac tube formation* (Lohr and Yost, 2000). In zebrafish, heartbeat is evident around 22 hpf as unidirectional peristaltic waves propelling the blood through the rudimentary circulatory system (Warren and Fishman, 1998). As in all vertebrates, the zebrafish heart tube undergoes rightward looping where the ventricular region adopts a pronounced rightward curvature (Kupperman *et al.*, 2000). In higher vertebrates this process of cardiac looping sets the stage for the formation of a four-chambered organ with separate systemic and pulmonary circuits. In the zebrafish, looping does not bring the venous inflow and atria as far cranially as in other species and septae do not form (Lohr and Yost, 2000). The process of *cardiac looping* is complete by 36 hpf in the zebrafish. At this point, the peristaltic contractions of the heart have developed into sequential contractions of the atrium and ventricle. In the zebrafish the main differentiation and chamber specification

of the heart is complete by 30 hpf (Gourdie *et al.*, 1995), and by 48 hpf the heart is a smooth walled tube with 4 segments separated by constrictions (Hu *et al.*, 2000). Further differentiation of the tube continues for up to 3 months. During this time the ventricle increases the number of trabeculae, the atria develops many branched pectinate muscles, and valves between the segments appear, mature, and thicken.

Studies of the development of the zebrafish vascular system have not been as thorough as those for zebrafish heart development. As with the heart, the vasculature of the zebrafish is similar to that of other vertebrates, consisting of endothelial cells surrounded by smooth muscle cells (Parker *et al.*, 1999). The formation of the vasculature and the molecular pathways controlling this development also appear to be similar to those of other vertebrates. In general, vascular development can be divided into two processes: vasculogenesis and angiogenesis (Poole and Coffin, 1989). In vasculogenesis, cells thought to derive primarily from cephalic and posterior trunk ventrolateral mesoderm differentiate into angioblasts (endothelial cell precursors), and migrate to sites of blood vessel formation (Fouquet *et al.*, 1997; Roman and Weinstein, 2000). Here, angioblasts form tubes with other endothelial primordial cells. Vessels that form by vasculogenesis include: the perineural and yolk sac vascular plexuses, anterior cardinal vein, major trunk vessels, and vessels that perfuse organs with endoderm derived epithelial layers (Roman and Weinstein, 2000; Pardanaud *et al.*, 1987). In angiogenesis, capillaries form by sprouting or elongating from existing vessels to form new tubes (Poole and Coffin, 1989). Vessels that form by angiogenesis include the internal carotid artery, trunk intersomitic vessels, and vessels that perfuse organs with ectodermally derived epithelial cells (Roman and Weinstein, 2000).

Vascularization begins in the zebrafish around the 24 somite stage (Fouquet *et al.*, 1997). By the 28 somite stage (24 hpf) a simple circulatory loop has been set up consisting, in part, of the ventral aorta, the mandibular arches, the dorsal aorta, and the caudal artery and vein (Isogai *et al.*, 2001). Over the next few days, vessel formation in the zebrafish is very dynamic as vessel tracts appear and disappear, and links between vessels sever and reconnect (Isogai *et al.*, 2001). The formation of the vasculature in the zebrafish, though dynamic, follows a plan similar to that of other vertebrates with a few unique features. These unique features are attributed to the necessity of gills, and the rapid development of the embryo. For example, the primary trunk vessels, dorsal aorta and posterior caudal vein form rapidly and without apparent secondary angiogenic remodeling. Also, some intermediate stages of development found in other vertebrates are missing, such as the transverse vessels and "primitive" subintestinal vein.

1. 7. Hypothesis and Objectives

Development of the vertebrate cardiovascular system is a highly complex process, and many factors need to be expressed in the right place and time for proper development. Studies of connexin knockout mice demonstrate the importance of connexins not only in heart and vascular development, but also in the propagation of the heartbeat. Though much information has already been obtained from the study of connexin knockout mice, their complex patterns of expression make understanding connexin function in the vascular system difficult. It is important to understand how connexins function in the vascular system as improper expression can lead to disease. Possibly through the use of model systems such as the zebrafish, which are conducive to

cardiovascular studies, cardiovascular development and function can be better deciphered. As well, the study of zebrafish cardiovascular devlopment may provide insights into how to prevent certain forms of heart disease.

The zebrafish genome has been shown to contain connexins orthologues to known vertebrate connexins (Cason *et al.*, 2001; Dermietzel *et al.*, 2000; Essner et *al.*, 1996). The zebrafish ortholouges of mammalian Cx43 (Valdimarsson, *personal communication*) and Cx45 (Essner *et al.*, 1996), two of the four major connexins expressed in the vertebrate heart, have been cloned and characterized in the zebrafish. It was hypothesized that the zebrafish genome contained the other two connexins expressed in the mammalian heart, and their expression was developmentally regulated. The objectives of this study were as follows:

1. To isolate a zebrafish connexin clone expressed in the cardiovascular system.

2. To analyze the function of the isolated connexin

3. To map the location of the gene.

4. To characterize the spatial and temporal expression pattern of the isolated zebrafish connexin

CHAPTER 2. METHODS

For the composition of commonly used buffers and solutions see Appendix II. For the sequence of primers used, see Appendix III.

2.1. Care of Fish

Fish were cared for by the staff in the University of Manitoba, Department of Zoology Animal Holding facility. Fish were maintained in 20-gallon tanks at 28.5°C, and kept on a cycle of approximately 14 hours of light, and 10 hours of dark. Fish were fed Nutrafin® flakes daily, #3 trout pellets twice a day, and blood worms and frozen brine shrimp once a week. For breeding purposes, five to ten fish were transferred to 10-gallon tanks equipped with special mesh bottomed containers to allow for the separation of adult fish and eggs. Zebrafish are photoperiodic in their breeding (Westerfield, 1995) and embryos produced just after dawn were collected from the bottom of the tank via siphoning with a pipette attached to rubber tubing. Debris and unfertilized embryos were removed, and approximately 100 embryos per 100 ml of egg water were maintained in glass beakers, and incubated in a 28°C water bath. Egg water was changed around 8 hpf (day 0), and every morning on subsequent days. When necessary, embryos were treated with 0.003% 1-phenyl-2-thiourea (PTU) (Sigma, St. Louis, MO) at 24 hpf, and with every subsequent water change to prevent pigmentation. By the third or fourth day, when embryos had hatched from their chorions, embryos were anaesthetized with 16.8 mg of 3-amino benzoic acidethylester (Tricane) (Sigma) per 100 ml of egg water, to aid in cleaning and collection of the embryos. When necessary, embryos were snap frozen by

transferring them to RNase free 1.5 ml tubes (Mandel, Guelph, ON) removing the excess water, and then immersing the lower half of the tube into a methanol and dry ice bath. The embryos were then stored at -80°C until required.

2.2. Isolation of zebrafish genomic DNA

Zebrafish genomic DNA was isolated for use in the polymerase chain reaction (PCR) as outlined in Westerfield (1995). Briefly, an adult zebrafish was frozen and ground to a powder in liquid nitrogen, suspended in 10 ml of buffer [10 mM Tris-HCl pH 8.0, 1.0% sodium dodecyl sulfate (SDS), 5 mM ethylenediaminetetraacetic acid salt (EDTA), 100 μg/ml proteinase K (Boehringer Mannheim, Indianapolis IN)], and incubated with shaking for 5 hours at 37°C. The solution was extracted once with an equal volume of phenol:chloroform:isoamyl alcohol (25:24:1), and then once with the same volume of chloroform. The DNA was precipitated overnight at -20°C with 0.3 M NaCl, and 2.5 volumes of 100% ethanol. The DNA was pelleted, washed with 70 % ethanol, and air-dried. The pellet was resuspended in 1 ml of suspension buffer (10 mM Tris-HCl pH 8.0, 1 mM EDTA). RNA was removed by the addition of NaCl and deoxyribonuclease-free ribonucleaseA (Sigma) to a 100 mM and 100 μg/ml final concentration respectively, and incubation for 3 hours at 37°C. SDS was added to a final concentration of 0.2%, and the reaction was phenol-chloroform extracted and precipitated again. The resulting genomic DNA pellet was resuspended in 1 ml of suspension buffer. The concentration of DNA was determined spectrophotometrically by measuring UV absorbance at 260 nm with an Ultrospec4000 (Pharmacia Biotech, Baie d'Urfé, QC)

assuming 1 unit of optical density (OD) = 50 μg/ml DNA. The DNA was diluted with suspension buffer to a concentration of 0.5 μg/μl and stored at 4°C.

2.3. PCR genomic clone

2.3.a. PCR

Primers for PCR were designed based on conserved regions of connexin nucleotide sequences obtained from GenBank (www.ncbi.nlm.nih.gov/). Nucleotide sequences were aligned using the Clustal W Multiple sequence alignment program (Canadian Bioinformatics Resource) (www.ca.embnet.org/). For the forward primer, areas of high nucleotide identity were located and translated into amino acid sequences. For the reverse primer, areas of high identity within the nucleotide sequence were difficult to locate, so nucleotide sequences were translated into amino acid sequences and areas of high amino acid identity were located. With the help of a zebrafish codon usage table (www.kazusa.or.jp/codon), these areas of amino acid sequence were back-translated into nucleotide sequence. The forward and reverse primers (alpha3/F/1 and alpha3/R/1) were designed against areas corresponding to the nucleotides coding for regions in the NH_2- terminus and the fourth transmembrane region, respectively. Primers were purchased from Life Technologies (GibcoBRL, Burlington, ON).

Hotstart PCR was performed with genomic zebrafish DNA, and the above primers. The following reagents were combined in a total volume of 40 μl and brought to 80°C: 1 μl of 2'deoxynucleoside 5'-triphosphates (dNTP)(10 mM each; dATP, dGTP, dCTP, dTTP), 1 μl of each primer (10 μM), 3μl of 50 mM $MgCl_2$, and 0.1 μg of zebrafish genomic DNA. When the above reagents reached 80°C, 2 units of Taq (Invitrogen,

Carlsbad, CA), and 1x PCR buffer (20 mM Tris-HCl pH 8.4, 50 mM KCl)(Invitrogen) were added to result in a final reaction volume of 50 µl. The following PCR program was then run: denaturation at 94°C for 2 minutes, followed by 35 cycles of: 94°C for 45 seconds to denature the DNA, 52°C for 45 seconds for primer annealing, and 72°C for 1 minute for elongation of the DNA. A final 8 minutes at 72°C was added for further elongation of the PCR products. To confirm amplification of the zebrafish genomic DNA, a 10 µl sample of the PCR with 1x DNA loading buffer was run on a 1% agarose gel in 1x Tris-Borate EDTA (TBE) buffer, alongside 1 µg of the 1 Kb Plus DNA Ladder (Invitrogen) as a size reference. The gel was stained with 0.5 µg/ml ethidium bromide (EtBr) in 0.1 M ammonium acetate, and visualised with UV light.

2.3.b. Cloning

The PCR product was cloned using the pCR®2.1 cloning kit (Invitrogen). Fresh PCR product was obtained, and purified with the QIA quick PCR purification kit (Qiagen, Mississauga, ON). The purified PCR product was eluted with 50 µl elution buffer (10 mM Tris-HCl pH 8.5). The following ligation reaction was set up in a total volume of 10 µl and incubated overnight at 14°C: 1 µl of fresh, purified PCR product, 1x ligation buffer (6 mM Tris-HCl pH 7.5, 6 mM $MgCl_2$, 5 mM NaCl, 0.1 mg/ml BSA, 7 mM β-mercaptoethanol, 0.1 mM ATP, 2 mM dithiothreitol (DTT), 1 mM spermidine) (Invitrogen), 50 ng pCR®2.1 vector (Invitrogen), and 4 Weiss units of T4 DNA ligase (Invitrogen). A 2 µl sample of the ligation reaction was transformed into INVαF' One Shot® competent cells (Invitrogen). Briefly, one vial of frozen competent cells (50µl) was thawed on ice prior to the addition of 2 µl of 0.5 M β-mercaptoethanol, and 2 µl of the ligation reaction. The vials were incubated on ice for 30 minutes, and then heat shocked

for exactly 30 seconds in a 42°C water bath. The cells were removed and placed on ice for 2 minutes, and 250 µl of SOC medium was added to each tube. The cells were shaken at 225 rpm for one hour at 37°C in a rotary shaking incubator. As a positive control, 1 µl of control PCR product from the Qiagen kit was also transformed into INVαF' One Shot® cells in the same manner. Various amounts of the transformation reactions were plated onto 90 mm Luria-Bertani (LB) plates supplemented with 50 µg/ml ampicillin (Amp), and grown overnight at 37°C. Prior to innoculation, the plates were spread with 40 µl of 40 µg/ml 5-bromo-4-chloro-3-indolyl-β-D-galactosidase (X-gal in dimethyl formamide) (Invitrogen) for color selection. White colonies from the experimental transformation were selected and grown overnight in 9 mL of LB medium supplemented with 50 µg/ml Amp (NOTE: all LB-Amp plates and overnight cultures were supplemented with 50 µg/ml Amp unless otherwise stated). Plasmid DNA was isolated from 1.5 ml of each overnight culture using the High Pure Plasmid Isolation kit (Boehringer Mannheim). The concentration of DNA in each eluate was determined spectrophotometrically. As EcoRI restriction sites are present on either side of the multiple cloning site, a restriction digest was performed with EcoRI to determine the size of the cloned PCR product. In a total volume of 10 µl, 0.8 µg of plasmid DNA, 5 units of EcoRI (Gibco BRL), and 1x React 3 buffer (50 mM Tris-HCl pH 8.0, 10 mM $MgCl_2$, 100 mM NaCl)(Gibco BRL) were combined and digestion was allowed to proceed for two hours at 37°C. The full digest was run on a 1% TBE agarose gel. One positive clone was maintained and sequenced, using the vector primers M13/pUC/F/1 (M13 forward) and M13 reverse, at the University Core DNA and Protein Services at the University of

Calgary. Sequence obtained was entered into BLAST® (Basic Local Alignment Search Tool) (www.ncbi.nlm.nih.gov/BLAST) to determine any sequence relationships.

2.4. PAC genomic clone #1

2.4.a. Probe preparation

To obtain the entire coding sequence, as well as up and downstream sequence, a clone was isolated from a zebrafish P1 artificial chromosome (PAC) library. A probe template was created by digesting 8 µg of the PCR clone with 20 units of EcoRI (Gibco BRL) and 1x React 3 buffer at 37°C for 2 hours. The digest was run on a 0.8% low melting point agarose gel in 1x TAE buffer. The insert band was cut out of the gel using a fresh razor blade, and water was added to obtain a concentration of about 5 ng/µl.

To create a labeled probe, the following reaction was set up in a total volume of 50 µl and incubated at 37°C for two hours: 10 µl OLB, 35 ng of the heat-denatured PCR clone template, 5 µg of bovine serum albumin (BSA) (New England BioLabs, Beverly MA), 6.5 units Klenow (DNA Polymerase) (Invitrogen), and 8 µl of 370 MBq/ml alpha ^{32}P 2'-deoxycytidine 5'-triphosphate (dCTP) (Perkin Elmer™ Life Science, Boston, MA). The labelled probe was purified by running the sample through a NICK column (Pharmacia Biotech), eluting the probe with 400 µl of buffer (10 mM Tris-HCl pH 7.5, 1 mM EDTA). To determine the strength and labelling efficiency of the probe, the counts per minute (CPM) from 1 µl of the probe prior to purification, and 1 µl of the probe after purification were read with a Beckman LS 6000TA scintillation counter. Immediately before use, the probe was denatured for 5 minutes with 40 µl of 3 M NaOH, and then neutralized with 40 µl of 3 M HCl.

2.4.b. PAC Library Hybridization

The PAC library (German Human Genome Project, RZPD), consisting of 110,600 clones spotted in duplicate on four filters, was prepared for hybridization during the probe incubation. The filters were brought to room temperature, rolled up into glass bottles, and prehybridized in 10-15 ml of PAC HYB solution for one hour at 55°C. The labelled, purified, and denatured probe was added to the tubes containing the filters with enough PAC HYB solution to obtain 3-5 x 10^6 CPM per ml of hybridization solution, and hybridized overnight at 55°C. The filters were washed three times for 1 hour each at 65°C in 10 ml of PAC wash solution, and then rinsed with 4x standard saline-citrate (SSC). The PAC filters were placed on filter paper, pre-wet with 2x SSC, and wrapped tightly in plastic wrap. The edges of the filter paper were marked with distinctive fluorescent stickers to aid with later alignment. The wrapped filters were placed in autoradiography cassettes with intensifying screens (Fisher Biotech, Nepean, ON), and exposed to Kodak BioMax Light film at -80°C. Following exposure, the cassettes were allowed to come to room temperature, and the film then developed by rocking for 5 minutes in each of the following solutions: Kodak GBX developer, water, Kodak GBX fixer, and water. The films were checked for positive clones and re-exposed and developed as necessary until the location of the positive clones was clear.

2.4.c. Isolating PAC clone

Clones were ordered from RZPD based on the coordinates of the positive signals, and then re-screened. To re-screen, each clone was diluted in LB media, and plated onto LB plates, both supplemented with 50 μg/ml kanamycin (Kan). (NOTE: all LB-Kan plates and overnight cultures were supplemented with 50 μg/ml Kan unless otherwise

stated). The plates were incubated overnight at 37°C. A 1 cm x 1 cm grid was marked and numbered in duplicate on two 150 mm diameter nitrocellulose membranes (0.45 microns, Millipore, Bedford, MA). Using sterile toothpicks, approximately 20 individual colonies from each clone were streaked on the filters in duplicate and then incubated overnight at 37°C on LB-Kan plates. After the incubation, one of the duplicate plates was wrapped in parafilm and stored at 4°C for use later. The other filter was pre-treated for hybridization in the following solutions: **1)** 25% sucrose, 1.5 mg/ml lysozyme (Sigma), 50 mM Tris pH 7.5, **2)** 0.2% TritonX-100 (BDH, Toronto, ON), 0.5 M NaOH, **3)** 0.5 M NaOH, **4)** 1 M Tris pH 7.5, **5)** 0.15 M NaCl, 0.1 M Tris pH 7.5. For each solution two blotting papers were set up, one dry, and one wet with the appropriate solution. The filter was placed on the wet blotting paper for one minute, and then on the dry blotting paper for one minute. This process was repeated two more times (6 minutes in total). This whole process was then repeated with the four other solutions. When finished, the treated filter was left to air dry, and then baked for one hour at 80°C to crosslink the DNA to the membrane.

The processed filter was wet in 2x SSC prior to prehybridization for 2 hours at 42°C in hybridization (HYB) solution. The filters were hybridized overnight at 42°C with the same ^{32}P-dCTP labeled PCR clone probe as in section 2.4.a., in enough HYB solution to obtain 3-5 x 10^6 CPM/ml. The filters were washed three times for 20 minutes each at 55°C in 0.1x SSC and 0.1% SDS, and then rinsed with 4x SSC before placing on filter paper pre-wet with 2x SSC. The filter was wrapped and marked with fluorescent stickers, and then exposed to Kodak BioMax Light film and developed as described previously (section 2.4.b.). Each of the original clones were scored for the proportion of

colonies hybridizing to the probe, and one positive colony was randomly selected for further amplification.

The clone selected for amplification was streaked from the original unprocessed filter onto a new LB-Kan plate and incubated overnight. A single colony from this plate was inoculated into 3 ml of LB-Kan media, and incubated for 8 hours shaking at 37°C. A 0.5 ml aliquot of this starter culture was added to 500 ml of LB-Kan media and incubated in a 37°C room with shaking for 16 hours. Plasmid DNA was isolated from this overnight culture using the Qiagen Large Construct kit. DNA was eluted from the column with 15 ml of Buffer QF (1.25 M NaCl, 50 mM Tris-HCl pH 8.5, 15% isopropanol), prewarmed to 65°C. The DNA was precipitated, pelleted, and washed as described previously (section 2.2.). The pellet was allowed to air dry for 5-10 minutes prior to being redissolved in water. The amount of PAC plasmid DNA obtained was determined spectrophotometrically. The clone was sequenced with primers based on PCR clone sequence (zfCx45.6/F/1, zfCx45.6/R/1) to confirm the identity of the clone.

2.5. PAC Genomic Clone #2

To confirm the sequence obtained from the first PAC clone, a second PAC clone was isolated using a different method. The original PAC clones were replated and screened as for the first PAC isolation. Two colonies were randomly chosen to restreak onto fresh LB-Kan plates. A single colony from each clone was inoculated into 2 ml LB medium supplemented with 25 mg/ml Kan, and incubated overnight at 37°C in a rotary shaking incubator. PAC plasmid DNA was isolated using a modification of the standard QIAGEN-tip method used to isolate the first PAC clone (www.chori.org/bacpac/bacpac

mini.ht – Children's Hospital Oakland Research Institute, Oakland, CA). The overnight culture was centrifuged, the supernatants were decanted, and the pellet resuspend in 300 µl of P1 solution [15 mM Tris-HCl pH 8, 10 mM EDTA, 100 µg/ml RNase A (Sigma)]. The cells were lysed with 300 µl of P2 solution (0.2 N NaOH, 1% SDS) and incubated for 5 minutes at room temperature. Genomic DNA was precipitated with 300 µl of P3 solution (3 M KOAc, pH 5.5) and incubation on ice for 5 minutes. The tube was centrifuged, and the supernatant containing the PAC DNA was transferred to a 1.5 ml tube. The PAC DNA was precipitated with 800 µl of ice-cold isopropanol overnight at -20 °C, and then pelleted. The pellet was washed with 70% ethanol, and air-dried. The PAC DNA was resuspended in 40 µl of TE buffer, and the amount of DNA obtained was determined spectrophotometrically. Prior to sequencing, the PAC clone was subcloned as described below.

2.6. PAC HindIII Subclones

Both PAC clones were subcloned to obtain the coding region, as well as some upstream and downstream sequence, in a more manageable sized fragment. Test restriction digests were performed on samples of the PAC plasmid with an excess of HindIII (Promega, Madison, WI), BamHI (New England BioLabs), or XbaI (GibcoBRL) to determine an enzyme which would cut the PAC clone optimally for subcloning. An aliquot of each digest was run on a 1% TBE agarose gel to determine the digestion pattern. After choosing a suitable enzyme, 5 µg of the pBluscript vector (Stratagene, LaJolla, CA) was digested overnight at 37°C with the same enzyme selected to digest the PAC clone. The vector was treated for 20 minutes at 37°C with 1 unit of Calf Intestinal

Alkaline Phosphatase (CIAP) (GibcoBRL) per 25 µl of sample to remove phosphates from the ends of the vector, and thus prevent self-ligation. To stop the reaction, 1 µl of 0.5 M EDTA was added for every 25 µl of sample, and the reaction was incubated for 1 minute at 65°C. Both the plasmid and vector digests were phenol-chloroform extracted (section 2.2.), and precipitated at –80°C for a few hours by adding 1/10th of the estimated volume of 3 M sodium acetate pH 5.2, and double the estimated volume of 100% ice cold ethanol. The precipitate was pelleted, washed in 75% ethanol, and dissolved in 11 µl of water. The amount of product obtained was estimated based on 50% recovery from the extraction.

PAC clone restriction fragments were cloned into pBluescript (Stratagene), and transformed into SoloPack® Gold cells (Stratagene). The following ligation reaction was set up in a microfuge tube in a total volume of 15 µl and incubated overnight at 14°C: ~500 ng of digested PAC clone, ~ 450 ng of digested pBluescript, 1x ligation buffer (Invitrogen), and 4 units of T4 ligase (Invitrogen). The plasmid was transformed into SoloPack® Gold cells by the addition of 1 µl of the ligation reaction to one tube of cells (50 µl), following a method similar to that outlined in section 2.3.b. Plasmids containing all or a portion of the coding region of the connexin were isolated by screening white colonies from the experimental transformation in the same fashion as the original PAC clones were screened (section 2.4.c.) (NOTE: Amp was used as the antibiotic instead of Kan).

Positive subclones were cultured overnight at 37°C in LB-Amp media, and plasmid DNA was isolated using the High Pure Plasmid Isolation miniprep kit (Boehringer Mannheim). The amount of DNA isolated was determined

spectrophotometrically. To determine the size of the cloned insert, an aliquot of the clone was digested with an excess of EcoRI (GibcoBRL), and run on a 1% TBE agarose gel. Subclones were sequenced over the entire coding region, each region at least twice, using primers designed from PCR and PAC clone sequence.

2.7. Functional Analysis

2.7.a. Cloning

To determine the functional properties of the cloned connexin, the coding region of the connexin was cloned into the pCS2+ vector (Turner and Weintrab, 1994). As the pCS2+ vector does not have the required elements for color selection, the coding region of the connexin was first subcloned into pDrive (Qiagen). To obtain a PCR product of the coding region for cloning, primers were designed approximately 10 bp upstream from the start codon, and 10bp downstream from the stop codon (zfCx45.6/F/5 and zfCx45.6/R/6 respectively). The following reagents were combined in a microfuge tube in a total volume of 50 µl: 0.4 mM of each dNTP, 0.6 µM of each primer, and 0.5 µg of the HindIII PAC subclone (section 2.3.c.) as template. To this mixture the following reagents were added in a volume of 50 µl: 2.5 units of Pwo polymerase (a proof reading polymerase) (Roche), and 10 µl of 10x Pwo PCR buffer (100 mM Tris HCl pH 8.85, 250 mM KCl, 50 mM $(NH_4)_2SO_4$, 20 mM $MgSO_4$) (Roche) resulting in a total reaction volume of 100 µl. A second reaction without template was set up as a negative control. The following PCR program was performed on both samples: 94°C for 2 minutes, and 14 cycles of: 94°C for 15 seconds, 60°C for 30 seconds, 72°C for 1 minute. This was followed by 19 cycles of: 94°C for 15 seconds, 60°C for 30 seconds, 72°C for 1 minute

with 5 seconds added at each cycle, followed by an elongation step of 72°C for 7 minutes. A 10 µl sample of the PCR was run on a 1% TBE gel to confirm amplification. A 3'-A overhang, required for cloning into the pDrive vector, was added to the PCR product by incubating the remaining 90 µl of the PCR with 2 units of Taq (Invitrogen), 0.2 mM of each dNTP, and 1x PCR buffer (Invitrogen) at 72°C for 8 minutes. The reaction was iced briefly and purified using the QIA quick PCR purification kit (Qiagen). The product was eluted with 30 µl of elution buffer and a portion was run on a 1% TBE agarose gel to estimate the amount of DNA present.

The 1.2 kb purified and Taq extended PCR product was ligated into the pDrive vector (Qiagen). Approximately 50 ng of pDrive, 140 ng of the PCR product (a 5-10x molar excess), and 1x ligation master mix were combined in a 10 µl volume. The reaction was incubated at 6°C for 30 minutes and then stored at -20°C. The cloned PCR insert was transformed into Qiagen EZ competent cells by the addition of 2 µl of the ligation reaction into one tube of cells. Various amounts of the reaction were plated onto LB plates supplemented with 100 µg/ml of Amp, and spread with 40 µl of 40 mg/ml X-gal plus 40 µl of 100 mM IPTG for color selection. The plates were incubated overnight at 37°C. Individual colonies were grown overnight at 37°C in LB culture supplemented with 100 µg/ml Amp. Plasmid DNA was isolated with the QIA prep spin Miniprep kit (Qiagen). One positive clone was maintained and sequenced at the University of Calgary with the M13 forward and reverse vector primers.

The full coding region of the connexin was digested out of 7 µg of the pDrive clone with 25 units of EcoRI (Gibco BRL) and 1x React3 buffer (Gibco BRL), for 3 hours at 37°C. The full digest was run on a 1% TBE agarose gel, and the insert band was

cut out of the gel using a fresh razor blade. The insert band was purified using Biolab's Geneclean spin kit, eluting the purified product in 20 µl. The amount of DNA recovered from the column was estimated as 50% of the original amount. The pCS2+ vector had previously been digested with EcoRI, treated with CIAP, and phenol-chloroform extracted (by a labmate). The following ligation reaction was set up in a microfuge tube in a total volume of 20 µl and incubated overnight at 14°C: 0.26-0.4 µg of the purified insert, 1 unit of T4 ligase (Invitrogen), 0.075 µg of the digested pCS2+ vector, and 1x ligation buffer (Invitrogen). The cloned connexin in pCS2+ was transformed into Solopack® Gold Competent cells (Strategene) by the addition of 1 µl of the ligation reaction to one tube of cells as outlined in section 2.6. Various amounts of the transformation reaction were plated onto LB-Amp plates (100 µg/ml of Amp) and incubated at 37°C overnight. Overnight cultures and minipreps were performed as previously described to isolate the plasmid. As the pCS2+ vector does not have the required elements for color selection, a test digest with EcoRI was performed and run on a 1% TBE-agarose gel to verify the presence of an insert of expected size. To determine the orientation of the cloned connexin, 1.5 µg of plasmid DNA was digested at 50°C for 3.5 hours with 10 units of BstXI (Promega), 1x buffer D (6 mM Tris-HCl pH7.9, 150 mM NaCl, 6 mM $MgCl_2$, 1 mM DTT) (Promega), and 5 µg of BSA (Promega) in a 20 µl volume, and run on a 1% TBE-agarose gel. The plasmid was sequenced using pCS2+/F/1 and internal primers previously created for sequencing of the HindIII PAC subclone.

To ensure the cloned connexin transcribed in pCS2+, an in vitro transcription was performed following the same method as used to create a probe for whole-mount ISH

(section 2.10.b.). Ten micrograms of the cloned connexin in pCS2+ was linearized to create an antisense template with 35 units of XbaI (GibcoBRL) and 1x React2 buffer (50 mM Tris-HCl pH 8.0, 10 mM $MgCl_2$, 50 mM NaCl)(GibcoBRL) for 5 hours at 37°C. The digestion was phenol-chloroform extracted and precipitated, and an *in vitro* transcription was set up with 1 μg of linearized template and 40 units Sp6 polymerase (NOTE: DIG-11-UTP was not added to the reaction). The reaction was run on a denaturing formaldehyde agarose gel to observe transcription products.

2.7.b. Electrophysiology

Fifteen micrograms of uncut plasmid was dried down using a Savant Centrivap and sent to Dr. T. White (SUNY, Stoney Brook, NY) so functional properties of the cloned connexin could be analyzed using the paired *Xenopus* oocyte system (Cason *et al.*, 2001).

2.8. Chromosomal Mapping: LN54 Radiation Hybrid Panel

A LN54 RH panel consisting of genomic DNA from 93 cell lines and 3 controls (generously supplied by Marc Ekker, Loeb Institute) was used to map the chromosomal location of the cloned connexin. A test PCR was first performed to ensure the primers chosen did not amplify regions from the mouse chromosomes. The first primer set amplified a 536 bp nucleotide sequence encoding for the region encompassing parts of the COOH- terminus (C-tail) and the 3' UTR (zfCx45.6/F/3, zfCx45.6/R/3). The second primer set amplified a 317 bp nucleotide sequence encoding for the region extending from the 5' UTR into the first transmembrane region (zfCx45.6/F/2, zfCx45.6/R/1). The following reagents were combined in a 20 μl volume for each primer set: 1x PCR buffer

(20 mM Tris-HCl pH 8.4, 50 mM KCl)(Invitrogen), 0.2 mM of each dNTP, 0.25 μM of each primer, 1 unit of Taq (Invitrogen), and varying amounts of $MgCl_2$ (1.5 mM, 0.75 mM, or 3 mM). To these reagents, either 0.1 μg of mouse genomic DNA (generously supplied by Dr. R. McGowan, University of Manitoba), or 0.5 μg of zebrafish genomic DNA was added, thus resulting in six different PCRs for each primer set. The following PCR was performed with all samples: 94°C for 3 minutes, and then 30 cycles of 94°C for 45 seconds, 65°C for 45 seconds, 72°C for 75 seconds, followed by 10 minutes of 72°C. A 5 μl sample of each reaction was run on a 1% TBE agarose gel to determine the optimal primer set and concentration of $MgCl_2$ to use for PCR with the panel.

The panel PCR was run in essentially the same fashion as above, but 100 ng of DNA from each cell line was used as template. A 5 μl sample of each PCR was run on a 1% TBE agarose gel to determine the cell lines containing positively amplified PCR products. Each cell line was scored as follows: 1-positive, 0-negative, 2-ambiguous or missing data. PCR was re-run and scored two more times in the same fashion. Results from all three runs were compiled and entered into the LN54 panel web page (http://mgchdl.nichd.nih.gov:8000/zfrh/beta.cgi), and the chromosomal location of the gene was statistically determined.

2.9. Northern Analysis

2.9.a. Poly A^+ blot

A polyA^+ mRNA blot was created by a lab-mate to use for Northern analysis. Total RNA was isolated from embryos staged 0 days post fertilization (dpf) to 5 dpf, as well as adult brain, eye (minus the lens), liver, and ovary using TRIzol® Reagent

(Invitrogen). The embryos or tissue were homogenized in 1ml of TRIzol®, and incubated for 5 minutes at room temperature. The organic phase and the aqueous phase containing the RNA were separated by the addition of 0.2 ml of chloroform followed by centrifugation. The aqueous phase was transferred to a fresh tube and the RNA was precipitated with 0.5 ml of isopropyl alcohol. The samples were incubated for ten minutes at room temperature, and then centrifuged to pellet the RNA. The resulting pellet was washed once with 75% ethanol, dried, and dissolved in 11 µl of diethylpyrocarbonate (DEPC) (Sigma) treated water. The amount of RNA isolated was determined spectrophotometrically. PolyA$^+$ mRNA was isolated from total RNA using the Oligotex mRNA Mini kit (Qiagen). Using this kit, 100 to 200 µg of total RNA was run through an Oligotex column that contained beads covalently linked with $dC_{10}T_{30}$ oligonucleotides. The poly-A tail of the mRNA hybridized to the beads while the tRNA and rRNA was washed off. PolyA$^+$ mRNA was eluted with low salt conditions, and then precipitated with glycogen and NaOAc in absolute ethanol. Two micrograms of polyA$^+$ mRNA from each sample, with the addition of 1x RNA loading buffer, were run on a 1% agarose denaturing formaldehyde gel (see appendix). The gel was rinsed in 10x SSC and then blotted by capillary action onto a nylon Magnacharge membrane (0.45 microns, Osmonics, Minnetonka, MN) (Sambrook *et al.*, 1989). The blot was dissassembled and washed for 5 minutes in 2x SSC at 65°C to remove any gel stuck to the membrane. The blot was dried and crosslinked with UV, and stored at room temperature.

2.9.b. PstI probe

A clone containing a portion of the coding region was created to use as a probe for Northern analysis. A 10 µg sample of the first HindIII PAC subclone was digested

with 10 units of PstI (GibcoBRL), and 1x React2 buffer (50 mM Tris-HCl pH 8.0, 10 mM $MgCl_2$, 50 mM NaCl)(GibcoBRL) for 2 hours at 37 °C. Computer-aided restriction mapping (BCMs Web cutter, http://searchlauncher.bcm.tmc.edu/seq-util/seq-util.html) determined that digestion with PstI would result in about a 600 bp fragment encompassing nucleotides coding for the 4^{th} transmembrane region and a portion of the C-tail (base pairs 449 to 1052 of the coding region). The full digest was run on a 1% TAE agarose gel. Using a fresh razor blade, a band of approximately 600 bp was cut out of the gel and purified using the Gene Clean spin kit (Bio 101, Carlsbad, CA), eluting the sample in 20 µl. Recovery from the column was estimated as 50% of the original amount. The vector, pBluescript (Strategene), was prepared for cloning as previously described (section 2.6.), but was digested with an excess of PstI before being treated with CIAP. The vector was phenol-chloroform extracted, and precipitated as described previously.

The insert was cloned by ligation into the pBluescript vector, and transformation into Solo Pack Gold cells (Stratagene). The following ligation reaction was set up in a 10 µl volume in a microfuge tube, and incubated overnight at 14°C: 167 ng of the purified 600 bp band, 20 ng of digested pBluescript, 1x ligation buffer (Invitrogen), and 1 unit T4 DNA ligase (Invitrogen). The ligation was transformed into SoloPack® Gold cells as described previously (section 2.6.). Various amounts of the transformation were plated onto LB-Amp plates and incubated overnight at 37°C. Three white colonies were selected and cultured overnight in LB-Amp media. Plasmid DNA was obtained from overnight cultures using the QIA prep Spin Miniprep kit (Qiagen). Samples were run on a 1% TBE agarose gel to estimate the concentration of DNA obtained. The orientation of

the ligated insert was determined by test digests with 3 μg of DNA and an excess of either BstXI (Promega), or HincII (GibcoBRL). The reactions were digested at 55°C and 37°C respectively for 2 hours, and run on a 1% TBE agarose gel.

2.9.c. Hybridization and detection

An antisense probe template was created by linearizing 10 μg of the PstI clone with an excess of BamHI (New England Biolabs), and 1x BamHI buffer (150 mM NaCl, 10 mM Tris-HCl pH 7.9, 10 mM $MgCl_2$, 1 mM DTT) (New England Biolabs) for 2 hours at 37°C. A sample of the digest was run on a 1% TBE agarose gel to verify digestion. The digest was phenol-chloroform extracted, precipitated, and dissolved in 11 μl of water. The amount of template recovered was determined spectrophotometrically. The following transcription reaction was set up in a total volume of 20 μl and incubated for 30 minutes at 37°C: 1x T7 buffer (40 mM Tris-HCl pH 8.0, 8 mM $MgCl_2$, 2 mM spermidine-$(HCl)_3$, 25 mM NaCl) (Invitrogen), 0.1 M DTT (Invitrogen), 20 units RNasin (Promega), 0.5 mM of each NTP, 1 μg of linearized and purified template, 5 μl of 370 MBq/ml ^{32}P uridine 5' – triphosphate (UTP) (Perkin Elmer™), and 50 units of T7 RNA polymerase (GibcoBRL). To digest the DNA template, the reaction was incubated with 1 unit of RQ1 RNase-Free DNase (Promega) for 15 minutes at 37°C. To stop the digestion reaction 1 μl of 0.5 M EDTA was added. The ^{32}P-labelled RNA probe was purified using the mini Quick Spin RNA Column (Boehringer Mannheim), diluting the sample to 75 μl with DEPC water prior to addition to the column. The labelling of the probe was assessed with a Beckman scintillation counter as outlined in section 2.4.a.

The $polyA^+$ blot was prepared for hybridization in the same fashion as described for the PAC clone rescreening (section 2.4.c.), but was incubated in HYB solution for 2

hours at 55°C. The RNA probe was denatured by heating for 5 minutes at 65°C, immediately before addition to the tube with enough hybridization solution to obtain 5 x 10^6 CPM/ml. The blot was hybridized overnight at 55°C. Unbound probe was removed with 3 washes of at least 30 minutes each in 0.1x SSC and 0.1% SDS at 68°C. The blot was then rinsed in 2x SSC, prior to wrapping and exposing to film as for the original PAC genomic clone (section 2.4.b.).

As a loading control, the same blot was probed by a lab-mate in the same fashion as above with a ^{32}P-UTP labeled antisense RNA probe created from the zebrafish elongation factor 1 alpha (ZfeF1alpha) (a generous gift from Dr. Ross Johnson, Minneapolis, MN). This gene is transcribed at a relatively constant level in all tissues and in embryos at all stages. The vector was linearized with EcoRI and transcribed with T3 RNA polymerase, and the blot was hybridized overnight at 55°C with 5x10^6 CPM/ml of probe. The blot was then rinsed and exposed to film as above.

2.10. Reverse Transcriptase – PCR

2.10.a. Obtaining cDNA

Reverse Transcriptase-PCR (RT-PCR) was performed to confirm the expression pattern of the cloned connexin in the adult and embryonic zebrafish. Total RNA was isolated from various embryonic zebrafish stages (1.5 hpf to 5 dpf), and adult tissue (heart, lens, liver, brain and ovary) using TRIzol® Reagent (Invitrogen) (section 2.8.a). Residual DNA was removed with RQ1 RNase-free DNase (Promega). In a total reaction volume of 10 µl, 3 µg of RNA was treated for 30 minutes at 37°C with 3 units of RQ1 RNase-free DNase (Promega), and 1x RQ1 RNase-free DNase buffer (40 mM Tris-HCl

pH 8.0, 10 mM $MgSO_4$, 10 mM $CaCl_2$)(Promega). DNase treatment was stopped by incubation for 10 minutes at 65°C with 1 µl of RQ1 DNase stop solution (Promega). The reaction was phenol-choloroform extracted, precipitated, and dissolved in 10 µl of DEPC treated water. The amount of RNA recovered from the extraction was estimated as half the original amount.

First strand cDNA was created from the RNA of each embryonic stage and adult tissue using Superscript ^{TM} II RNase H^- Reverse Transcriptase (Invitrogen). For each RNA sample, 500 ng of Oligo $(dT)_{12-18}$ (Invitrogen), approximately 1.5 µg of purified RNA, and 0.5 mM of each dNTP was mixed in a total reaction volume of 12 µl, and heated for 5 minutes at 65°C. To the mixture, 4 µl of 5x first strand buffer (50 mM Tris-HCl pH 8.3, 75 mM KCl, 3 mM $MgCl_2$)(Invitrogen), 2 µl of 0.1 M DTT (Invitrogen), and 1 µl (40 units) of RNaseOUT Recombinant Ribonuclease Inhibitor (Invitrogen) were added. The reaction was mixed gently, and incubated for 2 minutes at 42°C. To create cDNA, the reaction was incubated with 1 µl (200 units) of SuperscriptII for 50 minutes at 42°C (final reaction volume of 20 µl). The Superscript enzyme was inactivated by heating at 70°C for 15 minutes. The volume of the reaction was brought to 50 µl by the addition of 30 µl of DEPC treated water, and then phenol-chloroform extracted to remove residual enzymes and reagents.

2.10.b. PCR

PCR was performed using cDNA obtained from the various embryonic stages and adult tissues, and primers (zfCx45.6/F/4, zfCx45.6/R/3) amplifying about a 775 bp region of nucleotides coding for a region extending from within the C-tail into the 3' UTR. PCR was performed using the same Hotstart program used to isolate the PCR clone (section

2.3.a.). In a total reaction volume of 50 µl the following reagents were combined: 1x PCR buffer (Invitrogen), 1.5 mM $MgCl_2$, 0.2 mM of each dNTP, 0.2 µM of each primer, 2 units of Taq (Invitrogen), and 10% of the first strand cDNA. As a control, PCR was set up in a similar fashion using primers designed against a region of the zebrafish elongation factor 1 alpha that spans an intron (ZfeF1alpha/F/1, ZfeF1alpha/R/1). The expected size of the amplicon from cDNA is 569 bp, and 733 bp from genomic DNA. This gene is transcribed at a relatively constant level in all tissues and in embryos at all stages. A 10 µl sample of each PCR reaction was run on a 1% TBE agarose gel to visualise the amplification product.

2.10.c. Blotting and probing

To increase sensitivity and confirm the identity of the RT-PCR product, the experimental samples were blotted onto a nylon membrane and probed with a ^{32}P-labeled DNA probe. Fresh PCR products were obtained and 10 µl aliquots of each reaction were run on a 1% TBE agarose gel. The gel was prepared for blotting by washing it in the following solutions: 1) 0.25 M HCl for 15 minutes to fragment the DNA, **2)** 1.0 M NaCl/0.5 M NaOH for 30 minutes to denature the DNA, and **3)** 0.5 M Tris-HCl pH 8.0, 0.5 M NaCl for 30 minutes to neutralize the gel. The gel was then blotted onto a nylon membrane as outlined in section 2.9.c. After blotting, the membrane was probed with a ^{32}P-labeled DNA probe, created from the original PCR clone, as outlined in section 2.4. The membrane was prepared for hybridization by incubating in HYB solution at 42°C for a few hours, and then hybridized with 5-7 x 10^6 CPM per ml of labeled probe in HYB solution overnight at 42°C. The membrane was washed 3 times for 30 minutes each at

55°C in 0.1% SDS, 0.1x SSC, and then exposed to Kodak BioMax Light film as previously described (section 2.4.b.).

2.11. Whole-mount *In-Situ* Hybridization - DIG labelled

2.11.a. Heart cDNA clone

A new probe template of the isolated connexin was created from adult zebrafish heart cDNA. RNA was isolated from the adult zebrafish heart, and first strand cDNA was created as outlined in section 2.9.a. Primers used to create the cDNA probe template were located 151 bp upstream from the start codon, and 150 bp downstream from the stop codon of the cloned connexin (zfCx45.6/F/2 and zfCx45.6/R/3 respectively). RT-PCR was performed in the same manner as outlined in section 2.9.b. using 5 µl of the adult zebrafish heart first strand cDNA. An aliquot of the PCR reaction was run on a 1% TBE agarose gel to verify amplification.

The PCR product was ligated into the pCRII®-TOPO vector (Invitrogen) by combining 4 µl of the PCR product, 1 µl of salt solution (1.2 M NaCl, 60 mM $MgCl_2$) (Invitrogen), and 10 ng of the vector in a microfuge tube, and incubating for 30 minutes at room temperature. A 2 µl aliquote of the ligation reaction was transformed into one vial of TOP10 One Shot® cells (Invitrogen) in a method similar to that outlined in section 2.3.b. Aliquots of the transformation were spread onto LB-Amp plates, with the addition of 40 µl of 40 mg/ml X-gal (Invitrogen) for color selection, and incubated overnight at 37°C.

A test PCR reaction was performed to isolate positive colonies. Using a sterile probe, 20 colonies were picked and stirred into 20 µl of the following solution in

individual tubes: 1x PCR buffer (Invitrogen), 0.2 mM of each dNTP, 0.2 μM of both the M13 reverse primer and the M13 forward primer, 2 units of Taq (Invitrogen), and 3 mM of $MgCl_2$. The tubes were heated for 10 minutes at 94°C to lyse the cell membranes and denature the DNA. The following PCR program was then performed: 35 cycles of 94°C for 30 seconds, 53°C for 30 seconds, 72°C for 1 minute, and a final 8 minutes of elongation at 72°C. An aliquot of the PCR was run on a 1% TBE agarose gel to determine which of the 20 colonies contained vectors with an insert of expected size. One colony was selected and grown overnight in LB-Amp, and plasmid DNA was obtained from the overnight culture using the QIAprep Spin Miniprep Kit (Qiagen). The amount of DNA obtained was determined spectrophotometrically. The clone was sequenced using internal primers designed from PAC clone sequence. The sequence obtained from the cDNA clone was compared to the sequence obtained from the PAC clones and subclones.

2.11.b. DIG-labelled probe

Templates for antisense and sense probes were created by linearizing 10 μg of the heart cDNA clone with 80 units of BamHI (New England Biolabs) and 1x NEBamHI buffer (New England Biolabs), or 80 units of EcoRV (New England Biolabs) and 1x NE2 buffer (50 mM NaCl, 10 mM Tris-HCl pH 7.9, 10 mM $MgCl_2$, 1 mM DTT) (New England Biolabs) respectively. Both reactions were digested overnight at 37°C, and samples of the digestion were run on a 1% TBE agarose gel to verify complete digestion. The reactions were phenol-chloroform extracted and precipitated, and the pellet was dissolved in 11 μl of DEPC treated water. The amount of template recovered was

determined spectrophotometrically. DEPC treated water was added to bring the final concentration of the template to 0.2 μg/μl.

An *in vitro* transcription was set up to create a digoxygenin (DIG)-11-UTP-labelled probe by combining the following reagents in a 20μl volume and incubating for 2 hours at 37°C: 1 μg of linearized template, 2 μl of 10x NTPs (10 mM each ATP, CTP, GTP, and 6.5 mM UTP + 3.5 mM DIG-11-UTP) (Roche, Laval, QC), 4 μl of 5x transcription buffer (200 mM Tris-HCl pH 7.9, 30 mM $MgCl_2$, 10 mM spermidine, 50 mM NaCl) (Promega), 2 μl of 100mM DTT (Invitrogen), 40 units of RNasin (Promega), and 40 units of T7 RNA polymerase (for the antisense probe) (GibcoBRL), or 40 units of Sp6 RNA polymerase (for the sense probe) (Roche). Residual template was removed by the addition of 1 μl of RQ1 RNase free DNase (Promega) for 15 minutes at 37°C. The reaction was stopped and the probe precipitated overnight at -80°C by the addition of 75 μl of 100% ice-cold ethanol, 2 μl of 0.2 M EDTA, and 2.5 μl of 4 M LiCl. The RNA probes were pelleted, washed once with 75% ethanol and left to air dry. The pellet was dissolved in 50 μl DEPC treated water with the addition of 1 μl RNasin.

To check the efficiency of the transcription, 2-5 μl samples of the probes were run on a mini 1% formaldehyde gel and blotted onto a nylon membrane as for the Northern analysis (section 2.8.a.). The membrane was dried and the RNA was cross-linked to the membrane with 120000 $\mu J/cm^2$ from a Spectrolinker™ XL-1000 UV CrossLinker (Spectronics Corporation, Lincoln, NE). The membrane was wet in 2x SSC and rinsed in TBS-T prior to being blocked for 1 hour in 3% skim milk powder in TBS-T at room temperature. The blot was probed with sheep anti-digoxigenin alkaline phosphatase conjugated Fab fragments (anti-DIG antibody) (Boehringer Mannheim) (1:5,000 in block

solution) for 1 hour at room temperature. Antibody was removed with 3 washes of 10 minutes each in TBS-T. The blot was rinsed once in NTM buffer, and developed with 3.5 µl/ml of 5-bromo-4-chloro-3-indolyl phosphate (BCIP) (Boehringer Mannheim), and 4.5 µl/ml of nitroblue tetrazolium (NBT) (Boehringer Mannheim) in NTM buffer. The color reaction was stopped by rinsing with 50 mM Tris pH 7.0. The intensity of the incorporation of DIG into the sense and antisense probes was compared, and if necessary the amount of each probe used for hybridization was altered so as to obtain similar color intensity.

2.11.c. Embryo preparation

Whole-mount *in-situ* hybridization (ISH) was performed on various stages of embryos between 0 dpf and 5 dpf following the protocol set out by Thisse *et al.* (1993) with slight modifications. Embryos were fixed overnight in 4% paraformaldehyde (PFA) in PBS at 4°C, and washed twice in PBS at room temperature for at least 5 minutes each. Chorions were removed during the first wash using watchmaker's forceps. Embryos were stored in 90% methanol at -20°C for at least 1 hour to help reduce background. For ISH, embryos were allowed to reach room temperature, transferred to 1.5 ml microfuge tubes, and rehydrated by incubating for 5 minutes in each of the following solutions: **1)** 75% methanol/25% PBS, **2)** 50% methanol/50% PBS, **3)** 25% methanol/75 % PBS. Embryos were rinsed briefly in PBS, and then washed twice for 5 minutes each in 100 % PBS-T. Embryos were fixed again for 20 minutes in 4% PFA, rinsed briefly in PBS-T, and then washed twice in PBS-T for 5 minutes each. To permiabilize the plasma membranes, embryos were treated with 10µg/ml of proteinase K (Boehringer Mannheim) in PBS-T at room temperature as follows: 0 dpf - no treatment, 1 dpf – 15 minutes, 2 and

3 dpf – 20 minutes, 4 and 5 dpf – 30 minutes. Embryos were then rinsed in PBS-T and washed in PBS-T for at least 5 minutes. Embryos were fixed again in 4% PFA in PBS-T for 20 minutes at room temperature. The embryos were then washed three times in PBS-T for 5 minutes each.

At this point, pre-adsorption of the antibody (see section 2.10.e.) was initiated by combining 1 µl of the anti-DIG antibody (Boehringer Mannheim), approximately 50 µl of rehydrated fixed embryos, 400 µl of PBS-T, 2 mg/ml BSA (Promega) and 2% normal goat serum (NGS) (Zymed, San Francisco, CA). The tube was incubated with shaking at room temperature for 2 hours, and then stored at 4°C until needed.

2.11.d. Whole-mount ISH

The tubes containing embryos were placed on a rotary shaker (25 rpm) for 10 minutes at 60°C in 400 µl of ISH hybridization (HYB*) buffer. The HYB* buffer was replaced with 700 µl of fresh HYB* buffer, and the embryos were left rocking slowly for 3-5 hours at 60°C. Embryos were hybridized overnight at 60°C with about 2 ng/µl of either the sense or antisense DIG-labelled connexin probe in HYB*. Unbound probe was removed by washing embryos briefly in 100% HYB*, and then 15 minutes at 60°C in each of the following solutions: **1)** 75% HYB$^-$ (HYB* minus Heparin and *Torula* RNA)/25% 2x SSC, **2)** 50% HYB$^-$/50% 2x SSC, **3)** 25% HYB$^-$/75% 2x SSC, **4)** 2x SSC. The embryos were then washed twice in 50% formamide/0.2x SSC for 30 minutes at room temperature, followed by the following washes for 10 minutes each at room temperature: **1)** 75% 0.2x SSC/25% PBS-T, **2)** 50% 0.2x SSC/50% PBS-T, **3)** 25% 0.2x SSC/75% PBS-T, **4)** 100% PBS-T.

2.11.e. Detection of probe and observation of embryos

Embryos were rinsed in PBS with the addition of 2 mg/ml BSA (Promega) and 2% NGS (Zymed), and then blocked in the same solution for 1 hour at room temperature. Embryos were incubated with the preabsorbed anti-DIG antibody (1:4,000 – 1:5,000 dilution) in the above block solution rocking slowly overnight at 4°C. Unbound antibody was removed by rinsing embryos in PBS-T, and then washing in PBS-T at room temperature 6 times for at least 15 minutes each. Embryos were transferred to glass well plates and washed twice in NTM buffer with the addition of 5 mM levamisole (Sigma) at room temperature for 10 minutes each. The last wash was replaced with the same solution plus the addition of 4.5 µl/ml NBT, and 3.5 µl/ml BCIP. Color was allowed to develop for anywhere from 10-48 hours. To stop the color reaction, embryos were rinsed in PBS, and then fixed overnight at 4°C in 4% PFA with the addition of 1% glutaraldehyde.

Embryos for whole-mount observations were washed twice in PBS at room temperature for 5 minutes each. The embryos were dehydrated by the gradual addition of 100% methanol. Embryos were incubated in 100% methanol for 5 minutes, and then cleared with 100% glycerol. Embryos were mounted in glycerol on glass microscope slides, and observed with a Zeiss Axioskop light microscope (Carl Zeiss, Toronto, ON) using Nomarski optics. Images were captured and saved in Northern Eclipse 6.0 (Empix Imaging Inc., Mississauga, ON).

Embryos for sectioning were infiltrated with multiple washes of catalyzed JB-4™ Solution A (Polysciences Inc., Warrington, PA)(one of the infiltration washes was overnight at 4˚C). Embryos were then placed in flat bottomed BEEM® capsules, the

infiltration solution was replaced with a 1:25 mixture of JB-4 Solution B: Solution A, and the capsules capped. The blocks were left for a few hours at room temperature to polymerize. The capsules were cut open and exposed to air overnight prior to sectioning into 3-5 μm sections with a microtome. The sections were heat fixed to a glass slide, and observations were made as for whole-mounts.

2.12. Whole-mount *In situ* Hybridization – Double Staining

2.12.a. Cmlc2 DNP-labelled probe

A dinitrophenol (DNP)–labelled probe was created to aid in orientation of staining by the DIG-labelled connexin heart cDNA probe. Plasmid containing about a 1 kb cDNA fragment of the 3' end of the cardiac myosin light chain 2 gene (cmlc2), in the pGEM-T vector (Promega) was obtained from Dr. D. Stainier (University of California San Franscisco) (Yelon *et al.*, 1999). The plasmid, spotted on filter paper, was eluted by heating the filter in 100 μl of TE buffer for 5 to10 minutes at 65°C. The plasmid was transformed into SoloPack® Gold Competent cells (Strategene) as in section 2.6. Various amounts of the transformation were plated onto 100 μg/ml Amp-LB plates, and incubated at 37°C overnight. Individual colonies were grown overnight in LB culture supplemented with 100 mg/ml Amp. Plasmid DNA was isolated using the QIAprep spin miniprep kit (Qiagen), and the concentration of plasmid obtained was determined spectrophotometrically. To verify the presence of an insert, 1 μg of plasmid was linearized with 15 units of NotI (Invitrogen), and 1x React 3 buffer (50 mM Tris-HCl pH 8.0, 10 mM $MgCl_2$, 100 mM NaCl) (Invitrogen), and run on a 1% TBE agarose gel. The

digested transcript was then phenol-chloroform extracted, precipitated, and dissolved in 11 µl of water.

A DIG-labeled cmlc2 antisense RNA probe was created in the same fashion as described in section 2.10.b. using 1 µg of the NotI linearized cmlc2 template, and T7 RNA polymerase (GibcoBRL). A DNP-labeled cmlc2 antisense RNA probe was created by essentially following the protocol set by Long and Rebagliati (2002). A transcription reaction was set up by combining the following reagents in a 20 µl volume: 1 µg of purified linearized template, 1 mM of each NTP, 1x T7 transcription buffer (GibcoBRL), 10 mM DTT (Invitrogen), 40 units RNaseOUT (Invitrogen), and 40 units of T7 RNA polymerase (GibcoBRL). The transcription reaction was incubated at 37°C for 2 hours. To remove the DNA template, 1 µl of RQ1 RNase free DNase (Promega) was added and the mixture incubated at 37°C for 15 minutes. The transcription products were purified by running the reaction through a G50 RNA Quick spin column (Boehringer Mannheim). A 2 µl sample of the purified product was run on a 1% formaldehyde gel to estimate recovery. The remaining reaction (about 50 µl) was precipitated overnight at -80°C with the addition of 100 µl of 100% ice-cold ethanol, 2 µl of 0.2 mM EDTA, and 2.5 µl of 4 M LiCl. The RNA was pelleted, washed in 75% ethanol, and DEPC water was added to result in a dilution to approximately 0.2 µg/µl.

In a 20 µl volume, 2 µg of the transcript was combined with 1x labeling buffer A (MIRUS, Madison, WI), and 4 µl of reconstituted *Label*IT reagent (MIRUS), and then incubated for 1 hour at 37°C. This reaction results in DNP tags covalently attaching to nonbasepairing sites on the guanine ring within the probe. Unbound labelling reagent was removed by running the reaction through a G50 spin column provided with the kit.

Prior to adding the product to the column, the volume of the reaction was brought to 50 µl with 30 µl of 1x labeling buffer A. The DNP-labelled transcript was precipitated, washed, and dried. The probe was diluted to approximately 0.2 µg/µl with DEPC treated water, and stored at -80°C.

2.12.b. WM-ISH double staining

Initial tests with either the DIG- or DNP-labeled cmlc2 probes were performed on various staged embryos (as in sections 2.10.c-e.) to determine the location and strength of staining with each probe. Two-color WM-ISH was performed with the DIG-labelled connexin probe, and the DNP-labelled cmlc2 probe, essentially as outlined by Long and Rebagliati (2002). The embryos were prepared and probes hybridized as described previously (section 2.10.c. and 2.10.d.), except both probes were added to the overnight hybridization. As well, unbound probe was removed by washing embryos briefly in 100% HYB^-, and then at 60°C in each of the following solutions: **1)** 2 washes of 30 minutes each in 50% formamide/2xSSC/0.3% (3-[(3-Cholamidopropyl)-dimethylammonio]-1 propanesulfonate) (CHAPS) (Sigma), **2)** 2 washes of 15 minutes each in 2xSSC/0.3%CHAPS, and **3)** 2 washes of 30 minutes each in 0.2x SSC/0.3% CHAPS, and a final wash in PBS-T at room temperature for 15 minutes. After the DIG color reaction, embryos were fixed overnight in 4% PFA and then washed in the following solutions: **1)** 2 washes of 20 minutes each at room temperature in MAB-T, **2)** 10 minutes at 70°C in MAB-T and 10 mM EDTA. The embryos were dehydrated in 100% methanol for 10 minutes at room temperature, and then rehydrated with a graded methanol/MAB-T series. This was followed by 4 washes of 10 minutes each at room temperature in MAB-T. The embryos were blocked in 10% heat inactivated goat serum,

and 1% blocking reagent (Boehringer Mannheim) in MAB-T for 1-4 hours at room temperature. Embryos were incubated in preadsorbed anti-DNP antibodies (1:1,000) overnight at 4°C. Antibody was removed with multiple washes of MAB-T. To prepare for the DNP color reaction, the embryos were rinsed 3 times in NTM buffer for 5 minutes each, and then stained in NTM buffer with the addition of 3.5 µl/ml BCIP (Boehringer Mannheim) and 0.2 mg/ml p-Iodonitrotetrazolium (INT) violet (Sigma). Embryos were prepared for whole-mount observation as described previously (section 2.10.e.).

CHAPTER 3. RESULTS

3.1. Cloning

A genomic clone coding for the zebrafish orthologue to mammalian connexin40 was obtained by taking advantage of the high degree of sequence similarity between the connexins. PCR was performed using primers, designed with the help of a zebrafish codon usage table, and based on conserved regions of connexin nucleotide sequence obtained from GenBank. Hotstart PCR, with a low stringency annealing temperature of 52°C, resulted in amplification of an approximately 650 bp fragment from zebrafish genomic DNA. This product was cloned, and 634 bp of sequence was obtained using vector primers (Figure 4) (see Figure 3 for a representation of the location of this and other clones, and amplicons, with respect to the coding region of the cloned connexin). A BLASTN search of the non-redundant division of GenBank, using the 634 bp fragment as the query sequence, determined the clone shows the highest sequence similarity to the connexin40 orthologues (the α5 group), and to a lesser extent the connexin46 orthologues (the α3 group). This clone was used to probe a zebrafish PAC library at high stringency. A total of 8 strong and 40 very weak clone signals were observed on the radiographs. The PAC clones corresponding to the seven strongest signals were ordered and screened once by streaking approximately 20 individual colonies of each clone onto a nitrocellulose filter, and probing the filter with the PCR probe. Because the clones sent from DHGB are prepared as stabs picked directly from the microtitre plate containing the requested clone, there is a possibility that the stab could contain mixed colonies. Screening of the ordered clones in the above manner confirms their identity prior to subcloning. Two positive clones from the screen were randomly chosen, and

Figure 3. Clones and Amplicons of ZfCx45.6.

The coding region of zfCx45.6 is 1203 bp. This figure depicts the relative location and size of all clones and amplicons of zfCx45.6. The gray and black bars represent the clone or amplicon position in relation to the coding region or UTRs of zfCx45.6 (grey = in the coding region, black = in the 5' or 3' UTR). On either side of the bars, the primers used to create the clone or amplicon are noted. The numbers above the gray bars represent the approximate location of the primers with negative numbers (-) representing the distance into the 5' UTR. For example, the RT-PCR amplicon extends from within the coding region (520 bp), into the 3' UTR (92 bp) with an approximate size of 775 bp.

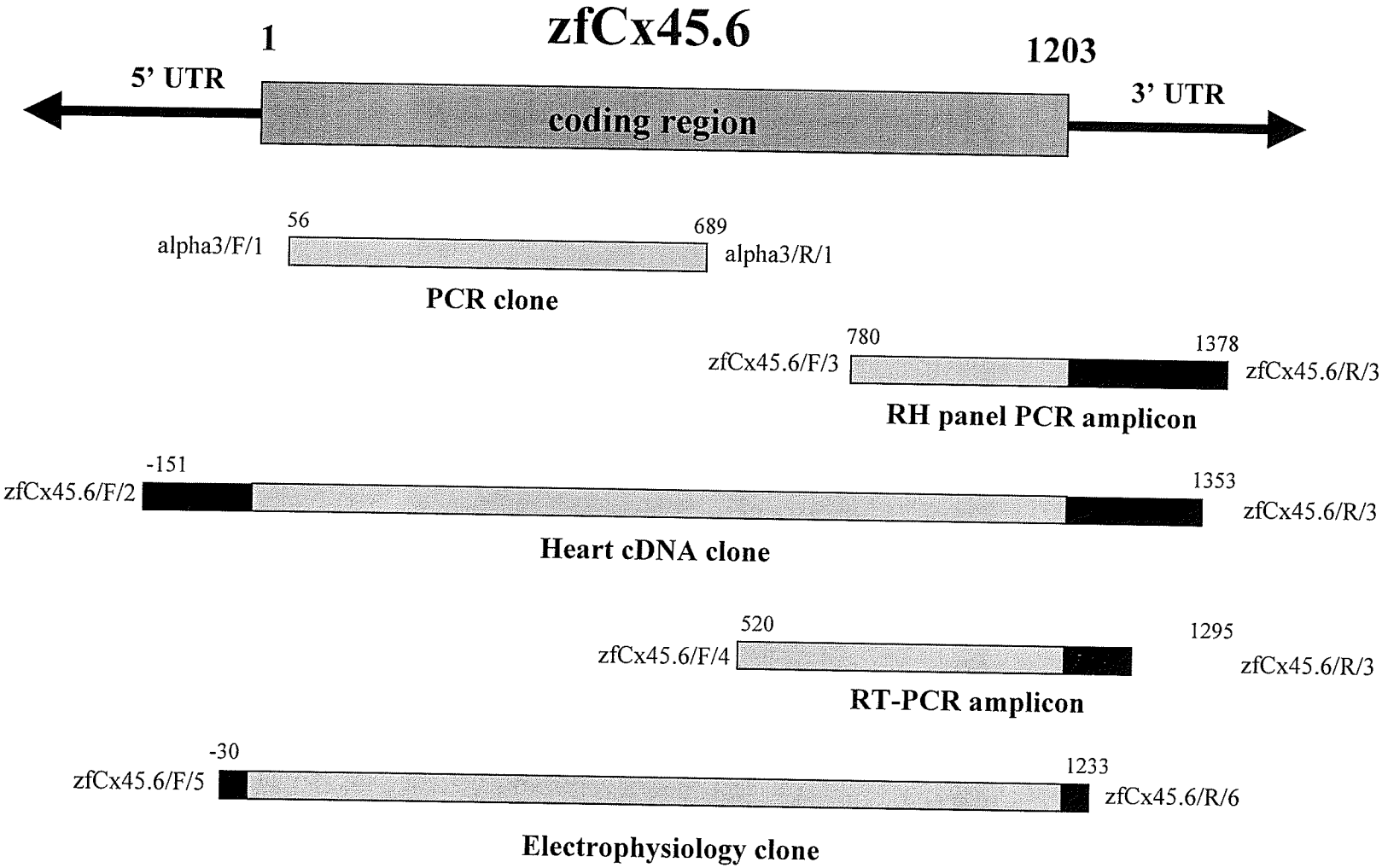
zfCx45.6
1
1203
5' UTR
coding region
3' UTR
56
689
alpha3/F/1
alpha3/R/1
PCR clone
780
1378
zfCx45.6/F/3
zfCx45.6/R/3
RH panel PCR amplicon
-151
1353
zfCx45.6/F/2
zfCx45.6/R/3
Heart cDNA clone
520
1295
zfCx45.6/F/4
zfCx45.6/R/3
RT-PCR amplicon
-30
1233
zfCx45.6/F/5
zfCx45.6/R/6
Electrophysiology clone

Figure 4. ZfCx45.6 Nucleotide Sequence.

A total of 1560 bp of nucleotide sequence was obtained from genomic PCR (bold underline) and PAC clones of zfCx45.6 (no underline, underline and bold underline). The start (ATG) and stop (TAG) codons (bold) encompassed an open reading frame of 1203 bp. Additional 161 bp of upstream sequence and 195 bp of downstream sequence were also obtained (no underline).

TTTGTCTTAGGACAACTTTGAAGTAATTTTTTGATCCCCTTCAAACGCTGA
CTACTGTATATCTTACTCAAAAGTACATTAATGTTATTGTTGTTTTTGTTCT
TCTTGTTGTTCCTCAGCAGTGTAGGTGAGGAGTA**ATG**GGGGACTGGAGTC
TCTTGGGTAATTTCCTCGAAGAAGTGCAGGAGCACTCTACGTCGGTTGGG
AAGGTGTGGTTAACCGTGCTGTTCATCTTCCGTATCCTGGTGTTAGGCACA
GCGGCAGAGTCATCATGGGGCGACGAGCAGTCCGACTTTATGTGTGATAC
TCTACAACCTGGTTGCACCAATGTCTGTTATGACCGAGCTTTCCCCATTGC
TCATATCCGCTACTGGGTGCTGCAGATCGTCTTCGTATCGACACCCTCCCT
CATCTACATGGGCCATGCCATGCACACCGTCCGCATGGAGGAGAAGAGA
AAACAAAAGGAGCAGGAGGAGAAGGCAGAGGCGGGAAAAGGAGAGAAG
GAGTATCTGGAACATAAAGAGAAATTCGAAAATACAAAGACAAAAATCC
ACCTGAAGGGGGCGCTGCTGCAGACATATGTTCTGAGCATTGTGATCCGC
CTGGTCATGGAAGTGACCTTCATTGTGATTCAGTACATGATGTACGGGAT
CTTCCTGGATGCTCTGTATCCATGTTCAATGCTTCCCTGCCCCAACCCTGT
GAACTGTTACATGTCCCGTCCAACTGAGAAAAATGTCTTTATTGTGTTCAT
GCTGGTGGTTGCAGCTGTTTCGCTCCTCCTCAGCGTCATAGAGTTATATCA
CCTTGGATGGAAACAGTGCAAAAAATGCCTTAGGAAACATGCTGACAAGC
ACGCCAATGACAAAATTCAAAACGTCAAAGCTGTTTCTGCAATTGAACCG
ATCAGGACAAGCATTCCAATGGATCTGCCTGAGAACAACCAGCCTCGTCT
CTCTCAAACCTGCACTCCACCTCCAGATTTCAACCAGTGCTTAAGATCAA
ACCAAGGTCCAACATCTCCTCCACATCTTCATTCTCACCATCTTCATCACA
TCCACCAAACCTGCCAGCCCTTCACCAACCATCTGGCACACCAGCAGAAC
TCCGTCAACATGGCCGCCGAGCGGCATCACCACAGCCATGATGGCCTGGA
GCCAGCCGTGGACTTCCTGCAGATGCATTATGGGAGTCCTGAGGCTCGGG
TTCGAAGTGAAATGACACCCAGTACCCCTTCCACACCATCCTCCCATCCAG
GGTTCTTCAGAGACAAGCGCAGGCTTAGCAAGACCAGTGGTACTAGTAGT
AACCGACTCAGACCAAGTGATCTGGCCGTG**TAG**ATCGTGAAAGTGGCAG
TTTCTGAGGAAAAGAAGCTGGAAGCCTTAAGATGAGAGATGTGAGTGTGT
GTGTGTGTGTGTGTTTGAATATGCTTGTTTGTTGGTACTATGAAATGGGAT
TTGGAATGAGAAAGGACTAAATACCACCATAAAACCAAGGCTAATTAGA
ATAAGATGGGAAGAATCTGTATCAGAGC

plasmids isolated by two different methods. Both plasmids were subcloned into more manageable portions, containing the full coding region of the connexin within a 12 kb HindIII restriction fragment. The first subclone was sequenced over the entire coding region, each region at least twice, and some regions multiple times. The second subclone was sequenced only once over the last three quarters of the coding region, as the sequence obtained confirmed that of the first subclone. Sequencing of the subclones was first performed with primers based on the PCR clone sequence, and then with primers based on PAC subclone sequence. A total of 1560 bp of sequence, including a predicted open reading frame of 1203 bp within one exon, was obtained from the PAC subclones (Figure 4). An additional 161 bp of sequence upstream from the start codon (ATG), and 195 bp of sequence downstream from the stop codon (TAG) was also obtained. A BLASTN search of the non-redundant division of GenBank, using the 1203 bp coding region of the connexin as the query sequence, confirmed the cloned connexin possesses the highest degree of sequence similarity to connexin40 orthologues.

The coding region of the cloned connexin translates into 400 amino acids with an estimated molecular weight of 45.6 kiloDaltons. In accordance with the standard naming system (Beyer *et al.*, 1987) the cloned connexin was named zebrafish connexin45.6 (zfCx45.6). ZfCx45.6 demonstrates typical connexin membrane topography with four transmembrane regions, and internal NH_2- and COOH- termini as depicted by a hydrophobicity plot of the amino acids (Figure 5). The high degree of similarity between zfCx45.6 and the connexin40 orthologues is highlighted by an alignment of their amino acid sequences (Figure 6). In this alignment, zfCx45.6 is shown to possess the three conserved cysteines present in the extracellular loops of all connexins. The highest

Figure 5. Hydrophobicity Plot of ZfCx45.6.

The hydrophobicity of the amino acid sequence of zfCx45.6 was plotted using the TMPRED program (Hofmann and Stoffel, 1993) to predict the membrane topology of the connexin. Amino acids plotted above zero indicated hydrophobic regions of the protein, while amino acids plotted below zero indicated hydrophilic regions of the protein. ZfCx45.6 demonstrates typical connexin membrane topology with four hydrophobic transmembrane regions (TM1, TM2, TM3, TM4), and internal hydrophilic NH_2- and COOH- termini (NH_2-, C-tail), resulting in two extracellular loops (E1, E2), and an internal cytoplasmic loop (IC).

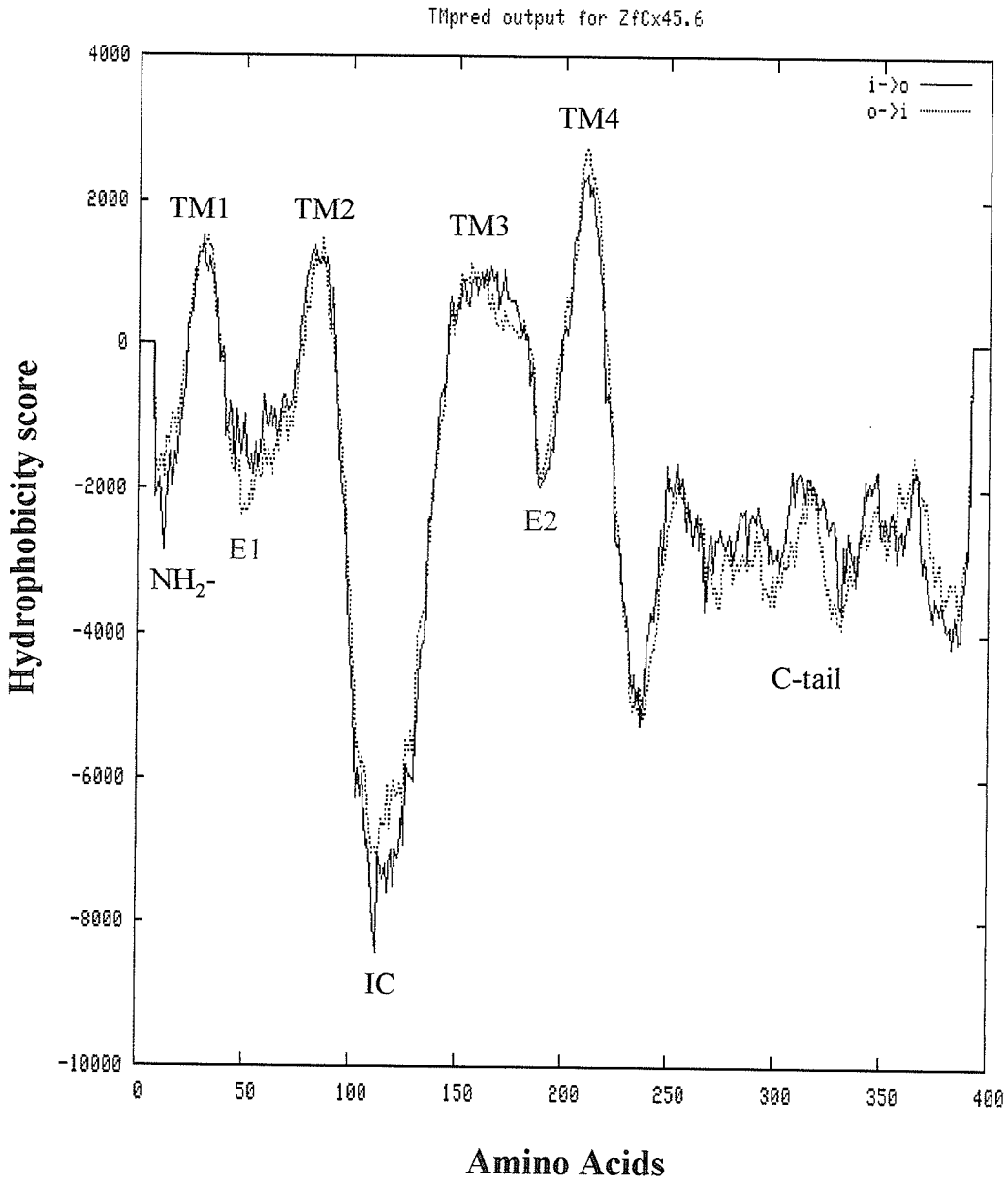
TMpred output for ZfCx45.6
i->o
o->i
TM1
TM2
TM3
TM4
E1
E2
IC
C-tail
NH2-
Hydrophobicity score
Amino Acids
4000
2000
0
-2000
-4000
-6000
-8000
-10000
0
50
100
150
200
250
300
350
400

Figure 6. Amino Acid Alignment of ZfCx45.6 and the Connexin40 Orthologoues.

A BLASTN search of the non-redundant division of GenBank, using the 1203 bp coding region of the connexin as the query sequence, confirmed zfCx45.6 possessed the highest degree of similarity to the connexin40 orthologues. This similarity is demonstrated by an alignment of the amino acid sequences of this group, whereby stars (*) denote identical amino acids, and semicolons (:) denote similar amino acids. Spaces represented by dashed lines have been added to optimize alignment. The shaded regions highlight the four predicted transmembrane regions, and the black circles highlight the three conserved cysteines in the extracellular loops. The highest divergence in similarity between the members of the group occurs in the cytoplasmic tail, where zfCx45.6 also possess extra sequence. Possible conserved regulatory phosphorylation sites are highlighted by open circles (o).

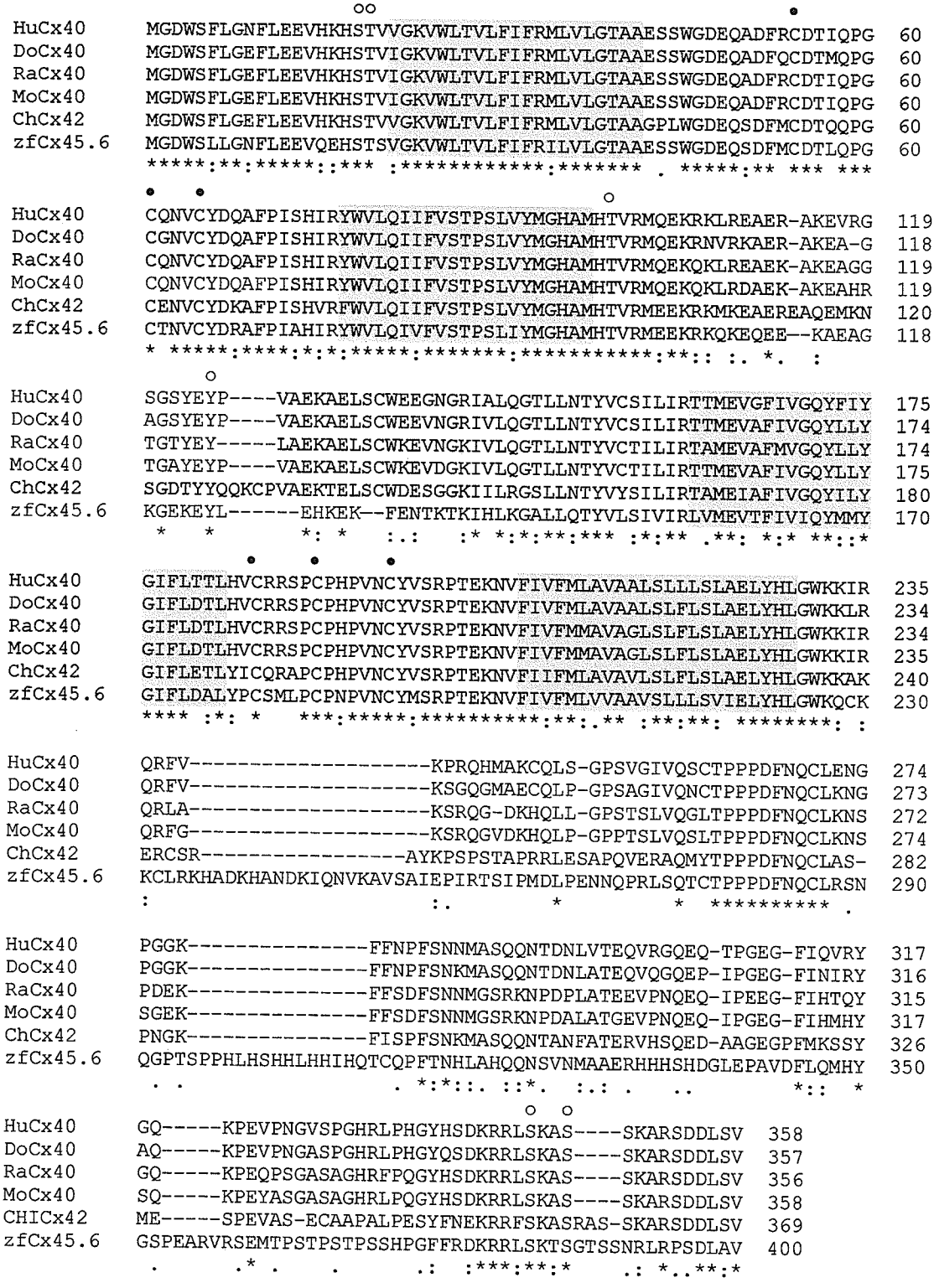
HuCx40 MGDWSFLGNFLEEVHKHSTVVGKVWLTVLFIFRMLVLGTAAESSWGDEQADFRCDTIQPG 60
DoCx40 MGDWSFLGEFLEEVHKHSTVIGKVWLTVLFIFRMLVLGTAAESSWGDEQADFQCDTMQPG 60
RaCx40 MGDWSFLGEFLEEVHKHSTVIGKVWLTVLFIFRMLVLGTAAESSWGDEQADFRCDTIQPG 60
MoCx40 MGDWSFLGEFLEEVHKHSTVIGKVWLTVLFIFRMLVLGTAAESSWGDEQADFRCDTIQPG 60
ChCx42 MGDWSFLGEFLEEVHKHSTVVGKVWLTVLFIFRMLVLGTAAGPLWGDEQSDFMCDTQQPG 60
zfCx45.6 MGDWSLLGNFLEEVQEHSTSVGKVWLTVLFIFRILVLGTAAESSWGDEQSDFMCDTLQPG 60
HuCx40 CQNVCYDQAFPISHIRYWVLQIIFVSTPSLVYMGHAMHTVRMQEKRKLREAER-AKEVRG 119
DoCx40 CGNVCYDQAFPISHIRYWVLQIIFVSTPSLVYMGHAMHTVRMQEKRNVRKAER-AKEA-G 118
RaCx40 CQNVCYDQAFPISHIRYWVLQIIFVSTPSLVYMGHAMHTVRMQEKQKLREAEK-AKEAGG 119
MoCx40 CQNVCYDQAFPISHIRYWVLQIIFVSTPSLVYMGHAMHTVRMQEKQKLRDAEK-AKEAHR 119
ChCx42 CENVCYDKAFPISHVRFWVLQIIFVSTPSLVYMGHAMHTVRMEEKRKMKEAEREAQEMKN 120
zfCx45.6 CTNVCYDRAFPIAHIRYWVLQIVFVSTPSLIYMGHAMHTVRMEEKRKQKEQEE--KAEAG 118
HuCx40 SGSYEYP----VAEKAELSCWEEGNGRIALQGTLLNTYVCSILIRTTMEVGFIVGQYFIY 175
DoCx40 AGSYEYP----VAEKAELSCWEEVNGRIVLQGTLLNTYVCSILIRTTMEVAFIVGQYLLY 174
RaCx40 TGTYEY-----LAEKAELSCWKEVNGKIVLQGTLLNTYVCTILIRTAMEVAFMVGQYLLY 174
MoCx40 TGAYEYP----VAEKAELSCWKEVDGKIVLQGTLLNTYVCTILIRTTMEVAFIVGQYLLY 175
ChCx42 SGDTYYQQKCPVAEKTELSCWDESGGKIILRGSLLNTYVYSILIRTAMEIAFIVGQYILY 180
zfCx45.6 KGEKEYL------EHKEK--FENTKTKIHLKGALLQTYVLSIVIRLVMEVTFIVIQYMMY 170
HuCx40 GIFLTTLHVCRRSPCPHPVNCYVSRPTEKNVFIVFMLAVAALSLLLSLAELYHLGWKKIR 235
DoCx40 GIFLDTLHVCRRSPCPHPVNCYVSRPTEKNVFIVFMLAVAALSLFLSLAELYHLGWKKLR 234
RaCx40 GIFLDTLHVCRRSPCPHPVNCYVSRPTEKNVFIVFMMAVAGLSLFLSLAELYHLGWKKIR 234
MoCx40 GIFLDTLHVCRRSPCPHPVNCYVSRPTEKNVFIVFMMAVAGLSLFLSLAELYHLGWKKIR 235
ChCx42 GIFLETLYICQRAPCPHPVNCYVSRPTEKNVFIIFMLAVAVLSLFLSLAELYHLGWKKAK 240
zfCx45.6 GIFLDALYPCSMLPCPNPVNCYMSRPTEKNVFIVFMLVVAAVSLLLSVIELYHLGWKQCK 230
HuCx40 QRFV--------------------KPRQHMAKCQLS-GPSVGIVQSCTPPPDFNQCLENG 274
DoCx40 QRFV--------------------KSGQGMAECQLP-GPSAGIVQNCTPPPDFNQCLKNG 273
RaCx40 QRLA--------------------KSRQG-DKHQLL-GPSTSLVQGLTPPPDFNQCLKNS 272
MoCx40 QRFG--------------------KSRQGVDKHQLP-GPPTSLVQSLTPPPDFNQCLKNS 274
ChCx42 ERCSR-----------------AYKPSPSTAPRRLESAPQVERAQMYTPPPDFNQCLAS- 282
zfCx45.6 KCLRKHADKHANDKIQNVKAVSAIEPIRTSIPMDLPENNQPRLSQTCTPPPDFNQCLRSN 290
HuCx40 PGGK---------------FFNPFSNNMASQQNTDNLVTEQVRGQEQ-TPGEG-FIQVRY 317
DoCx40 PGGK---------------FFNPFSNKMASQQNTDNLATEQVQGQEP-IPGEG-FINIRY 316
RaCx40 PDEK---------------FFSDFSNNMGSRKNPDPLATEEVPNQEQ-IPEEG-FIHTQY 315
MoCx40 SGEK---------------FFSDFSNNMGSRKNPDALATGEVPNQEQ-IPGEG-FIHMHY 317
ChCx42 PNGK---------------FISPFSNKMASQQNTANFATERVHSQED-AAGEGPFMKSSY 326
zfCx45.6 QGPTSPPHLHSHHLHHIHQTCQPFTNHLAHQQNSVNMAAERHHHSHDGLEPAVDFLQMHY 350
HuCx40 GQ-----KPEVPNGVSPGHRLPHGYHSDKRRLSKAS----SKARSDDLSV 358
DoCx40 AQ-----KPEVPNGASPGHRLPHGYQSDKRRLSKAS----SKARSDDLSV 357
RaCx40 GQ-----KPEQPSGASAGHRFPQGYHSDKRRLSKAS----SKARSDDLSV 356
MoCx40 SQ-----KPEYASGASAGHRLPQGYHSDKRRLSKAS----SKARSDDLSV 358
CHICx42 ME-----SPEVAS-ECAAPALPESYFNEKRRFSKASRAS-SKARSDDLSV 369
zfCx45.6 GSPEARVRSEMTPSTPSTPSSHPGFFRDKRRLSKTSGTSSNRLRPSDLAV 400

divergence in sequence between zfCx45.6 and the connexin40 orthologues occurres in the C-tail. ZfCx45.6 also possesses extra sequence in this region, thus resulting in a higher predicted molecular weight than the mammalian connexin40 orthologues. ZfCx45.6 possesses the highest amino acid similarity to chick Cx42 with 53% identity, and 63% similarity. This is followed by human Cx40 (52%/63%), dog Cx40 (51%/62%), rat Cx40 (50%/62%), and mouse Cx40 (49%/62%). This similarity is graphically depicted in Figure 7, which represents the structural relationships between connexins expressed in the cardiovascular system. ZfCx45.6 clearly groups with the mammalian connexin40 orthologues.

Possible zfCx45.6 regulatory serine (Ser), threonine (Thr), and tyrosine (Tyr) phosphorylation sites were predicted using NetPhos2.0 (www.cbs.dtu.dk/services /NetPhos/). In total, 19 Ser, 5 Thr, and 1 Tyr phosphorylation sites were predicted. The majority of the predicted sites were within the cytoplasmic regions, with only 6 of these sites being conserved across the connexin40 orthologues (Ser18, Ser383, Ser386, Thr19, Thr99, Tyr124) (Figure 6). All conserved sites had high "phosphorylation potential" scores of 0.82 and above, except for Thr19, which had a low score of 0.56 suggesting it may not be a potential phosphorylation site. These predicted sites are located in all of the cytoplasmic regions of the zfCx45.6 (N terminus, cytoplasmic loop, and C-tail).

3.2. Functional Analysis

The basic biophysical properties of zfCx45.6 channels were determined in studies performed by Dr. T. White using the paired *Xenopus* oocyte system. In all studies, oocyte pairs were injected with an oligonucleotide antisense to *Xenopus* Cx38 to minimize any

Figure 7. Phylogenetic Tree of Connexins Expressed in the Cardiovascular System.

Phylogenetic analysis was performed with CLUSTALX (1.4) (Thompson *et al.*, 1997) and TreeView (1.5) (Page, 1996). The phylogram graphically represents the structural relationships between connexins expressed in the cardiovascular system, whereby the linear distance between sequences is inversely proportional to the level of amino acid similarity. The distance indicated by the scale bar represents 0.1 amino acid substitutions per site. ZfCx45.6 clearly groups with the connexin40 orthologues.

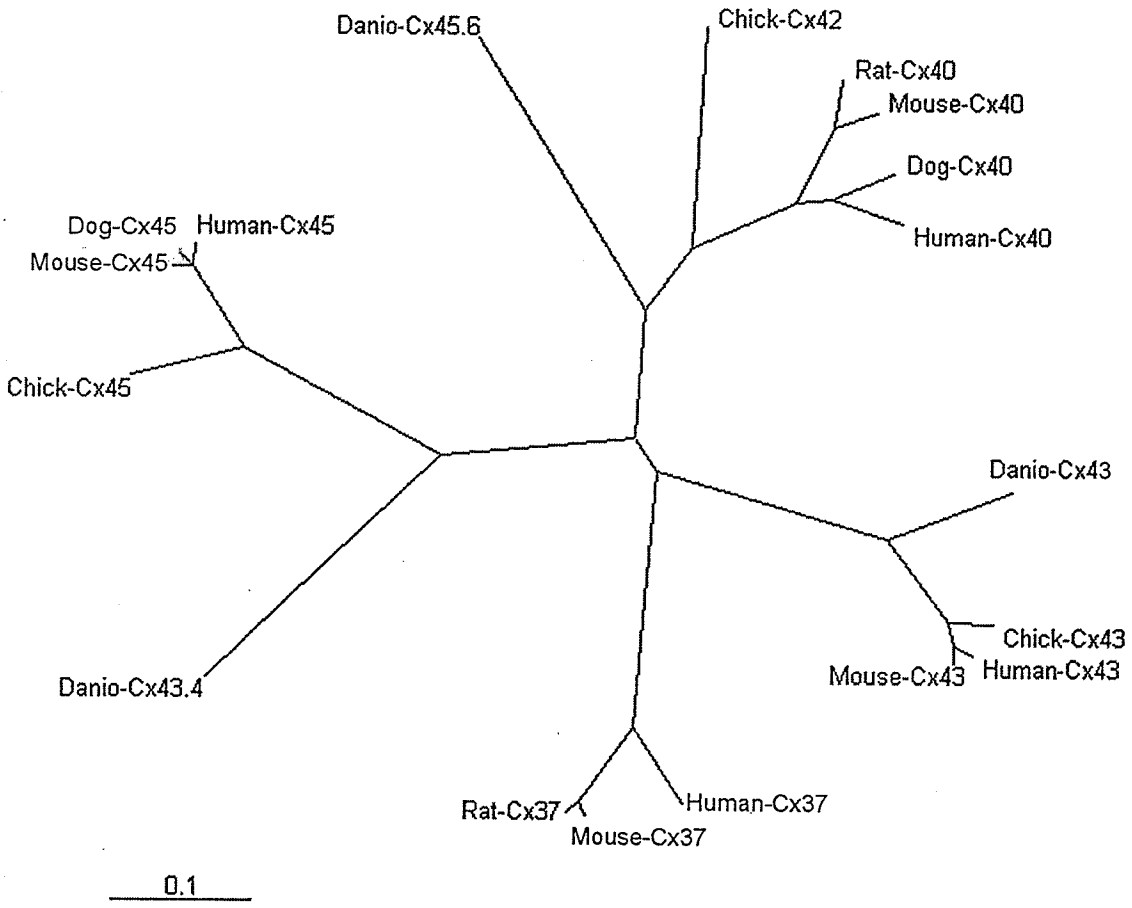
Danio-Cx45.6
Chick-Cx42
Rat-Cx40
Mouse-Cx40
Dog-Cx40
Human-Cx40
Dog-Cx45
Human-Cx45
Mouse-Cx45
Chick-Cx45
Danio-Cx43
Chick-Cx43
Mouse-Cx43
Human-Cx43
Danio-Cx43.4
Rat-Cx37
Human-Cx37
Mouse-Cx37
0.1

contributions of this endogenous connexin to recorded conductance values (Bruzzone *et al.*, 1993).

In the first set of experiments, two *Xenopus* oocytes were injected with zfCx45.6 mRNA, paired, and clamped at a set voltage to ensure the transjunctional voltage (Vj) was zero. A voltage step was applied to one oocyte, and the resulting macroscopic junctional current passing from the first to the second oocyte was recorded, and the junctional conductance (Gj) was plotted (Gj = junctional current / Vj). For zfCx45.6, the cells were found to be electrically coupled with a mean Gj = 33.57 +/- 11.95 μS (n=30), while control oocytes injected with water were not electrically coupled (Gj = 0.12 +/- 0.13 μS, n=24) (Figure 8.A.). Thus, zfCx45.6 forms functional gap junction channels.

In a second set of experiments, hyperpolarizing or depolarizing transjunctional voltage (Vj) steps of +/- 20 mV were applied to one oocyte, while the second oocyte was clamped at a set voltage. The resulting junctional current (Ij) between both oocytes was recorded. The junctional current was found to rapidly decay over time to a steady state within 0.5 seconds, in a symmetrical and exponential manner (Figure 8.B.). Thus, zfCx45.6 channels are voltage sensitive.

3.3. Mapping

To determine the chromosomal location of zfCx45.6, PCR was performed using the LN54 RH panel. As this panel consists of genomic DNA from fused mouse and zebrafish cells, and orthologous connexins possess a high degree of sequence similarity, initial tests were run to determine optimal PCR conditions that would amplify a region of zfCx45.6 from zebrafish DNA, but not Cx40 from mouse DNA. It was determined that

Figure 8. Functional Analysis of ZfCx45.6

The basic biophysical properties of zfCx45.6 channels were determined using the paired *Xenopus* oocyte system. **A.** ZfCx45.6 forms functional channels with a junctional conductance (Gj) = 33.57 +/- 11.95 μS (n=30) (control Gj = 0.12 +/- 0.13 μS, n=24). **B.** ZfCx45.6 forms voltage-dependant channels that close upon hyperpolarizing or depolarizing voltage steps. This is illustarted by the rapidly decaying junctional current (Ij) within 0.5 seconds.

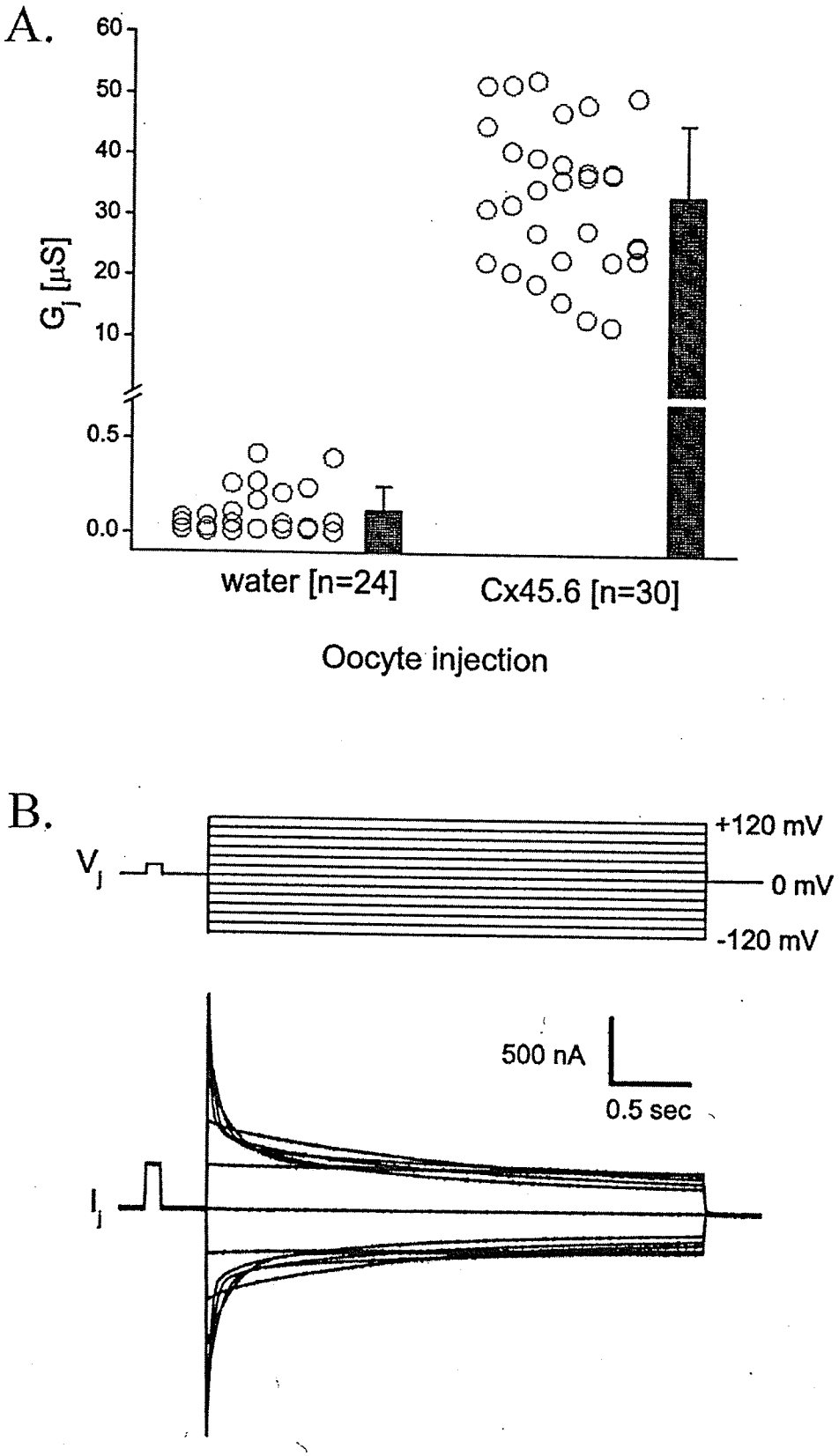
A.
60
50
40
30
20
10
0.5
0.0
G_j [µS]
water [n=24]
Cx45.6 [n=30]
Oocyte injection
B.
V_j
+120 mV
0 mV
-120 mV
500 nA
0.5 sec
I_j

PCR using either primer set tested, and a high annealing temperature of 65°C, amplified a band of expected size from zebrafish, but not mouse DNA. The primer set that amplified a 536 bp nucleotide sequence, encoding the region comprising parts of the C-terminus and the 3' UTR (zfCx45.6/F/3, zfCx45.6/R/3), was randomly chosen to use for PCR screening of the panel. As well, it was determined that a final concentration of 1.5 mM $MgCl_2$ was optimal for the PCR. PCR was performed three times with the panel using the same conditions each time. An aliquot of the PCR from each cell line was run on a gel and scored as positive (containing a portion of zfCx45.6), negative, or ambiguous. A cell line was scored positive if a strong band was observed in at least two of the three PCRs, and negative if a very faint band, or no band at all was observed. A cell line was scored as ambiguous if a strong band was observed only once out of the three runs. Compilation of the results revealed that 20 cells lines were positively amplified, only one cell line scored ambiguous, and PCR with seven cell lines resulted in faint bands, but were counted as negative in compliance with the above scoring criteria. The results were entered into the LN54 web page, and the program statistically determined that the best overall marker linked to zfCx45.6 was found on linkage group (LG) 9 with a lod score of 6.9 (Figure 9). The program mapped zfCx45.6 zero centirays from fb36h02, a previously mapped marker on LG9. The sequences of zfCx45.6 and this marker did not show any significant similarity. The best marker in the second best LG linked zfCx45.6 to LG15 with a lod score of 4.6.

Figure 9. ZfCx45.6 Maps to Linkage Group 9.

Using the LN54 RH panel, zfCx45.6 was mapped zero centirays from fb36h02, a previously mapped marker on zebrafish LG9 (LOD score 6.9). Sequence of zfCx45.6 and fb36h02 did not significantly line up.

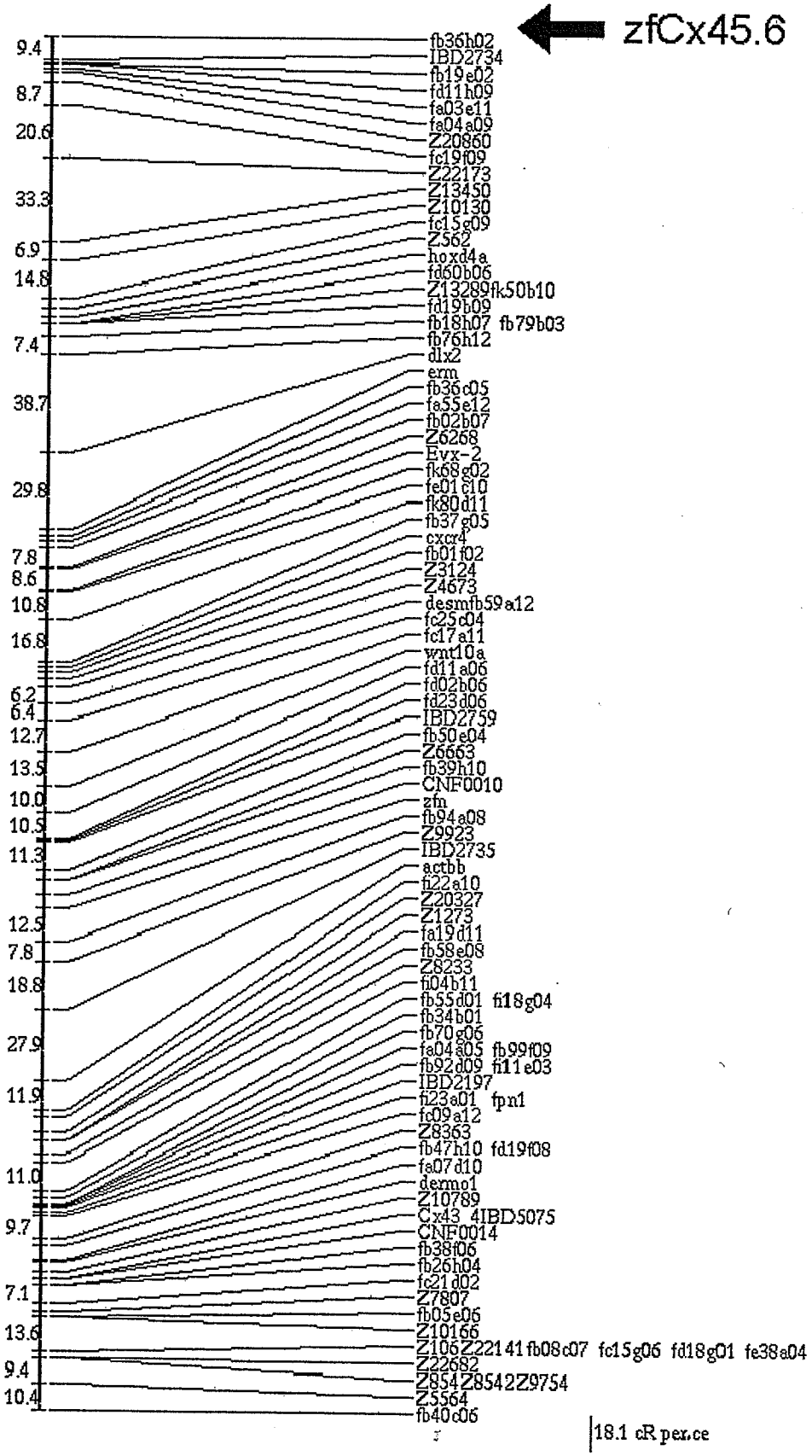
zfCx45.6
9.4
8.7
20.6
33.3
6.9
14.8
7.4
38.7
29.8
7.8
8.6
10.8
16.8
6.2
6.4
12.7
13.5
10.0
10.5
11.3
12.5
7.8
18.8
27.9
11.9
11.0
9.7
7.1
13.6
9.4
10.4
fb36h02
IBD2734
fb19e02
fd11h09
fa03e11
fa04a09
Z20860
fc19f09
Z22173
Z13450
Z10130
fc15g09
Z562
hoxd4a
fd60b06
Z13289fk50b10
fd19b09
fb18h07 fb79b03
fb76h12
dlx2
erm
fb36c05
fa55e12
fb02b07
Z6268
Evx-2
fk68g02
fe01c10
fk80d11
fb37g05
cxcr4
fb01f02
Z3124
Z4673
desmfb59a12
fc25c04
fc17a11
wnt10a
fd11a06
fd02b06
fd23d06
IBD2759
fb50e04
Z6663
fb39h10
CNF0010
zfn
fb94a08
Z9923
IBD2735
actbb
fi22a10
Z20327
Z1273
fa19d11
fb58e08
Z8233
fi04b11
fb55d01 fi18g04
fb34b01
fb70g06
fa04a05 fb99f09
fb92d09 fi11e03
IBD2197
fi23a01 fpn1
fc09a12
Z8363
fb47h10 fd19f08
fa07d10
dermo1
Z10789
Cx43 4IBD5075
CNF0014
fb38f06
fb26h04
fc21d02
Z7807
fb05e06
Z10166
Z106Z22141fb08c07 fc15g06 fd18g01 fe38a04
Z22682
Z8542Z8542Z9754
Z5564
fb40c06
18.1 cR pen.ce

3.4. Northern Analysis

To determine the embryonic and adult expression of zfCx45.6, a Northern blot composed of polyA$^+$ mRNA from 0 to 5 dpf embryos, and adult brain, eye (minus the lens), liver, and ovary was probed with a zfCx45.6 specific RNA probe. After 10 days of exposure, zfCx45.6 was detected on this blot as a 2.38 kb transcript in 1 to 5 dpf embryos, and all of the tissues tested (Figure 10). The signal intensity appeared to increase from 0 to 5 dpf, but the intensity also increased from 0 to 5 dpf in the loading control (zebrafish elongation factor 1 alpha – ZfeF1alpha), thus the increase in zfCx45.6 signal is probably not significant.

3.5. RT-PCR

To confirm the Northern blot results, RT-PCR was performed with cDNA generated from 0 to 5 dpf embryo RNA. In the first trial, zfCx45.6 was detected in 0 to 5 dpf embryo samples. A second trial was performed with cDNA isolated from new embryonic RNA, and zfCx45.6 was detected in 1 to 5 dpf embryo samples, but not from the 0 dpf sample. In both trials, about a 570 bp band was amplified with the zebrafish elongation factor 1 alpha primers from all the samples (i.e. there was no genomic DNA contamination). To confirm the band amplified by the test primers was zfCx45.6, and to obtain a higher sensitivity, the PCR products from the second trial were blotted onto a nylon membrane and probed with a zfCx45.6 specific DNA probe. A faint signal was detected on 0 dpf, and strong signals were detected from 1 to 5 dpf (Figure 11).

As it appeared zfCx45.6 could be detected at some point prior to 24 hpf, RT-PCR was performed with cDNA samples generated from various staged embryos throughout 0

Figure 10. Northern Analysis – PolyA$^+$ Blot.

To determine the expression patterns of zfCx45.6, Northern analysis was performed with a blot composed of polyA$^+$ mRNA isolated from various embryonic stages and adult tissues. ZfCx45.6 was detected as a 2.38 kb transcript in embryos 1 to 5 dpf, and in adult brain, eye (minus lens), liver, and ovary. The loading control (ZfeF1alpha) indicated that polyA$^+$ mRNA was present in all of the lanes tested, but not necessarily in equal amounts.

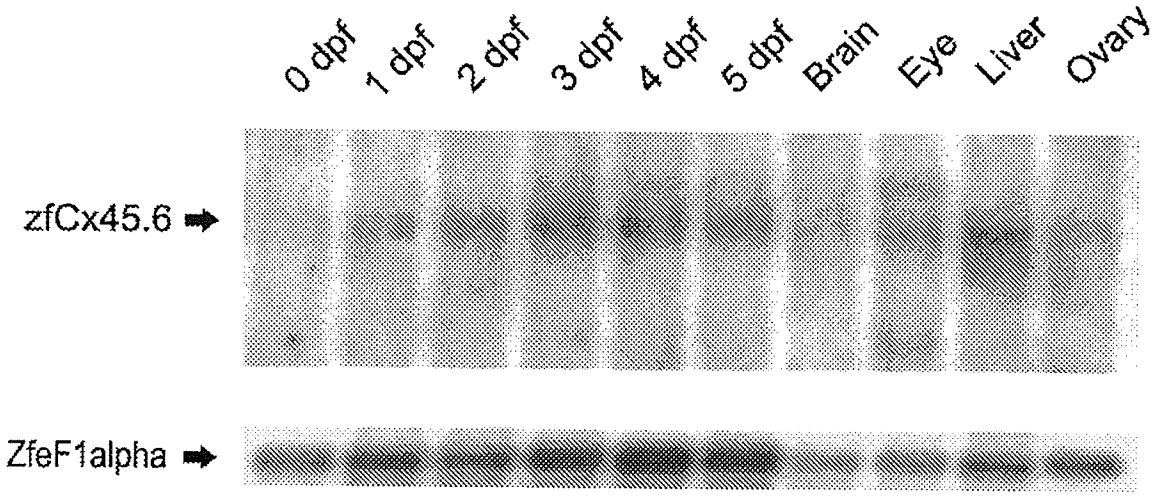
0 dpf
1 dpf
2 dpf
3 dpf
4 dpf
5 dpf
Brain
Eye
Liver
Ovary
zfCx45.6
ZfeF1alpha

Figure 11. RT-PCR – 0 to 5 dpf.

To confirm temporal expression pattern of zfCx45.6, RT-PCR was performed with cDNA generated from 0 to 5 dpf embryos. Products were blotted onto a membrane and probed with a zfCx45.6 specific DNA probe. A faint signal was detected on 0 dpf, and strong signals were detected from 1 to 5 dpf. In all samples tested a 570 bp band was amplified with the ZfeF1alpha primers indicating cDNA was present, and there was no genomic DNA contamination.

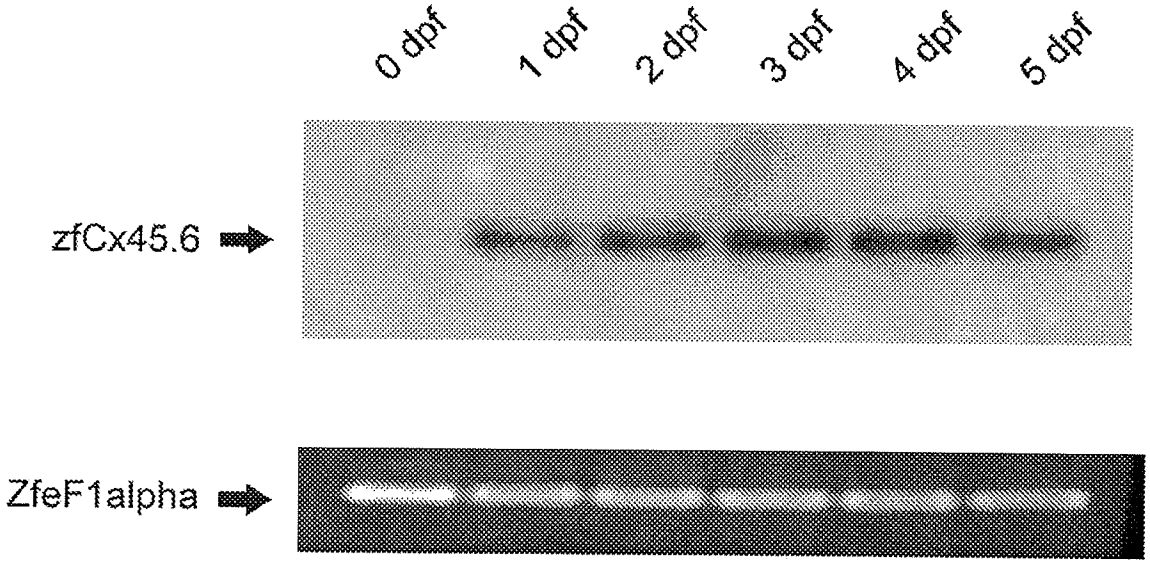
0 dpf
1 dpf
2 dpf
3 dpf
4 dpf
5 dpf
zfCx45.6
ZfeF1alpha

dpf (1.5-2 hpf, 2-2.5 hpf, 3.5-4 hpf, 4-4.5 hpf, 5-5.5 hpf, 8-8.5 hpf, 12-12.5 hpf, 12.5-13 hpf, 15-15.5 hpf, 22-23 hpf). Unlike the previous experiments where embryos were collected randomly throughout a specific day, embryos were collected and staged as accurately as possible according to Kimmel *et al.* (1995). For each stage, RT-PCR was performed at least twice using RNA isolated from different batches of embryos, though not every stage was tested in a single trial. Overall, zfCx45.6 expression was detected prior to 2.5 hpf (i.e. in the 1.5-2 hpf and 2-2.5 hpf stages), and in 12.5-13 hpf and later stages. ZfCx45.6 expression was not detected between 3.5 and 12.5 hpf. PCR was repeated with one sample of cDNA from every stage tested, and the products were run on a gel. In this case, zfCx45.6 expression was only detected in the 1.5-2 hpf samples, and from 12.5 to 23 hpf (i.e. zfCx45.6 was not detected in the 2-2.5 hpf sample). PCR products were blotted onto a nylon membrane and probed with a zfCx45.6 specific DNA probe as before to confirm the identity of the amplified products, and obtain a higher sensitivity (Figure 12). Results of the blot were the same as the gel with strong signals detected in the 1.5-2 hpf sample, and from 12.5 to 23 hpf. Faint bands could also be seen in most of the samples between 2 and 12.5 hpf, though the signals were significantly lower. Control PCR with the zebrafish elongation factor 1 alpha primers resulted in amplification in all but one stage (3.5-4 hpf) where the signal was lower.

RT-PCR was also performed multiple times using cDNA from adult heart, lens, liver, brain, and ovary. ZfCx45.6 expression was always strongly detected in the heart (6 positives/6 trials, where each trial PCR used template cDNA created from new RNA). ZfCx45.6 expression was also detected in the liver (3/3), brain (3/3), and ovary (2/2), but

Figure 12. RT-PCR – 1.5 to 23 hpf.

To more accurately determine when zfCx45.6 is expressed, RT-PCR was performed with cDNA isolated from various staged embryos throughout 0 dpf. Products were blotted onto a membrane and probed with a zfCx45.6 specific DNA probe. Overall, zfCx45.6 was detected before 2 hpf, and after 12.5 hpf. ZfCx45.6 expression was not strongly detected between 2 and 12 hpf. The loading control (ZfeF1alpha) indicated cDNA was present in all samples tested, and there was no genomic DNA contamination.

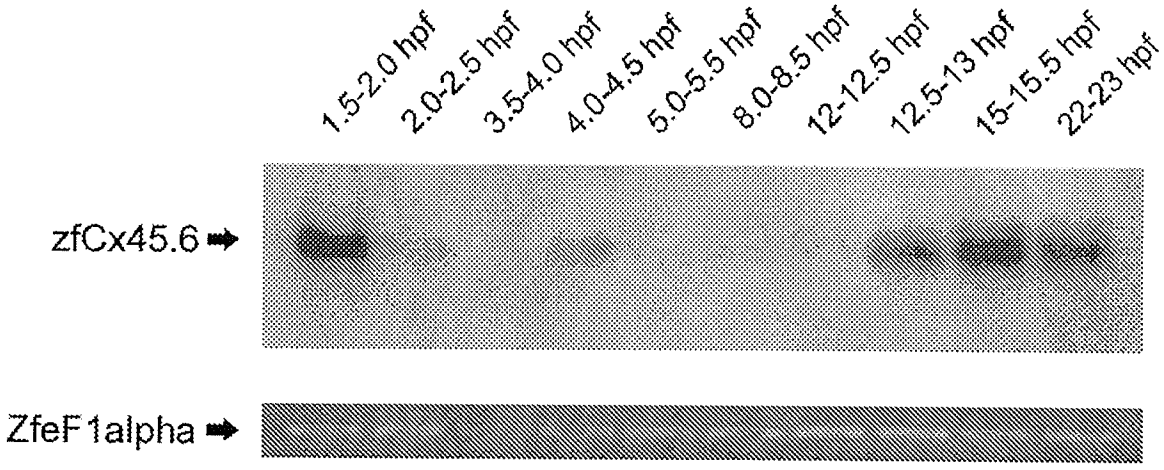
1.5-2.0 hpf
2.0-2.5 hpf
3.5-4.0 hpf
4.0-4.5 hpf
5.0-5.5 hpf
8.0-8.5 hpf
12-12.5 hpf
12.5-13 hpf
15-15.5 hpf
22-23 hpf
zfCx45.6
ZfeF1alpha

not in the lens (6 negatives/6 trials). As with the other trials, PCR products were blotted and probed to increase resolution and confirm the identity of the products (Figure 13).

3.6. Whole-mount ISH

3.6.1. DIG whole-mount ISH

To spatially localize the expression of zfCx45.6, whole-mount ISH was performed multiple times with 0 to 5 dpf embryos. Embryos were probed with sense (S) and antisense (AS) DIG-labeled RNA probes encompassing the entire coding region of zfCx45.6, as well as ~150 bp of upstream and ~150 bp of downstream sequence (about 1500 bp in total). Following hybridization with the DIG-labeled probes, embryos were incubated with an alkaline phosphatase conjugated anti-DIG antibody, which binds to the DIG moiety on the probe. This antibody was chromogenically detected with alkaline phosphatase substrates (BCIP, NBT) that produced a blue precipitate, resulting in specific blue staining patterns corresponding to the location of zfCx45.6 expression.

The color reactions were allowed to proceed for 10 to 24 hours in the younger embryos (0 to 3 dpf) and 15 to 30 hours in the older embryos. Specific expression patterns were not observed in the 0 dpf embryos (Figure 14.A), but the 0 dpf AS-embryos (probed with the zfCx45.6 AS-DIG probe) were generally darker than the S-embryos (probed with the zfCx45.6 S-DIG probe). By 1 dpf, the ventral portion of the tail of the AS-embryos was much darker than the dorsal portion, and specific patterns of zfCx45.6 expression were beginning to emerge. In the majority of cases, a darker band, possibly corresponding to the location of vasculature in the tail, could be detected in a lateral view just below the notochord (Figure 14.B, F). The location of this structure most closely

Figure 13. RT-PCR – Adult Tissues.

To confirm the adult spatial expression pattern of zfCx45.6, RT-PCR was performed with cDNA generated from various adult tissues. Products were blotted onto a membrane and probed with a zfCx45.6 specific DNA probe. ZfCx45.6 expression was detected in the heart, liver, brain, and ovary. ZfCx45.6 expression was not detected in the lens. The loading control (ZfeF1alpha) indicated cDNA was present in all samples tested, and there was no genomic contamination.

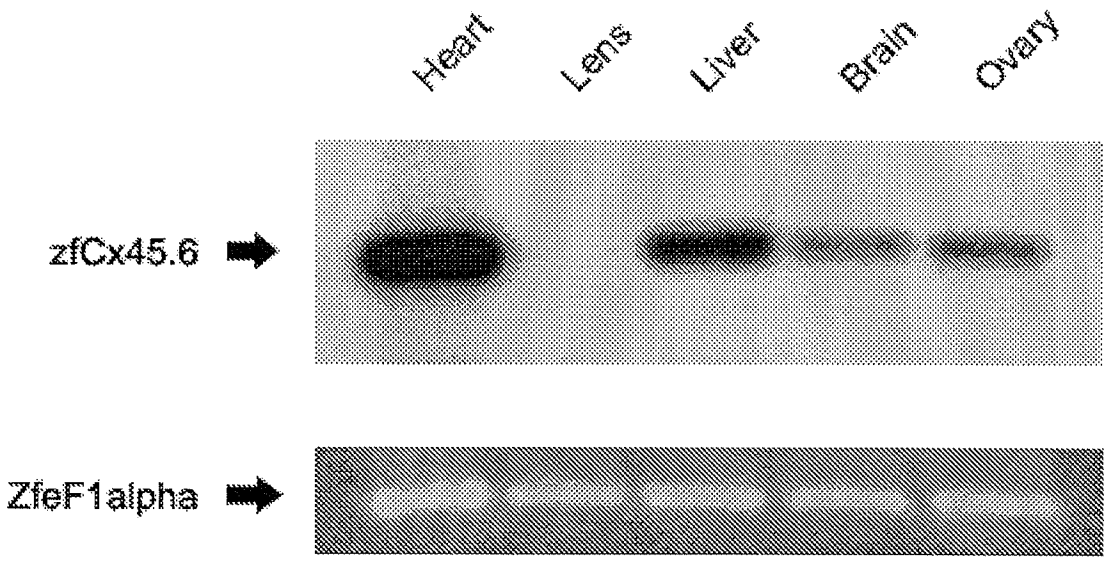
Heart
Lens
Liver
Brain
Ovary
zfCx45.6
ZfeF1alpha

Figure 14. Whole-mount ISH – ZfCx45.6 Expression in the Tail.

To localize the embryonic expression of zfCx45.6, whole-mount ISH was performed with DIG-labelled S- and AS-probes encompassing the entire coding region of zfCx45.6 as well as up and downstream sequence. This figure highlights zfCx45.6 expression in the tail region. In the youngest stages, zfCx45.6 expression was restricted to the ventral half of the embryo (A). As the embryos developed, a distinct band of expression was located in the tail, just below the notochord (B,E,F,G). The location of this structure most likely corresponds to the dorsal aorta (arrow in E,F,G). Embryos probed with the S-probe showed very little background (C,D). In all cases, anterior is to the left. The scale bar represents 400 μm in B, 200 μm in A and G, 100 μm in C,D,F, and 50 μm in E.

A. 0 dpf (~19 hpf), whole embryo (AS)

B. 1 dpf (~24 hpf), whole embryo (AS)

C. 1 dpf, lateral view head (S)

D. 1 dpf, lateral view tail (S)

E. 1 dpf, ventral view tail (AS)

F. 1 dpf, lateral view tail (AS)

G. 5 dpf, lateral view tail (AS)

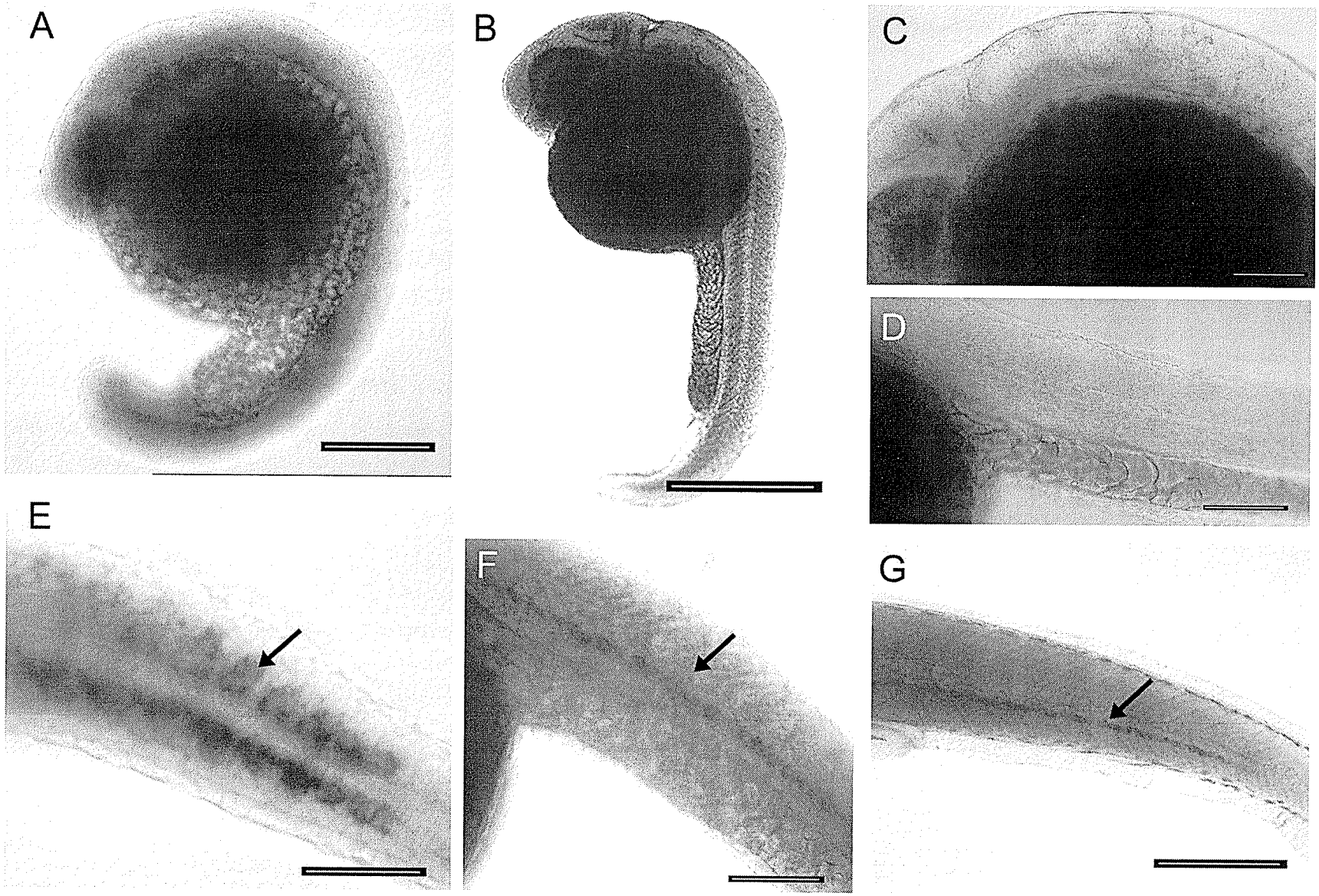
A
B
C
D
E
F
G

corresponds to the dorsal aorta, but other candidate vessels include the posterior (caudal) cardinal vein, the caudal artery, and/or the caudal vein. In a ventral view, this band appeared as two bands on either side of the notochord (Figure 14.E). ZfCx45.6 expression in the tail continued to be visible in the 5 dpf embryos (Figure 14.G). This area of the tail was always clear in the S-embryos (Figure 14.D). The heads of the AS-embryos (Figure 14.B) were also darker than those of the S-embryos (Figure 14.C), but specific expression patterns were not visible until later stages of development.

By 2 dpf and through to 5 dpf, very distinct expression patterns were visible in areas that appeared to correlate with the location of major blood vessels of the embryo. More specifically, zfCx45.6 expression was visible around the eyes, in the branchial arch region, in the limb buds, in the tail, and over the yolk sac. The identity of the zfCx45.6 positive vessels in the zebrafish was provisionally determined with the aid of confocal microangiograph figures of developing zebrafish vasculature (Isogai *et al.*, 2001) and "The interactive atlas of zebrafish vascular anatomy" web page (http://eclipse.nichd.nih.gov/nichd/Img.redirect.html).

Expression of zfCx45.6 around the eyes was visible in three major areas. A structure was visible surrounding the medio-ventral portion of the eye, just outside the retina, in embryos 2 dpf and older. This structure was best observed from a ventral view (Figure 15.B), but was also visible in the lateral view as a small line just below the eye (Figure 15.D). As there are many vessels surrounding the eye, the identity of this structure was not clear. Two possibilities include the optic vein (a vessel surrounding the ventral portion of the eye), and the primitive internal carotid artery (located ventral and

Figure 15. Whole-mount ISH –ZfCx45.6 Expression in the Anterior Portion of the Embryo.

ZfCx45.6 embryonic expression was observed in three major locations of the embryonic zebrafish head. Expression of zfCx45.6 was detected in a structure surrounding the ventro-medial 1/3 of the eye in embryos 2 dpf and older (arrow in B, also visible in D and E). ZfCx45.6 was also detected as "dots" at the posterior/ventral corner of the eye in embryos 2 dpf and older (arrow in C). The most distinct expression patterns of zfCx45.6 were visible in the branchial arch region of embryos 2 dpf and older (A-E). ZfCx45.6 expression was also apparent in the limb bud of embryos 1 dpf and older (D,E). There was no significant staining in embryos probed with the S-probe (F). In all cases anterior is to the left. The scale bar represents 100 μm.

A. 2 dpf, head ventral view (AS)

B. 3 dpf, head ventral view (AS)

C. 3 dpf, head ventral view (AS)

D. 4 dpf, head oblique view (AS)

E. 5 dpf, head ventral view (AS)

F. 3 dpf, head ventral view (S)

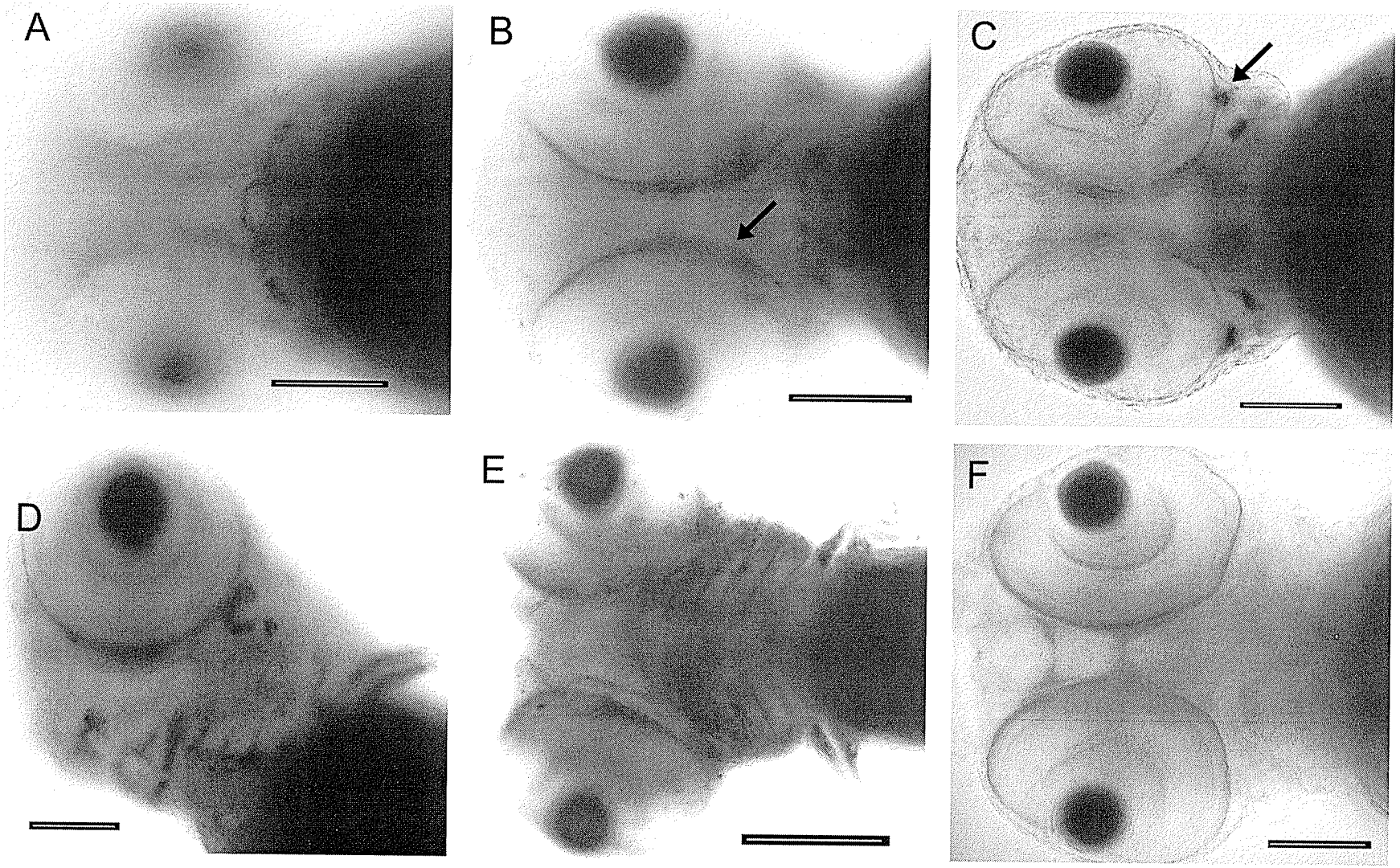
A
B
C
D
E
F

medial to the optic vein). The location of both of these structures corresponds most closely to the expression pattern of zfCx45.6 in this area.

ZfCx45.6 expression was also visible as "dots" of DIG precipitate at the posterior/ventral corner of the eye in embryos 2 dpf and older (Figure 15.C). At 2 dpf, only one "dot" was visible, but by 3 and 4 dpf, three "dots" were visible. This expression pattern was evident in both the ventral and lateral view. Though the identity of these structures is not clear, there are connections between vessels, and expansions of vessels, identified in angiograms of the area around the eye, that appear to correlate with the location of zfCx45.6 expression. The expression pattern observed most likely corresponds to connections between and around the ophthalmic vein, the primordial midbrain channel, and the cranial division of the internal carotid artery.

Though not visible in all cases, a third expression pattern visible around the eyes appeared as a "dot" of DIG precipitate in the dorsal/posterior corner of the eye. This "dot" was visible in the lateral and dorsolateral view in 3 dpf and 5 dpf embryos (results are not shown as this structure did not show up clearly in the images captured). By 5 dpf this area had expanded. The identity of this structure is unclear.

Some of the most distinctive expression patterns of zfCx45.6 occurred in the branchial arch region. Expression was visible by 2 dpf as bands through this area (Figure 15.A). As the embryo grew and the branchial area enlarged, the expression pattern of zfCx45.6 changed, corresponding to branchial arch remodeling and development. By 3 dpf, clear bands that appeared to correspond to the location of the branchial arches were visible (Figure 15.B). The most intricate staining was visible by 4 dpf, when expression of zfCx45.6 appeared to correspond to the location of the hypobranchial artery, the

opercular artery, and the 3rd, 4th 5th, and/or 6th branchial arches (Figure 15.D). The expression of zfCx45.6 continued to be visible in this area through to 5 dpf (Figure 15.E).

ZfCx45.6 expression was also distinct in other areas of the embryo such as the limb buds (from 1 to 5 dpf) (whole-mount Figure 15.D, E and section Figure 16.C), and the common cardinal vein over the yolk sac in the 1 dpf embryos (figure not shown as the location of the yolk sac interfered with capturing images).

Expression of zfCx45.6 in the embryonic zebrafish heart was generally difficult to detect. Clear images could only be captured from the 2dpf embryos of one trial. In this case, an area of zfCx45.6 expression outlined the location of the heart from both the lateral and ventral view (Figure 16.A, B). In the majority of cases, the heart appeared to express zfCx45.6, but visualization was difficult due to the location of the heart with respect to the yolk (see below). To confirm expression of zfCx45.6 in the heart and other locations in the zebrafish embryo, semi-thin plastic sections were obtained from 3 dpf embryos. In general, zfCx45.6 was detected in very low amounts in the myocardium and possibly the endocardium of the heart (Figure 16.D), but staining was not as distinct as through areas such as the limb buds (Figure 16.C), or branchial arch vessels (Figure 16.D).

In all cases, very little background staining was observed in the head and body of the S-embryos (Figure 14.C, D and Figure 15.F). The exception to this was that in all cases the lenses and yolk of both S- and AS-embryos darkened with increased exposure to the NTM color reaction. This staining was viewed as background, as a DIG precipitate was not visible in sections of these areas (Figures 16.D) suggesting instead that the

Figure 16. Whole-mount ISH and Sections: ZfCx45.6 Expression in the Heart and Limb.

ZfCx45.6 expression in the embryonic zebrafish heart was generally difficult to detect, but was visible in the 2 dpf embryos of one trial. In an oblique view zfCx45.6 expression outlined what appeared to be the entire heart (arrow in A), while in the ventral view a tubular structure in the same location as the heart was visible (arrow in B). Semithin plastic sections of the heart region showed zfCx45.6 was detected in very low amounts in the myocardium and possibly endocardium (arrow in D). Expression in the heart was not as distinct as sections through the vessels of the branchial arches (arrow in D), or limb buds (arrow in C). The scale bar represents 100 μm in A, B, and D (anterior is to the left), and 20 μm in C.

A. 2 dpf, head oblique view (AS)

B. 2 dpf, head ventral view (AS)

C. 5 dpf, limb bud (AS), 5 μm plastic section

D. 3 dpf head sagital section (AS), 5 μm plastic section

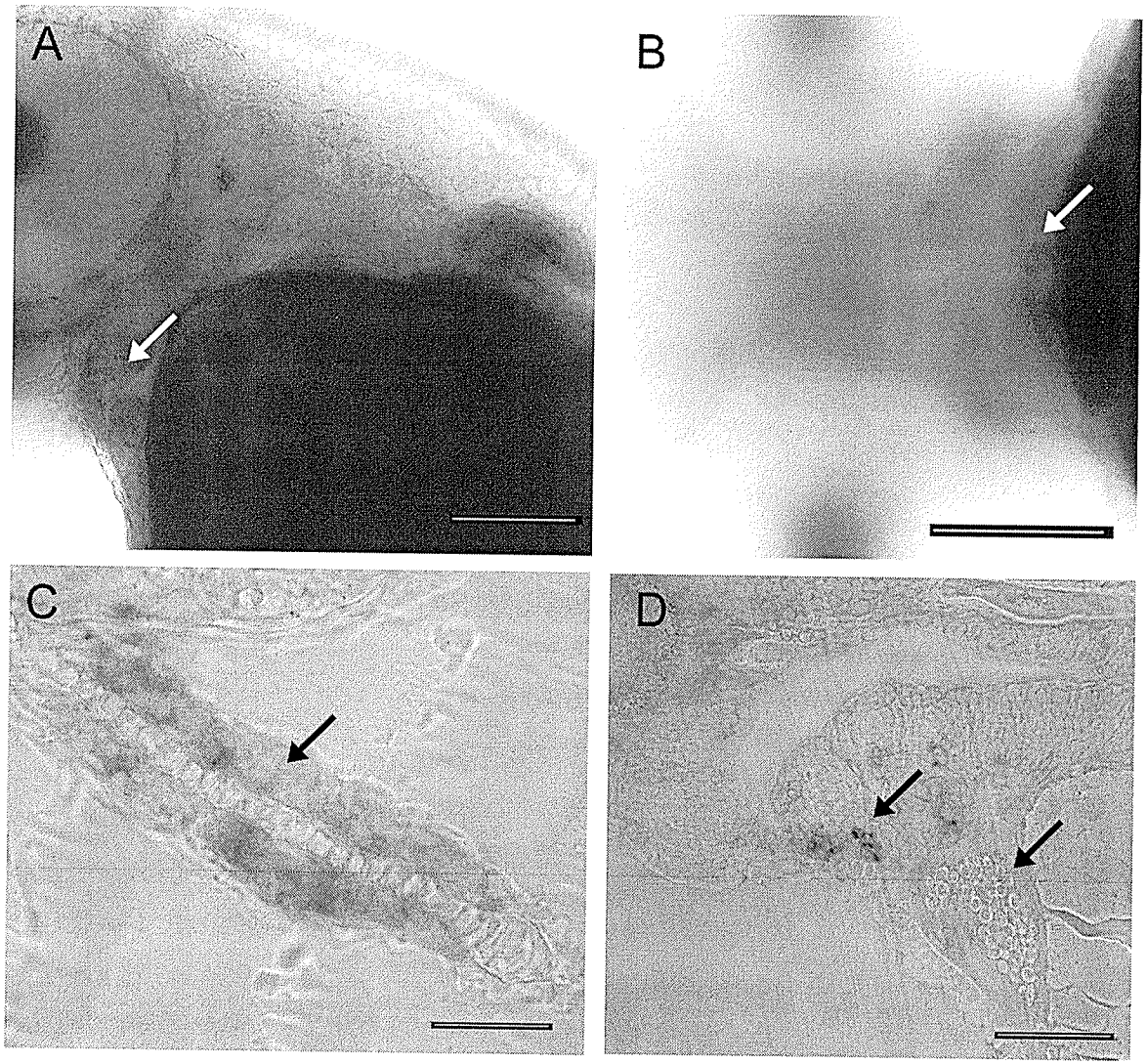
A
B
C
D

appearance of a precipitate in the whole-mounts occurred due to the inherent structure of the lens and yolk. Also, these structures stained equally with the S- and AS-probes.

3.6.2. Two-color whole-mount ISH

Two-color whole-mount ISH was performed in an attempt to confirm the localization of zfCx45.6 expression in the embryonic zebrafish heart. Whole-mount ISH was performed in essentially the same fashion as above, but two different probes were used. The first probe was the same DIG-labeled zfCx45.6 probe used in the one color ISH, thus resulting in a blue precipitate during the color reaction. The second probe was a DNP-labeled cmlc2 probe. Cmlc2 is a marker specific to heart muscle (Yelon *et al.*, 1999). The method of detection for this moiety is essentially the same as for DIG, but the alkaline phosphatase substrates used for antibody detection (BCIP, INT violet) result in a red precipitate during the color reaction. If both the DIG-labeled and DNP-labeled probes were detected in the same location, a brown product would result, thus confirming expression of zfCx45.6 in the zebrafish embryonic heart.

Initial tests were performed with the cmlc2 probe alone to confirm its specificity. Test whole-mount ISH with a DIG-labeled cmlc2 probe showed a very restricted expression pattern in the embryonic zebrafish heart as described previously by Yelon *et al.* (1999). It was noted that cmlc2 was detected very quickly as compared to the rate of detection of zfCx45.6, and a strong blue precipitate was visible after only 2 hours in the color reaction (Figure 17.A, B). Test whole-mount ISH with the DNP-labeled cmlc2 probe resulted in a slightly different effect. At least twice as long a time was required to

Figure 17. Two-color Whole-mount ISH.

Initial tests were performed with DIG-labelled cmlc2 probes (A,B) and DNP-labelled cmlc2 probes (D). A strong blue precipitate was visible in the heart of all embryos tested with the cmlc2-DIG probe (A), and expression was localized to the heart tissue as seen in sections (B). Tests with the cmlc2-DNP probe resulted in a spotty red precipitate throughout the heart, and increased background (D). Two-color whole-mount ISH with a DIG-labelled zfCx45.6 probe, and the DNP-labelled cmlc2 probe showed overlapping expression in the embryonic zebrafish heart (E,F), though this was best seen by comparing sections of the hearts of the cmlc2-DIG embryos (B) and the zfCx45.6 DIG-embryos (C). The arrow in C is highlighting the myocardium of the heart. The scale bar represents 100 microns in A,B,D, and 50 microns in C and F. In all cases, anterior is to the left.

A. 3 dpf, head lateral view, cmlc2-DIG

B. 3 dpf, heart semi-thin plastic section, cmlc2-DIG

C. 5 dpf, heart semi-thin plastic section, zfCx45.6-DIG

D. 5 dpf, head lateral view, cmlc2-DNP

E. 2 dpf, head ventral oblique view, two-color ISH

F. 2 dpf, heart lateral view, two-color ISH

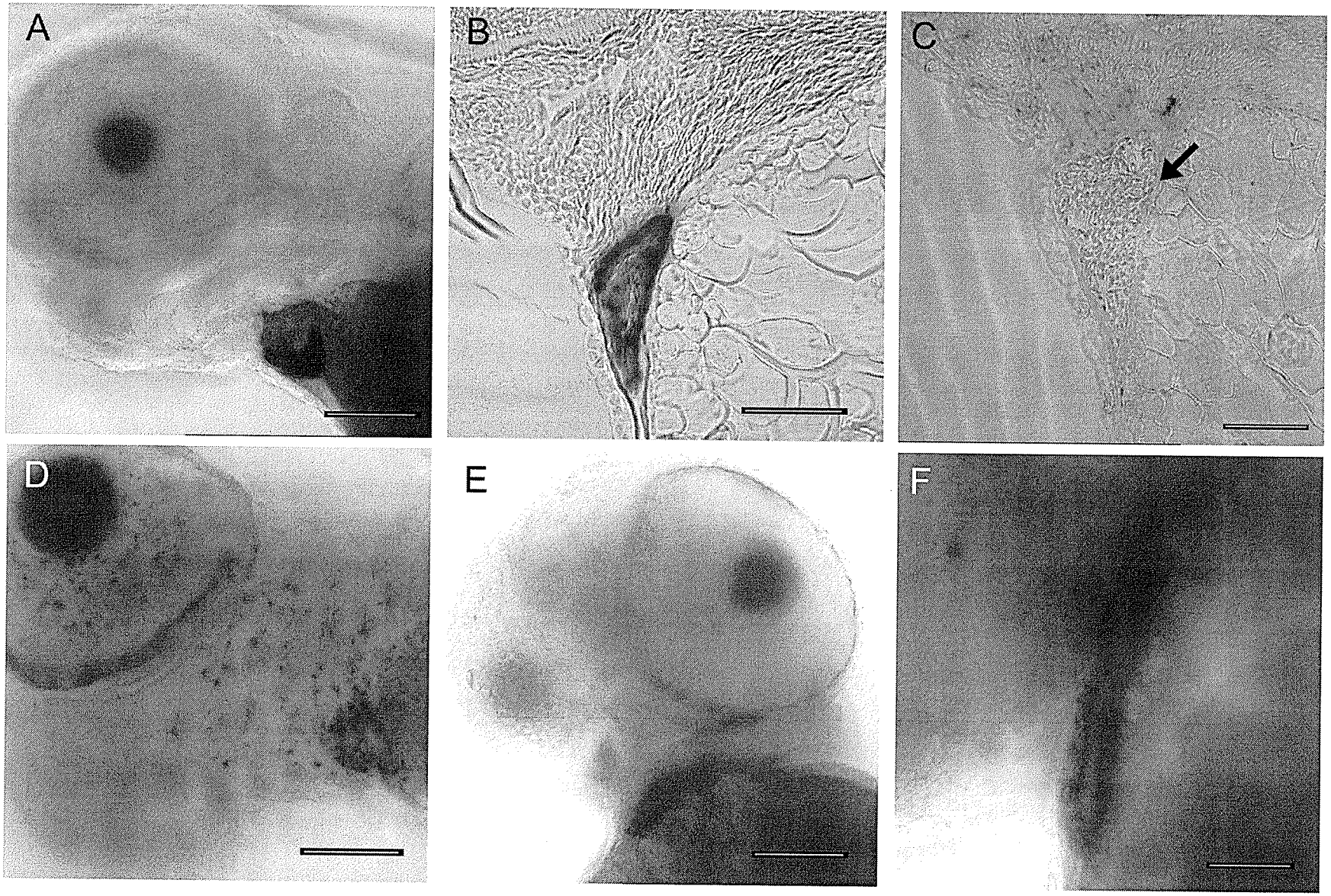
A
B
C
D
E
F

obtain an intense red precipitate. A side effect of this longer color reaction was higher background staining. The background staining looked like red melanophores throughout the skin (Figure 17.D). Another difference between the DIG and DNP precipitate was that the DNP precipitate was not visualized homogeneously throughout the heart. The red precipitate appeared in spotty patches in the heart, versus the DIG staining, which resulted in a homogeneous blue precipitate.

Overall, two color whole-mount ISH worked best in the 1 to 3 dpf embryos as compared to the 4 and 5 dpf embryos. In these younger embryos both DIG (zfCx45.6) and DNP (cmlc2) staining was observed in the areas observed in the single probe tests. Areas of expression of cmlc2 and zfCx45.6 did appear to overlap in the embryonic heart (best seen when comparing sections of the single probe ISH tests with either the DIG-labeled cmlc2 probe or the DIG-labeled-zfCX45.6 probe), but a brown product (clearly indicating overlapping expression in the same cells) was not visible. As well, the specific cell types with overlapping expression could not be determined from whole-mounts (Figure 17.E, F). Sections were attempted, but the DNP precipitate appeared to dissolve during the infiltration process.

Two-color ISH was also attempted with 4 and 5 dpf embryos, but results were not as good. The need for a longer staining time and increased background (more-so for the DIG staining) appeared to interfere with visualizing any overlap in DIG and DNP staining. Again, sections were not feasible due to the DNP precipitate dissolving during the infiltration process.

CHAPTER 4. DISCUSSION

4.1. Cloning of ZfCx45.6

To learn more about the role connexins play in heart and vascular development and function, one of the four major connexins expressed in the vertebrate cardiovascular system was cloned from zebrafish. This was accomplished by taking advantage of the high degree of sequence similarity between connexins to obtain a PCR clone, and then using the PCR clone to isolate a PAC clone containing the full coding region of the connexin. The cloned connexin is predicted to possess the sequence topology of a typical connexin with four transmembrane regions, internal NH_2- and COOH- termini, and three cysteine residues in conserved positions on each extracellular loop. As with the majority of connexins, the coding region is contained within one exon. The sequence of the cloned connexin encodes a polypeptide with a predicted molecular weight of 45.6 kDa, and thus was named zfCx45.6 according to standard protocol. ZfCx45.6 shows the highest degree of sequence similarity to the mammalian connexin40 orthologues, and also has similar RNA expression patterns. This sequence and expression similarity indicates a new member of the connexin40 orthologous group has been cloned.

The PCR clone of zfCx45.6 was obtained by taking advantage of the high degree of sequence similarity between orthologous connexins, combined with the use of a zebrafish codon usage table. A codon of three nucleotides encodes an amino acid, and different codons may encode the same amino acid. For example, Glycine is encoded by the synonymous codons: GGU, GGC, GGA, or GGG. The frequency of use of these synonymous codons varies from one gene to another, both within species, and between species (for a review see Yarden, ZFIN: http://zfin.org/cgi-bin/webdriver?MIval=aa-

ZDB_home.apg). Therefore, codon usage for a particular amino acid can be biased in a species-specific manner, and in compiling these biases, a codon usage table can be created for a particular species. Many codon usage tables have been created and are readily available on the web. In this study, a codon usage database compiled from the GenBank DNA sequence database was used to aid in creating the primers that were used to obtain the PCR clone (Nakamura *et al.*, 2000). Interestingly enough, a PCR clone was successfully obtained, but upon later inspection, the sequence of the primers used to obtain the PCR fragment, and the full connexin sequence (obtained from PAC clones) did not line up significantly. It is possible that regions of the primer sequence were similar enough to amplify a fragment under optimal PCR conditions, but not similar enough for current computer programs to line up. Another possibility is that there may be sequence differences between the strains of zebrafish used to isolate the genomic DNA from for PCR, and the strains used to create the PAC library.

4.2. Functional Analysis of ZfCx45.6

Most cells express more than one type of connexin therefore making it difficult to determine the unique channel properties of gap junctions formed by specific connexins *in vivo*. One method employed to study these unique properties involves expressing connexins in *Xenopus* oocytes, where the endogenous connexin expression has been minimized, and testing the gating parameters and permeability of the resulting channels (Dahl *et al.*, 1987). Studies of this sort have shown that gap junctions formed by different connexins have distinct conductance states, voltage sensitivities and ionic and dye permeabilities. These differences can be used to confirm orthology between

connexins when sequence similarity alone does not allow unequivocal assignment of orthologous relationship. Understanding the properties of channels composed of one type of connexin may also help to understand the function of intercellular communication in systems expressing multiple connexins.

Interestingly enough, studies with the paired *Xenopus* oocyte system have determined that some connexins do not form functional channels, for example, Atlantic croaker (*Micropongonia undulatus)* Cx32.7 (Bruzzone *et al.*, 1995), and rat Cx33 and Cx33.1 (Bruzzone *et al.*, 1994). It is speculated that these connexins do not form functional channels for one of three reasons. They may not form homotypic channels, they may act as dominant-negative inhibitors of other connexins, or cell-specific post-translational events required for functional competence are not carried out in *Xenopus* oocytes. Further studies will need to be performed to determine the exact reason some connexins do not appear to form functional channels.

Preliminary studies utilizing the paired *Xenopus* oocyte expression system have determined that zfCx45.6 forms functional, voltage sensitive channels in a manner similar to other connexins. For example, the macroscopic junctional conductance of zfCx45.6 mRNA injected oocytes is 280x higher than control values. This reveals that the channels formed by zfCx45.6 readily conduct current. Studies using the paired *Xenopus* oocyte system also show that the mean levels of conductance of channels formed by mouse Cx40 are 200 – 1000x higher than those of controls (Henneman *et al.*, 1992). Studies on mouse Cx40 also showed that the decay of junctional current in response to incremental changes in transjunctional voltage was described by a simple exponential function with a decreasing time constant for increasing transjunctional

voltage. Though a time constant for zfCx45.6 is not available for comparison, the same exponential function is observed. Both results demonstrate that each connexin forms channels that are voltage sensitive, and close upon application of a voltage stimulus. Studies on rat Cx40 revealed similar results to that of the mouse (Beblo *et al.*, 1995).

Though these preliminary results do not provide enough detail to establish a relationship between zfCx45.6 and the mammalian Cx40 orthologues, they are distinct from results obtained from other fish connexins. For example, zfCx55.5 shows a voltage induced channel opening in response to hyperpolarizing or depolarizing voltage steps, setting it apart from other connexins studied to this point (Dermietzel *et al.*, 2000). ZfCx44.1, zfCx27.5, and carp Cx43 have also been tested and show a similar, yet distinct response to zfCx45.6 with voltage induced channel closure. As appears to be the case with zfCx45.6, zfCx44.1 is more sensitive than zfCx27.5 and carp Cx43, and closes more rapidly upon application of voltage steps (Dermietzel *et al.*, 2000; Cason *et al.*, 2001). Further studies may provide more evidence for similarities or differences in voltage dependant closure to help establish the relationship between zfCx45.6 and the Cx40 orthologues.

Studies have shown that the C-tail region of a connexin is important in regulating properties of the channel, and this regulation can be altered by an increase in intracellular acidification and phosphorylation. For example, mammalian Cx40 experiences a considerable drop in pH sensitivity of the channels, and the lower conductance state (representing the residual conductance through the closed channel) disappears when the C-tail (CT) domain is removed (Stergiopoulos *et al.*, 1999). Normal function (or gating) and the unitary conductance profile of the channel can be restored by

the re-expression of the CT domain fragments of either Cx40 or Cx43 (Anumonwo *et al.*, 2001). From these and other studies, a ball and chain model has been proposed describing how some connexins are gated, whereby the CT domain is predicted to act as a gating particle under certain conditions to bind to a receptor in the pore and close the channel. The highest degree of divergence between zfCx45.6 and the connexin40 orthologues occurs within the C-tail, where zfCx45.6 contains more sequence, thus resulting in a higher predicted molecular weight. The reason for the disparity in length of the C-tail is unknown, though through other studies it appears that there is not a direct relationship between the pH sensitivity and the CT domain length (Stergiopolous *et al.*, 1999) therefore the extra sequence in the tail region of zfCx45.6 may not be functionally significant. Any significance could possibly be determined by creating clones that are missing one, or both of these "extra" regions, followed by functional analysis. Any functional changes would suggest the importance of this region in gating properties.

The permeability and single channel conductance of gap junctions composed of distinct types of connexins are also regulated differently by similar phosphorylating conditions (Kwak and Jongsma 1996; Kwak *et al.*, 1995a). For example, in SKHep1 cells, a decrease in transjunctional conductance through rat Cx43 channels was observed after treatment with protein kinase G (PKG) activators, while the same treatment had no effect on the transjunctional conductance of human Cx43 channels (Kwak *et al.*, 1995b). Connexin45 channel properties are also modulated under different phosphorylating conditions in HeLa cells such that activation of PKA decreases cell coupling, activation of PKC increase cell coupling, and activation of PKG has no effect on cell coupling (van Veen *et al.*, 2000). Studies have also shown that activation of PKA strongly increases the

macroscopic conductance and permeability of human Cx40 gap junctions in a communication-deficient SKHep1 cell line (van Rijen *et al.*, 2000). It is believed that these results suggest a role in the regulation of intercellular communication in the heart and vasculature by different phorphorylating conditions.

All predicted cytoplasmic regions of zfCx45.6 contain possible phorphorylation sites. Six of these sites are conserved, and 2 serine sites occur within the C-tail. Further studies need to be performed to determine if these sites are significant (such as site directed mutagenesis followed by functional studies), and if so, how they affect intercellular communication.

4.3. Chromosomal Mapping of ZfCx45.6 to Zebrafish Linkage Group 9

ZfCx45.6 was mapped to zebrafish LG9 with a first lod score of 6.9. The lod score is the logarithm of the likelihood ratio for linkage, with the first lod score representing the probability of the gene in question being found on the selected linkage group. ZfCx45.6 was mapped to zebrafish LG15 with a second lod score of 4.4. The second lod score represents the probability of the gene in question being found on any of the other 24 linkage groups. For these results to be significant, the first lod score must be greater than 5, and the second lod score must be at least 3 units away from the first. One of the possible reasons for the lack of significance with the second lod score (there was a difference of only 2.5 units between the lod scores) could lie in the fact that the panels may not have been scored consistently each time (i.e. human error). For example, a cell line may have been scored as positive one time, and ambiguous the next. Caution is required when scoring the panel, as the donor chromosomal fragments (i.e. the zebrafish

chromosome fragments) are present at various molarities among the hybrid cell lines, therefore detection of the PCR products will depend on the sensitivity of each PCR assay (Hukriede *et al.*, 1999). ZfCx45.6 was also mapped to the end of LG9, resulting in fewer distal markers to aid in mapping. ZfCx45.6 was mapped zero centirays from the previously mapped marker fb36h02, but no significant sequence similarity was found between zfCx45.6 and fb36h02. This is not unusual as for this panel, 1 centiray equals 118 kb (Hukreide *et al.*, 2001), and the sequence obtained from zfCx45.6 was only 1.5 kb.

Radiation hybrid panels are one of the best methods for mapping genes to chromosomes or chromosome segments because, unlike meiotic mapping, mapping with cell hybrids does not require gene polymorphisms. In the case of the RH panel, the frequency of breakpoints between two markers is proportional to the distance between them. In 1999, Hukriede and associates produced a zebrafish RH panel by fusing irradiated zebrafish fin AB9 cells with mouse B78 melanoma cells. At that point, the map covered 88% of the zebrafish genome, and showed 96% concordance with markers in meiotic maps and other RH maps. Recently, another 3119 expressed sequence tags (ESTs) and cDNA sequences have been placed on the map, joining the previously mapped 748 simple sequence length polymorphism (SSLP) markers, and 459 genes and ESTs (Hukriede *et al.*, 2001). Mapping ESTs and cloned genes with the LN54 RH panel should prove to be a valuable method for identifying candidate genes for specific mutations in zebrafish (Hukriede *et al.*, 1999).

It may seem redundant to have greater than one map for each model organism, but as already mentioned, each map does not necessarily cover 100% of the genome. On

ZFIN, a consolidated map of the zebrafish genome based on all the known zebrafish maps has been created. This ZMAP currently contains over 20,00 markers. This map will be a useful tool for researchers to compare the position of their gene or EST of interest, mapped via their method, to the position on the higher resolution consolidated ZMAP.

A study by Barbazuk *et al.* (2000) analyzed and compared over 500 zebrafish genes and ESTs mapped with the LN54 RH panel, and the corresponding mapped human genes. In this analysis, it was found that over 80% of the genes analyzed fell into syntenic groups (two or more genes that are found on the same chromosome in zebrafish are also found in one chromosome in humans) (Barbazuk *et al.*, 2000). Their analysis suggested that syntenic comparison between zebrafish and humans could be used to aid in positionally cloning zebrafish mutant genes, and/or to predict homology. Syntenic comparisons would also be especially useful in establishing orthologous relationships in the case of connexins, where the structure and sequence of connexins can be quite similar.

In the case of zebrafish LG9, nine genes have apparent orthologues, and a tenth gene a close homologue on the long arm of human chromosome 2 (Postlethwait *et al.*, 1998). Zebrafish LG9 also has syntenic regions with human chromosomes 11, 21 and X (Barbazuk *et al.*, 2000). Human Cx40 has been mapped to chromosome 1 (Willecke *et al.*, 1990). At this point, zfCx45.6 and human Cx40 do not appear to be in a syntenic group, therefore one cannot confirm their orthology with this method. Genes not in a syntenic group are referred to as singletons (Barbaziuk *et al.*, 2000). These singletons may reflect errors in orthology determination, or mapping. Due to the second lod score

not being significant, there is a possibility that zfCx45.6 was not mapped to the correct location.

Another possibility is that zfCx45.6 was mapped to the correct location, but not enough markers have been mapped to determine synteny. Interestingly enough, fb36h02, the marker most closely associated with zfCx45.6, shows similarity to a marker on human chromosome 12, even though a region of synteny has not been established between zebrafish LG9 and human chromosome 12. As well, other zebrafish markers mapped to the same position as fb36h02 are mapped to human chromosomes 1, 2 and 21 (http://zfish.wustl.edu/zebrafish_to_human_suppl_.pdf). Though synteny has not been established, these results suggest further mapping could reveal a linkage between a region of zebrafish LG9 and human chromosomes 1 and 12.

4.4. Expression Analysis of ZfCx45.6

The spatial and temporal expression of zfCx45.6 was determined through Northern analysis, RT-PCR, and whole-mount ISH. The first two methods were used to determine embryonic temporal and adult spatial expression. As polyA$^+$ mRNA was difficult to obtain, due to the large number of embryos required, RT-PCR was used to confirm and extend the results from the Northern analysis. Whole-mount ISH was used to localize embryonic expression. Through these methods zfCx45.6 expression was detected in embryos prior to 2.5 hpf, presumably representing maternal expression, and then not again until 12.5 hpf, after which it was continually expressed to 5 dpf. In the embryo, zfCx45.6 was detected in what appeared to be the major vasculature of the entire embryo, and to a lesser extent in the heart. ZfCx45.6 continued to be expressed in the

adult, and was detected in the heart, liver, eye (minus the lens), brain, and ovary. ZfCx45.6 was not detected in the lens of the embryo or adult zebrafish.

A 2.3 kb transcript of zfCx45.6 was detected by Northern analysis. The size of the transcript is relatively small when compared to the transcripts of the other connexin40 orthologues: 3 kb in chick (Beyer *et al.*, 1990), 3.3 kb in human and rat (Kanter *et al.*, 1994; Beyer *et al.*, 1992), 3.5 kb in the mouse (Hennemann *et al.*, 1992), and 2.5 kb in the dog (Beyer *et al.*, 1992). These size differences in the transcripts most likely reflect differences in the untranslated region of the mRNA.

In the zebrafish, zygotic transcription does not begin until midblastula transition at about the 1000 cell stage, or 3 hpf (Kane and Kimmel, 1993). The fact that zfCx45.6 is detected prior to 2.5 hpf suggests this message is maternally supplied to the embryo. It is well known that the earliest stages of embryogenesis are regulated by maternally inherited compounds stored within the oocyte, and zygotic expression takes over after these maternal compounds have decayed (Telford *et al.*, 1990). Genes may be expressed only maternally, maternally and embryonically, or only embryonically (Dworkin and Dworkin-Rastl, 1990). From the present study it appears that zfCx45.6 is expressed both maternally and embryonically, and could thus be crucial for early embryogenesis as well as later in development.

The maternal expression of gap junctions has been studied in *Xenopus*, where alpha and beta forms of gap junctions have been detected in the early embryo (Ebihara *et al.*, 1989; Gimlich *et al.*, 1990). For example, *Xenopus* Cx38 is a maternal transcript that disappears by the late gastrula stage, and is also detected in the mature ovary. The function of this maternal transcript was not determined. *Xenopus* Cx43 has been detected

in a similar manner, as it appears during organogenesis and is detected in a variety of organs, including oocytes, but degrades upon oocyte maturation (Gimlich *et al.*, 1990). It is proposed to participate in hormone regulated intrafollicular communication events during oogenesis, and in early oocyte maturation. As zfCx45.6 is also detected in the adult ovary, and only for a short time in the early embryo, there is the possibility that zfCx45.6 mRNA detected prior to 2.5 hpf is also residual, nonfunctional, maternal mRNA. In the adult ovary, zfCx45.6 may be present in the blood vessels, regulating blood vessel function and growth, or possibly in connections between the ovarian somatic cells and the oocyte, regulating early oocyte development. Any possible function of zfCx45.6 prior to 2.5 hpf, could be studied through the use of antisense technologies (see further for details).

ZfCx45.6 expression was detected by whole-mount ISH in the heart and major vasculature of the zebrafish embryo between 1 and 2 dpf. Though this technique did not detect specific expression patterns prior to this, RT-PCR, a more sensitive method, detected zfCx45.6 by 12.5 hpf in the whole embryo. One could speculate that zfCx45.6 is expressed in the heart and vasculature tissue around 12.5 hpf, but at levels below that which could be detected by whole-mount ISH. In the zebrafish, cardiac progenitors begin to arrive at the embryonic axis by 13 hpf (8 somite stage), and by about 16.5 hpf two tubular heart primordia have formed in the lateral plate mesoderm (Stainier *et al.*, 1993). Vascularization begins by 20-22 hpf (24 somite stage) (Fouquet *et al.*, 1997), and by 24 hpf (28 somite stage) a simple circulatory loop has been set up (Isogai *et al.*, 2001). The detection of the zfCx45.6 transcript in the whole embryo prior to these times, and the subsequent localization of the transcript in the heart and vascular tissue, suggests the

possibility that zfCx45.6 plays a role in zebrafish cardiovascular function and/or development.

The location of embryonic expression of zfCx45.6 is actually quite similar to the embryonic expression of Cx40 in the mouse. In the 9.5 days post coitum (dpc) mouse, cardiac contractions have started, and looping is complete, but the chambers have not been specified yet (Delorme *et al.*, 1997). At this stage whole-mount ISH detects high levels of Cx40 transcripts in the vasculature (Delorme *et al.*, 1997). In the mouse, Connexin40 was specifically located in the paired dorsal aortae, the intersegmental arteries sprouting from the aortas, the branchial arch arteries, the primary head arteries and branching vessels, the common aorta and vitteline, umbilical, and caudal vessels. Connexin40 was also detected in the atrium and common ventricular chamber.

One question that arises when comparing the embryonic expression of these orthologues, is why does mouse Cx40 appear to be expressed at much higher levels in the heart than zfCx45.6? Studies by Delorme *et al.* (1997) have determined that the levels of mouse Cx40 are regulated during mouse cardiovascular development. At 8.5 dpc, connexins for the most part are not detected in the heart or vascular system through whole-mount ISH, though a moderate signal is detected in the paired dorsal aortas. RT-PCR does indicate low levels of Cx40 in both the 8.5 and 9.5 dpc mouse. By 9.5 dpc Cx40 is detected in the atrial wall, but not in the endocardium, and by 10.5 dpc and later stages of development, Cx40 is more highly expressed in the atrial myocytes than previously. Possibly, zfCx45.6 expression in the heart is regulated in much the same way it is in the mouse, as zfCx45.6 is detected in the embryonic heart at very low levels, but is easily detected in the adult heart. ZfCx45.6 may play more of a role in heart function,

and therefore not be highly expressed until later stages of development, when detection via whole-mount ISH appears not to work as well. Real time quantitative PCR with TaqMan® probes (Applied Biosystems, Foster City, CA) and isolated embryonic zebrafish hearts at younger stages of development could be used to confirm this, but this would be difficult due to the small size of their hearts.

ZfCx45.6 may also be regulated at the protein level. Even though mRNA levels of zfCx45.6 are not easily detected in the embryonic stages, high levels of protein could still be produced. Analysis of Cx40 distribution in the tissues of the mouse suggest this posttranscriptional regulation, as the amount of mRNA detected in the lungs is greater than detected in the heart, but the reverse is true for the levels of protein (Traub *et al.*, 1994). Western analysis or immunohistochemistry would help to determine any control over the translation of zfCx45.6.

It is also possible that in the zebrafish a different connexin is expressed at higher levels in the heart and takes over the role played by Cx40 in the mammalian heart. In all animals studied, the level and location of specific connexin expression varies throughout the heart. For example, in the adult chick, Cx42 is the major connexin expressed in the myocardium of the atria and ventricles, and little if any Cx43 is expressed in the myocytes (Minkoff *et al.*, 1993). In the adult rat, Cx40 is not found between the myocytes, and Cx43 is the major connexin expressed (Bruzzone *et al.*, 1993). Interestingly enough, Cx32 and Cx43 are the major connexins expressed in the goldfish heart (in the myocardium and endocardial cushion tissues respectively), yet Cx40 is not detected at all (Becker *et al.*, 1998). Now that three of the major connexins expressed in the mammalian heart have been cloned in the zebrafish, studies can be performed to

determine the relative levels of connexin expression. These studies could possibly help to decipher the roles of connexins in zebrafish cardiovascular development and function.

As with studies on the heart, the localization of specific connexin subtypes in the vascular system appears to be not only species specific, but also vessel specific. For example, in studies by Yeh *et al.* (1997), Cx40 was expressed in the EC of the rat coronary arteries, the atrial endocardium, and in some locations of the ventricular endocardium, but not in the media or SMC of the vessels. This correlates with results from Rummery *et al.* (2002) who noted Cx40 was absent from the media of the rat thoracic aorta and caudal artery, but was present in the endothelium. These results are in conflict with studies that did detect Cx40 in the media of blood vessels of multiple species, including the SMC of the rat coronary artery (though not the SMC of the aorta)(van Kempen and Jongsma, 1999). The unifying result from the majority of these studies is that the expression of specific connexins in EC and SMC varies in different segments of the vasculature, and between species. One possible function of this difference is the potential for complex regulation of growth, development and vasomotor responses (Yeh *et al.*, 1997). For example, Cx43 is dynamically regulated in confluent EC by specific flow patterns whereby its expression is increased in areas of increased flow (DePaola *et al.*, 1999). Further comprehensive comparative studies will need to be performed and repeated to obtain a full understanding of how this regulation may work.

ZfCx45.6 was detected in all of the adult organs tested except the lens. It is most likely that zfCx45.6 is expressed in the vasculature of these organs, though this would best be confirmed through immunohistochemistry. ZfCx45.6 was not detected in the embryonic or adult zebrafish lens. Through whole-mount ISH, the lens of AS-embryos

did appear to stain dark. As the lenses of S-embryo also stained, and sections of both S- and AS- embryos did not show any DIG staining, this was interpreted as a discoloration resulting from the inherent structure of the lens. Supporting this idea is the fact that whole-mount ISH with DNP-labeled probes also resulted in the same phenomenon. The fact that zfCx45.6 was not detected in the lens is consistent with other studies (Beyer, 1990). It is also consistent with the fact that even though Cx40 expression in different organisms is not always the same, its expression does appear to be restricted to the heart, and vascular tissue, or adult vascularized organs. As the lens is an avascular tissue, one would not expect to find zfCx45.6 expressed there.

CHAPTER 5. SUMMARY AND FUTURE STUDIES

In summary, the zebrafish orthologue of Cx40 was cloned from genomic DNA. The gene was linked to zebrafish LG9, and paired *Xenopus* oocyte studies determined that zfCx45.6 forms functional gap junction channels with voltage dependant gating. In the embryo, zfCx45.6 mRNA was detected by 12.5 hpf, and was localized to the major vasculature of the entire embryo, and to a lesser extent the heart. ZfCx45.6 was also detected prior to 2.5 hpf, suggesting it is maternally expressed. ZfCx45.6 continues to be expressed in the adult and is detected in all major organs tested with the exception of the lens, an avascular tissue.

More studies need to be carried out to fully characterize the role zfCx45.6 plays in the formation and function of the cardiovascular system. First, western analysis and/or immunohistochemistry would need to be performed to determine if and when zfCx45.6 is translated *in vivo*, and where this protein localizes. The temporal and spatial localization of zfCx45.6 protein could possibly help to determine whether zfCx45.6 plays a role in heart and vascular function and/or development. Even though zfCx45.6 RNA is detected before the cardiovascular system forms, the protein may not be translated until after the heart or vascular system has developed. This would suggest the connexin plays more of a role in function rather than development. In these studies, one would need to keep in mind that the connexin may be expressed in very low levels, below the ability to detect it, but still in functional amounts.

The role of zfCx45.6 could be further analyzed through the use of antisense morpholino-modified oligonucleotides (morpholinos, MO). Morpholinos are biologically

stable DNA analogues made from ribonucleosides that are effective in blocking the translation of targeted mRNAs when injected into one or two cell staged embryos (for reviews see Heasman, 2002; Ekker and Larson, 2001). Morpholinos are an attractive choice for antisense studies because they are highly soluble in water, immune to a wide range of nucleases and therefore highly biologically stable (Summerton and Weller, 1997). They also demonstrate high antisense efficacy, high sequence specificity, little or no non-antisense activity, and are easily delivered into culture cells (Summerton and Weller, 1997). Though the genetics of cardiovascular development in zebrafish is similar to that of mammals, developmental differences prevent molecular techniques used to determine gene function in mammals from being used in zebrafish. Morpholinos overcome these developmental differences between fish and mammals, and result in a similar effect to those of mouse "knockouts", whereby a gene is removed from the mouse genome. The major difference with morpholinos is that the targeted gene is not destroyed as in conventional mouse knockouts, and therefor this approach is known as a gene "knockdown" strategy.

Studies have shown that injection of morpholinos into single cell zebrafish embryos results in effective transfer of the morpholino to all the cells in the embryo, and reduced expression of the target gene in almost every cell (Nasevicius and Ekker, 2000; Muller *et al.*, 2001; Zhongan *et al.*, 2001; Bauer *et al.*, 2001; Shepherd *et al.*, 2001). A study by Heasman and colleagues (2000) has also shown that morpholinos can effectively block maternal gene function as long as there is no stored pool of protein. With the previous cloning of two other cardiovascular connexins in the zebrafish, double and triple

knockdown studies could be performed to determine how the cardiovascular connexins interact with one another, and if they can compensate for one another.

Though embryonic stages of zebrafish are initially easier to handle than mammalian embryos, zebrafish embryos do not grow very large over the first few days of development, and this could make analysis of cardiovascular development or defects difficult to observe. Through MO studies, initial analysis of the effects of blocking the translation of zfCx45.6 and the other cardiovascular connexins would be readily visibly in the optically transparent zebrafish embryo, as heart rate and function and would be easily detected. As the zebrafish has been utilized as a model system for over 20 years, many invasive and non-invasive techniques have also been developed for the measurement of multiple cardiovascular functions in minute animals and embryos. These techniques could be used to determine if there are any functional defects in blood pressure, stroke volume, heart rate, and changes in blood flow (for a review see Burggren and Fritsche, 1995). For example, blood pressure can be measured in slightly anesthetized embryos with a servo-null micropressure system (Pelster and Burggren, 1996). Cardiomyocytes from whole embryonic hearts can also be cultured, and patch-clamp recording can be taken to asses channel activity (Baker *et al.*, 1997). Also, with the development of transgenic zebrafish expressing GFP in endothelial cells (Motoike *et al.*, 2000), the course of development of the vasculature could be observed in real time with confocal microscopy (Isogai *et al.*, 2001). Any defects observed in the MO embryos could also be compared to those from the cardiovascular mutants isolated from the large-scale mutagenesis screens (Stainier *et al.*, 1996; Chen *et al.*, 1996). This could possibly

help to identify zfCx45.6 as the gene responsible for the observed effect of a mutant screen embryo, or genes that are interacting up or downstream of zfCx45.6

APPENDIX I

SUMMARY OF CONNEXIN KNOCKOUT MICE AND THEIR RELATED CARDIOVASCULAR DEFECTS.

Connexin	Defects
$Cx43^{-/-}$ [1]	-embryonically lethal at birth -impaired cardiac looping results in obstruction of right ventricular subpulmonary outflow tract
$Cx43^{-/-}$, cardiac specific [2]	-normal heart structure and function -die by 2 months due to spontaneous ventricular arrhythmias
$Cx43^{-/-}$, endothelial cell specific [3]	-survive to maturity -hypotensive and bradycardic
$Cx45^{-/-}$ [4,5]	-embryonically lethal at E10 (Cx45+/- is viable and fertile) -cardiac arrest within 24 h of the first heart contractions due to impaired atrial contractions and/or impaired transmission of the atrial impulse through the AV canal -endocardial cushion and cardiac looping defect -essential for vascular development: vasculogenesis is normal, but the subsequent transformation into mature vessels is interrupted
$Cx40^{-/-}$ [6,7]	-viable and fertile -conduction through His-Purkinji system slowed resulting in altered ventricular contractions
Cx40 and Cx43 double-deficient mice [8]	-additive effects of Cx40 and Cx43 haploinsufficiency on ventricular conduction and cardiac morphogenesis -no additive effects on atrial conduction -overall, haploinsufficiency aggravates defects observed in $Cx40^{-/-}$ phenotype, but not the $Cx43^{-/-}$ phenotype

1. Reaume *et al.*, 1995, 2. Gutstein *et al.*, 2001, 3. Liao *et al.*, 2001, 4. Kumai *et al.*, 2000

5. Kruger *et al.*, 2000, 6. Simon *et al.*, 1998, 7. Kirchoff *et al.*, 1998, 8. Kirchoff *et al.*, 2000

APPENDIX II

COMMON BUFFERS AND SOLUTIONS

Buffer A
1 ml 0.125 M Tris-HCl pH 8.0 / 0.125 M $MgCl_2$
18 µl β-mercaptoethanol
5 µl 100mM each dATP/dTTP/dGTP

Denhardt's 50x
5 g Ficoll (Type 400 Pharmacia Biotech)
5 g polyvinylpyrrolidone (Fisher Biotech)
5 g BSA (Fraction V, Sigma)
H_2O to 500ml

DEPC H_2O
1 ml diethylpyrocarbonate
1 L H_2O
stir overnight, autoclave

DNA loading buffer 6x
30% glycerol
0.25% bromophenol blue
in H_2O

Egg water
1.5 ml salt solution
1 L distilled H_2O
pH to 7.2-7.4

Gel staining buffer
0.5 µg/ml ethidium bromide
0.1 M ammonium acetate

HYB
50% deionized formamide
5x SSPE
0.1% SDS
100 µg/ml sheared, heat denatured salmon sperm DNA
5x Denhardt's

HYB*
50% deionized formamide
5x SSC
50 mg/ml Torula RNA (type VI, Sigma)
100 µg/µl heparin (Sigma)
1x Denhardt's
0.1% Tween 20 (BDH)
0.1% CHAPS (Sigma)
5 mM EDTA

HYB-
HYB* minus the heparin and *Torlua* RNA

LB medium
10 g Bacto-Tryptone (Difco)

	5 g Bacto-yeast extract (Difco) 10 g NaCl ddH_2O to 1 L autoclave, add desired antibiotic
LB plates	15 g Bacto-agar (Difco) 1 L of LB medium autoclave, add desired antibiotic, pour into petrie plates
MAB-T	100 mM maleic acid 150 mM NaCl 0.1% Tween20 (BDH) pH to 7.7
MOPS buffer 10x	0.2 M MOPS 50 mM NaOAc 10 mM EDTA, pH 7.0 DEPC treat and autoclave
NTM buffer	100 mM NaCl 100 mM Tris pH 9.5 50 mM $MgCl_2$
OLB	50 OD units of random primer hexanucleotides (Pharmacia) 555 µl double distilled water 375 µl buffer A 925 µl 2 M HEPES
PAC HYB	7% SDS 0.5 M Na Phosphate, pH 7.2 1 mM EDTA
PAC Wash	40 mM Na Phosphate, pH 7.2 0.1% SDS
PBS	0.8% NaCl 0.02% KCl 0.02 M PO_4 pH 7.3
PBS-T	PBS plus 0.1% Tween 20
Salt solution	40 g "Instant Ocean" Sea Salts in 1L distilled water
10 % SDS	100 g sodium dodecyl sulfate 1 L water, pH 7.2

SOC medium	2% Tryptone 0.5% yeast extract 10 mM NaCl 2.5 mM KCl 10 mM $MgCl_2$ 10 mM $MgSO_4$ 20 mM glucose
SSC 20x	175.3 g NaCl 88.2 g sodium citrate H_2O to 1 L pH to 7.0
SSPE 20x	175.3 g NaCl 27.6 g NaH_2PO_4-H_2O 7.4 g EDTA, pH 7.4 H_2O to 1 L
TAE 50x	242 g Tris base 57.1 ml glacial acetic acid 100 mL EDTA (0.5 M, pH 8.0) H_2O to 1 L
TBE 5x	54 g Tris base 27.5 g boric acid 20 ml EDTA (0.5 M, pH 8.0) H_2O to 1 L
TBS-T	20 mM Tris pH7.5 500 mM NaCl 0.05% Tween 20
TE buffer	1 mM EDTA pH 8.0 10 mM Tris-HCl (at the pH required of buffer)
Tricane	400 mg Tricane powder 97.9 ml ddH_2O ~2.1 ml 1 M Tris pH 9.0 adjust pH to ~7 add 4.2 ml of stock to 100 ml of egg water for use as anesthetic
1M Tris	121.1 g Tris H_2O to 1 L

APPENDIX III

LIST OF PRIMERS

Primer name (bp)	Sequence
M13/pUC/F/1 (18)	5' - TCACGACGTTGTAAAACG - 3'
M13 Reverse (16)	5' - AACAGCTATGACCATG - 3'
ZfeF1alpha/F/1	5' – CAAGGGCTCCTTCAAGTACGCCTG – 3'
ZfeF1alpha/R/1	5' – GGCAGAATGGCATCAAGGGCA – 3'
alpha3/F/1 (31)	5' - AGTGATCGGAAAGGTTTGGTTAACCGTCCTG - 3'
alpha3/R/1 (33)	5' - CTTTAACTTTTTCCATCCCAGGTGGTAGATCTC - 3'
zfCx45.6/F/1 (22)	5' - CCCTGTGAACTGTTACATGTCC - 3'
zfCx45.6/F/2 (19)	5' - TCCTGTCCTAAAACCACGG - 3'
zfCx45.6/F/3 (21)	5' - TGGATCTGCCTGAGAACAACC - 3'
zfCx45.6/F/4 (22)	5' - GCTCTGTATCCATGTTCAATGC - 3'
zfCx45.6/F/5 (20)	5' - GTTGTTCCTCAGCAGTGTAG - 3'
ZFcX45.6/R/1 (22)	5' - GCCTAACAACAGGATACGGAAG - 3'
zfCx45.6/R/3 (21)	5' - GCTCTGATACAGATTCTTCCC - 3'
zfCx45.6/R/6 (18)	5' - GCTTCCAGCTTCTTTTCC - 3'

REFERENCES

Angst B.D., Khan L.U.R., Severs N.J., Whitely K., Rothery S., Thompson R.P., Magee A.I., Gourdie R.G. 1997. Dissociated spatial patterning of gap junctions and cell adhesion junctions during postnatal differentiation of ventricular myocardium. *Circ. Res.* 80:88-94.

Anumonwo J.M.B., Taffet S.M., Gu H., Chanson M., Moreno A.P., Delmar M. 2001. The carboxyl terminal domain regulates the unitary conductance and voltage dependance of connexin40 gap junction channels. *Circ. Res.* 88(7):666-673.

Baker K., Warren K.S., Yellen G., Fishman M.C. 1997. Defective "pacemaker" current (I_h) in a zebrafish mutant with a slow heart rate. *Proc. Natl. Acad. Sci. USA.* 94: 4554-4559.

Barbazuk W.B., Korf I., Kadavi C., Heyen J., Tate S., Wun E., Bedell J.A., McPherson J.D., Johnson S.L. 2000. The syntenic relationship of the zebrafish and human genomes. *Genome Res.* 10(9):1351-1358.

Bauer H., Lele Z., Rauch G.J., Geisler R., Hammerschmidt M. 2001. The type I serine/threonine kniase receptor Alk8/Lost-a-fin is required for Bmp2b/7 signal transduction during dorsoventral patterning of the zebrafish embryo. *Development.* 128(6):849-858.

Beblo D.A., Wang H.Z., Beyer E.C., Westphale E.M., Veenstra R.D. 1995. Unique conductance, gating, and selective permeability properties of gap junction channels formed by connexin40. *Circ. Res.* 77:813-822.

Becker D.L., Cook J.E., Davies C.S., Evans W.H., Gourdie R.G. 1998. Expression of major gap junction connexin types in the working myocardium of eight chordates. *Cell Biol. Int.* 22(7-8):527-543.

Bergoffen J., Scherer S.S., Wang S., Scott M., Bone L.J., Paul D.L., Chen K., Lensch M.W., Chance P.F., Fischenbeck K.H. 1993. Connexin mutations in X-linked Charcot-Marie-Tooth disease. *Science.* 262 (5142): 2039-2042.

Beyer E.C., Paul D.L., Goodenough D.A. 1987. Connexin43: a protein from rat heart homologous to a gap junction protein from liver. *J. Cell Biol.* 105(6 Pt 1):2621-2629.

Beyer E.C. 1990. Molecular cloning and developmental expression of two chick embryo gap junction proteins. *J. Biol. Chem.* 265(24):14439-14443.

Beyer E.C., Reed K.E., Westphale E.M., Kanter H.L., Larson D.M. 1992. Molecular cloning and expression of rat connexin40, a gap junction protein expressed in vascular smooth muscle. *J. Membr. Biol.* 127(1):69-76.

Bleeker W.K., Mackaay A.J., Masson-Pevet M., Bouman L.N., Becker A.E. 1980. Functional and morphological organization of the rabbit sinus node. *Circ. Res.* 46(1):11-22.

Bruzzone R., Haefliger J.A., Gimlich R.L., Paul D.L. 1993. Connexin40, a component of gap junctions in vascular endothelium, is restricted in its ability to interact with other connexins. *Mol. Biol. Cell.* 4(1):7-20.

Bruzzone R., White T.W., Paul D.L. 1994. Expression of chimeric connexins reveals new properties of the formation and gating behavior of gap junction channels. *J. Cell Sci.* 107(Pt 4):955-967.

Bruzzone R., White T.W., Yoshizaki G., Patino R., Paul D.L. 1995. Intercellular channels in teleosts: functional characterization of two connexins from Atlantic croaker. *FEBS Letter.* 358(3):301-304.

Bruzzone R., White T.W., Goodenough D.A. 1996a. The cellular internet: on-line with connexins. *BioEssays.* 18(9):709-718.

Bruzzone R., White T.W., Paul D. 1996b. Connections with connexins: the molecular basis of direct intercellular signaling. *Eur. J. Biochem.* 238:1-27.

Burggren W., Fritsche R. 1995. Cardiovascular measurements in animals in the milligram range. *Braz. J. Med. Biol. Res.* Nov-Dec 28(11-12):1291-1305.

Cason N., White T.W., Cheng S., Goodenough D.A., Valdimarsson G. 2001. Molecular cloning, expression analysis, and functional characterization of connexin44.1: a zebrafish lens gap junction protein. *Dev. Dyn.* 221(2):238-247.

Chen J.N., Haffter P., Odenthal J., Vogelsang E., Brand M., van Eeden F.J., Furutani-Seiki M., Granato M., Hammerschmidt M., Heisenberg C.P., Jiang Y.J., Kane D.A., Kelsh R.N., Mullins M.C., Nusslein-Volhard C. 1996. Mutations affecting the cardiovascular system and other internal organs in zebrafish. *Development.* 123:293-302.

Christ G.J., Spray D.C., el-Sabban M., Moore L.K., Brink P.R. 1996. Gap junctions in vascular tissues. Evaluating the role of intercellular communication in the modulation of vasomotor tone. *Circ. Res.* 79(4):631-646

Coppen S.R., Dupont E., Rothery S., Severs N.J. 1998. Connexin45 expression is preferentially associated with the ventricular conduction system in mouse and rat heart. *Circ. Res.* 82:232-243.

Coppen S.R., Severs N.J., Gourdie R.G. 1999. Connexin45 (alpha6) expression delineates an extended conduction system in the embryonic and mature rodent heart. *Dev. Genet.* 24(1-2):82-90.

Curtin K.D., Zhang Z., Wyman R.J. 1999. Drosophila has several genes for gap junction proteins. *Gene.* 232(2):191-201.

Dahl G., Miller T., Paul D., Voellmy R., Werner R. 1987. Expression of functional cell-cell channels from cloned rat liver gap junction complementary DNA. *Science.* 236:1290-1293.

Davis L.M., Kanter H.L., Beyer E.C., Saffitz J.E. 1994. Distinct gap junction protein phenotypes in cardiac tissues with disparate conduction properties. *J. Am. Coll. Cardiol.* 24(4):1124-1132.

deCarvalho A.C., Masuda M.O., Tanowitz H.B., Wittner M., Goldenberg R.C., Spray D.C. 1994. Conduction defects and arrhythmias in Chagas' disease: possible role of gap junctions and humoral mechanisms. *J. Cardiovasc. Electrophysiol.* 5(8):868-898.

Delorme B., Dahl E., Jarry-Guichard T., Briand J.P., Willecke K., Gros D., Theveniau-Ruissy M. 1997. Expression pattern of connexin gene products at the early developmental stages of the mouse cardiovascular system. *Circ. Res.* 81(3):423-437.

DePaola N., Davies P.F., Pritchard W.F. Jr., Florez L., Harbeck N., Polacek D.C. 1999. Spatial and temporal regulation of gap junction connexin43 in vascular endothelial cells exposed to controlled disturbed flows in vitro. *Proc. Natl. Acad. Sci. USA.* 96(6):3154-3159.

Dermietzel R., Kremer M., Paputsoglu G., Stang A., Skerrett I.M., Gomes D., Srinivas M., Janssen-Bienhold U., Weiler R., Nicholson B.J., Bruzzone R., Spray DC. 2000. Molecular and functional diversity of neural connexins in the retina. *J. Neurosci.* 20(22):8331-8343.

Driever W., Fishman M.C. 1996. The zebrafish: heritable disorders in transparent embryos. *J. Clin. Invest.* 97(8):1788-1794.

Driever W.L., Solnica-Krezel L., Schier A.F., Neuhauss S.C.F., Malicki J., Stemple D.L., Stanier D.Y.R., Zwartkrus F., Abdelilah S., Rangini Z., Belak J., Boggs C. 1996. A genetic screen for mutations affecting embryogenesis in zebrafish. *Development.* 123:37-46.

Dupont E., Matsushita T., Kaba R.A., Vozzi C., Coppen S.R., Khan N., Kaprielian R., Yacoub M.H., Severs N.J. 2001. Altered connexin expression in human congestive heart failure. *J. Mol. Cell Cardiol.* 33(2)359-371.

Dworkin M.B., Dworkin-Rastl E. 1990. Functions of maternal mRNA in early development. *Mol. Reprod. Dev.* 26(3):261-297.

Ebihara L., Beyer E.C., Swenson K.I., Paul D.L., Goodenough D.A. 1989. Cloning and expression of a *Xenopus* embryonic gap junction protein. *Science.* 243(4895):1194-1195.

Ekker S.C., Larson J.D. 2001. Morphant technology in model developmental systems. *Genesis.* 30(3):89-93.

Essner J.J, Laing J.G., Beyer E.C., Johnson R.G., Hackett P.B. Jr. 1996. Expression of zebrafish connexin43.4 in the notochord and tail bud of wild-type and mutant no tail embryos. *Dev. Biol.* 177(2):449-462.

Fouquet B., Weinstein B.M., Serluca F.C., Fishman M.C. 1997. Vessel patterning in the embryo of the zebrafish: guidance by notochord. *Dev. Biol.* 183(1):37-48.

Gimlich R.L., Kumar N.M., Gilula N.B. 1990. Differential regulation of the levels of three gap junction mRNAs in *Xenopus* embryos. *J. Cell Biol.* 110(3):597-605.

Gourdie R.G., Harfst E., Severs N.J., Green C.R. 1990. Cardiac gap junctions in rat ventricle: localization using site-directed antibodies and laser scanning confocal microscopy. *Cardioscience.* 1(1):75-82.

Gourdie R.G. 1995. A map of the heart: gap junctions, connexin diversity and retroviral studies of conduction myocyte lineage. *Clinical. Sci.* 88:257-262.

Gros D.B., Jongsma H.J. 1996. Connexins in mammalian heart function. *BioEssays.* 18(9):719-730.

Gutstein D.E., Morley G.E., Tamaddon H., Vaidya D., Schneider M.D., Chen J., Chein K.R., Stuhlmann H., Fishman G.I. 2001. Conduction slowing and sudden arrhythmic death in mice with cardiac-restricted inactivation of connexin43. *Circ. Res.* 88(3):333-339.

Haffter P., Granato M., Brand M., Mullins M.C., Hammerschmidt M., Kane D.A., Odenthal J., van Eeden F.J., Jiang Y.J., Heisenberg C.P., Kelsh R.N., Furutani-Seiki M., Vogelsang E., Beuchle D., Schach U., Fabian C., Nusslein-Volhard C. 1996. The identification of genes with unique and essential functions in the development of the zebrafish, *Danio rerio. Development.* 123:1-36.

Haefliger J.A., Bruzzone R., Jenkins N.A., Gilbert D.J., Copeland N.G., Paul D.L. 1992. Four novel members of the connexin family of gap junction proteins. Molecular cloning, expression, and chromosome mapping. *J. Biol. Chem.* 267(3):2057-2064.

Harvey R.P. 1999. Seeking a regulatory roadmap for heart morphogenesis. *Cell Dev. Biol.* 10:99-107.

Heasman J. 2002. Morpholino oligos: making sense of antisense? *Dev. Biol.* 243(2):209-214.

Heasman J., Kofron M., Wylie C. 2000. Beta-catenin signaling activity dissected in the early *Xenopus* embryo: a novel antisense approach. *Dev. Biol.* 222(1):124-134.

Hennemann H., Suchyna T., Lichtenberg-Frate H., Jungbluth S., Dahl E., Schwarz J., Nicholson B.J., Willecke K. 1992. Molecular cloning and functional expression of mouse connexin40, a second gap junction gene preferentially expressed in lung. *J. Cell Biol.* 117(6):1299-1310.

Hirschi K.K., Xu C., Tsukamoto T., Sager R. 1996. Gap junction genes Cx26 and Cx43 individually supress the cancer phenotype of human mammary carcinoma cells and restore differentiation potential. *Cell Growth Dev.* 7:861-870.

Hofmann K., Stoffel W. 1993. TMbase - A database of membrane spanning proteins segments. *Biol. Chem.* 374:166.

Hoh J.H., John S.A., Revel J.P. 1991. Molecular cloning and characterization of a new member of the gap junction gene family, connexin-31. *J. Biol. Chem.* 266(10):6524-31.

Hu N., Sedmera D., Yost H.J., Clark E.B. 2000. Structure and function of the developing zebrafish heart. *Anat. Rec.* 260:148-157.

Hukriede N.A., Joly L., Tsang M., Miles J., Tellis P., Epstein J.A., Barbazuk W.B., Li F.N., Paw B., Postlethwait J.H., Hudson T.J., Zon L.I., McPherson J.D., Chevrette M., Dawid I.B., Johnson S.L., Ekker M. 1999. Radiation hybrid mapping of the zebrafish genome. *Proc. Natl. Acad. Sci. USA.* 96(17):9745-9750.

Hukriede N., Fisher D., Epstein J., Joly L., Tellis P., Zhou Y., Barbazuk B., Cox K., Fenton-Noriega L., Hersey C., Miles J., Sheng X., Song A., Waterman R., Johnson S.L., Dawid I.B., Chevrette M., Zon L.I., McPherson J., Ekker M. 2001. The LN54 radiation hybrid map of zebrafish expressed sequences. *Genome Res.* 11(12):2127-2132.

Isogai S., Horiguchi M., Weinstein B.M. 2001. The vascular anatomy of the developing zebrafish: an atlas of embryonic and early larval development. *Dev. Bio.* 230:278-301.

Jongsma H.J. 2000. Diversity of gap junctional proteins: does it play a role in cardiac excitation? *J. Cardiovasc. Electrophysiol.* 11:228-230.

Jalife J., Morley G.E., Vaidya D. 1999. Connexins and impulse propagation in the mouse heart. *J. Cardiovasc. Electrophysiol.* 10:1649-1663.

Kane D.A., Kimmel C.B. 1993. The zebrafish midblastula transition. *Development.* 119(2):447-456.

Kanter H.L., Saffitz J.E., Beyer E.C. 1994. Molecular cloning of two human cardiac gap junction proteins, connexin40 and connexin45. *J. Mol. Cell. Cardiol.* 26(7):861-868.

Kelsell D.P., Dunlop J., Stevens H.P., Lench N.J., Liang J.N., Parry G., Mueller R.F., Leigh I.M. 1997. Connexin 26 mutations in hereditary non-syndromic sensorineural deafness. *Nature.* 387(6628):80-83.

Kimmel B., Ballard W., Kimmel S.R., Ullmann B., Schilling T.F. 1995. Stages of embryonic development of the zebrafish. *Dev. Dyn.* 203:253-310.

Kirchhoff S., Nelles E., Hagendorff A., Kruger O., Trab O., Willecke K. 1998. Reduced cardiac conduction velocity and predisposition to arrhythmias in connexin40-deficient mice. *Curr. Biol.* 8:299-230.

Kirchhoff S., Kim J.S., Hagendorff A., Thonnissen E., Kruger O., Lamers W.H., Willecke K. 2000. Abnormal cardiac conduction and morphogenesis in connexin40 and connexin43 double-deficient mice. *Circ. Res.* 87(5):399-405.

Kruger O., Plum A., Kim J.S., Winterhager E., Maxeiner S., Hallas G., Kirchhoff S., Traub O., Lamers W.H., Willecke K. 2000. Defective vascular development in connexin 45-deficient mice. *Development.* 127(19):4179-4193.

Kumai M., Nishii K., Nakamura K., Takeda N., Suzuki M., Shibata Y. 2000. Loss of connexin45 causes a cushion defect early in cardiogenesis. *Development.* 127:3501-3512.

Kupperman E., An S., Osborne N., Waldron S., Stanier D.Y.R. 2000. A sphingosine-1-phosphate receptor regulates cell migration during vertebrate heart development. *Nature.* 406:192-195.

Kwak B.R., Hermans M.M., De Jonge H.R., Lohmann S.M., Jongsma H.J., Chanson M. 1995a. Differential regulation of distinct types of gap junction channels by similar phosphorylating conditions. *Mol. Biol. Cell.* 6(12):1707-1719.

Kwak B.R., Saez J.C., Wilders R., Chanson M., Fishman G.I., Hertzberg E.L., Spray D.C., Jongsma H.J. 1995b. Effects of cGMP-dependent phosphorylation on rat and human connexin43 gap junction channels. *Pflugers Arch.* 430(5):770-778.

Kwak B.R., Jongsma H.J. 1996. Regulation of cardiac gap junction channel permeability and conductance by several phosphorylating conditions. *Mol. Cell Biochem.* 157(1-2):93-99.

Liao Y., Day K.H., Damon D.N., Duling B.R. 2001. Endothelial cell-specific knockout of connexin 43 causes hypotension and bradycardia in mice. *Proc. Natl. Acad. Sci. USA.* 98(17):9989-9994.

Locke D., Perusinghe N., Newman T., Jayatilake H., Evans W.H., Monaghan P. 2000. Developmental expression and assembly of connexins into homomeric gap junction hemichannels in the mouse mammary gland. *J. Cell Physiol.* 183(2):228-237.

Lohr J.L., Yost H.J. 2000. Vertebrate model systems in the study of early heart development: *Xenopus* and zebrafish. *Am. J. Med. Genet.* 97:248-257.

Long S., Rebagliati M. 2002. Sensitive two-color whole-mount in situ hybridization using Digoxygenin- and Dinitrophenol-labeled RNA probes. *Biotechniques.* 32(3): 494-500.

Minkoff R., Rundus V.R., Parker S.B., Beyer E.C., Hertzberg E.L. 1993. Connexin expression in the developing avian cardiovascular system. *Circ. Res.* 73(1):71-78.

Motoike T., Loughna S., Perens E., Roman B.L., Liao W., Chau T.C., Richardson C.D., Kawate T., Kuno J., Weinstein B.M., Stainier D.Y., Sato T.N. 2000. Universal GFP reporter for the study of vascular development. *Genesis.* 28(2):75-81.

Muller F., Lakatos L., Dantonel J., Strahle U., Tora L., TBP is not universally required for zygotic RNA polymerase II transcription in zebrafish. 2001. *Curr. Biol.* 11(4):282-287.

Nakamura Y., Gojobori T., Ikemura T. 2000. Codon usage tabulated from the international DNA sequence databases: status for the year 2000. *Nucl. Acids Res.* 28:292.

Nasevicius A., Ekker S.C. 2000. Effective targeted gene 'knockdown' in zebrafish. *Nature Genetics.* 26:216-220.

Nilius B., and Drogsman G. 2001. Ion channels and their functional role in vascular endothelium. *Physiol. Rev.* 81(4):1415-1459.

Opitz J.M., Clark E.B. 2000. Heart development: an introduction. *Am. J. Med. Genet.* 97:238-247.

Page R.D.M. 1996. TreeView: an application to display phylogenetic trees on personal computers. *Comput. Appl. Biosci.* 12(4):357-8.

Pardanaud L., Altmann C., Kitos P., Dieterlen-Lievre F., Buck C.A. 1987. Vasculogenesis in the early quail blastodisc as studied with a monoclonal antibody recognizing endothelial cells. *Development.* 100(2):339-349.

Parker L.H., Zon L.I., Stainier D.Y.R. 1999. Vascular and blood gene expression. *Methods Cell Biol.* 59:313-336.

Pelster B., Burggren W.W. 1996. Disruption of hemoglobin oxygen transport does not impact oxygen-dependent physiological processes in developing embryos of zebrafish (*Danio rerio*). *Circ. Res.* 79: 358-362.

Phelan P., Starich T.A. 2001. Innexins get into the gap. *BioEssays.* 23(5):388-396.

Poole T.J., Coffin J.D. 1989. Vasculogenesis and angiogenesis: two distinct morphogenetic mechanisms establish embryonic vascular pattern. *J. Exp. Zool.* 251(2):224-231.

Postlethwait J.H., Yan Y.L., Gates M.A., Horne S., Amores A., Brownlie A., Donovan A., Egan E.S., Force A., Gong Z., Goutel C., Fritz A., Kelsh R., Knapik E., Liao E., Paw B., Ransom D., Singer A., Thomson M., Abduljabbar T.S., Yelick P., Beier D., Joly J.S., Larhammar D., Rosa F., et al. 1998. Vertebrate genome evolution and the zebrafish gene map. *Nat. Genet.* 18(4):345-349.

Pozzi A., Risek B., Kiang D.T., Gilula N.B., Kumar N.M. 1995. Analysis of multiple gene products in the rodent and human mammary gland. *Exp. Cell Res.* 220(1):212-219.

Reaume A.G., de Sousa P.A., Kulkarni S., Langille B.L., Zhu D., Davies T.C., Juneja S.C., Kidder G.M., Rossant J. 1995. Cardiac malformation in neonatal mice lacking connexin43. *Science.* 267:1831-1834.

Reed K.E., Westphale E.M., Larson D.M., Wang H.Z., Veenstra R.D., Beyer E.C. 1993. Molecular cloning and functional expression of human connexin37, an endothelial cell gap junction protein. *J. Clin. Invest.* 91(3):997-1004.

Risek B., Guthrie S., Kumar N., Gilula N.N. 1990. Modulation of gap junction transcript and protein expression during pregnancy in the rat. *J. Cell Biology.* 100(2):269-282.

Roman B.L., Weinstein B.M. 2000. Building the vertebrate vasculature: research is going swimmingly. *Bioessays.* 22(10):882-893.

Rose B., Mehta P.P., Loewenstein W.R. 1993. Gap junction protein gene supressor tumorigenicity. *Carcinogenesis.* 14(5):1073-1075.

Rummery N.M., Hickey H., McGurk G., Hill C.E. 2002. Connexin37 is the major connexin expressed in the media of the caudal artery. *Arterioscler. Thromb. Vasc.* Biol. 22:1427-1432.

Sambrook J., Fritsch E.F., Maniatis T. 1989. Molecular Cloning: A Laboratory Manual 2nd edition. Cold Spring Harbor, NY.

Seul K.H., Beyer E.C. 2000. Heterogeneous localization of connexin40 in the renal vasculature. *Microvasc. Res.* 59(1):140-148.

Severs N.J.1994. Pathophysiology of gap junctions in heart disease. *J Cardiovasc Electrophysiol.* 5(5):462-475.

Severs N.J. 1995. Cardiac muscle cell interaction: from microanatomy to the molecular make-up of the gap junction. *Histol. Histopathol.* 10(2):481-501

Severs N.J., Rothery S., Dupont E., Coppen S.R., Yeh H.I., Ko Y.S., Matsushita T., Kaba R., Halliday D. 2001. Immunocytochemical analysis of connexin expression in the healthy and diseased cardiovascular system. *Microsc. Res. Tech.* 52(3):301-322.

Shepherd I.T., Beattie C.E., Raible D.W. 2001. Functional analysis of zebrafish GDNF. *Dev. Biol.* 231(2):420-435.

Shiels A., Mackay D., Ionides A., Berry V., Moore A., Bhattacharya S.A. 1998. Missense mutation in the human connexin50 (GJA8) underlies autosomal dominant "zonular pulverulent" cataract, on chromosome 1q. *Amer. J. Hum. Genet.* 62(3):526–532.

Simon A.M., Goodenough D.A., Li E., Paul D.L. 1997. Female infertility in mice lacking connexin 37. *Nature.* 385(6616):525-529.

Simon A.M., Goodenough D.A., Paul D.L. 1998. Mice lacking connexin40 have cardiac conduction abnormalities characteristic of atrioventricular block and bundle branch block. *Curr. Biol.* 8:295-298.

Skerrett I.M., Aronowitz J., Shin J.H., Cymes G., Kasperek E., Cao F.L., Nicholson B.J. 2002. Identification of amino acid residues lining the pore of a gap junction channel. *J. Cell Biol.* 159(2):349-360.

Stanier D.Y., Fishman M.C. 1992. Patterning the zebrafish heart tube: acquisition of anteroposterior polarity. *Dev. Biol.* 153:91-101.

Stainier D.Y., Fouquet B., Chen J.N., Warren K.S., Weinstein B.M., Meiler S.E., Mohideen M.A., Neuhauss S.C., Solnica-Krezel L., Schier A.F., Zwartkruis F., Stemple D.L., Malicki J., Driever W., Fishman M.C. 1996. Mutations affecting formation and function of the cardiovascular system in the zebrafish embryo. *Development.* 123: 285-292.

Starich T, Sheehan M, Jadrich J, Shaw J. 2001. Innexins in *C. elegans*. *Cell Adhes. Commun.* 8(4-6):311-314.

Stergiopoulos K., Alvarado J.L., Mastroianni M., Ek-Vitorin J.F., Taffet S.M., Delmar M. 1999. Hetero-domain interactions as a mechanism for the regulation of connexin channels. *Circ. Res.* 84(10):1144-1155.

Summerton J., Weller D. 1997. Morpholino antisense oligomers: design, preparation, and properties. *Antisense Nucleic Acid Drug Dev.* 7:187-195.

Telford N.A., Watson A.J, Schultz G.A. 1990. Transition from maternal to embryonic control in early mammalian development: a comparison of several species. *Mol. Reprod. Dev.* 26(1):90-100.

Thisse C., Thisse B., Schilling T.F., Postlethwait J.H. 1993. Structure of the zebrafish snail1 gene and its expression in wild-type spadetail and notail mutant embryos. *Development.* 119:1203-1215.

Thompson J.D., Gibson T.J., Plewniak F., Jeanmougin F., Higgins D.G. 1997. The CLUSTAL_X windows interface: flexible strategies for multiple sequence alignment aided by quality analysis tools. *Nucleic Acids Res.* 25(24):4876-4882.

Traub O., Eckert R., Lichtenberg-Frate H., Elfgang C., Bastide B., Scheidtmann K.H., Hulser D.F., Willecke K. 1994. Immunochemical and electrophysiological characterization of murine connexin40 and -43 in mouse tissues and transfected human cells. *Eur. J. Cell. Biol.* 64(1):101-112.

Turner D.L., Weintraub H., 1994. Expression of achaete-scute homologue 3 in *Xenopus* embryo converts ectodermal cells to a neural fate. *Genes and Dev.* 8:1434-1447.

Valiunas V., Weingart R., Brink P.R. 2000. Formation of heterotypic gap junction channels by connexins 40 and 43. *Circ. Res.* 86:e42.

VanderBrink B.A., Link M.S., Aronovitz M.J., Saba S., Sloan S.B., Homoud M.K., Estes III N.A., Wang P.J. 1999. Assessment of atrioventricular nodal physiology in the mouse. *J. Interv. Card. Electrophysiol.* 3(3):207-212.

Vanderbrink B.A., Sellitto C., Saba S., Link M.S., Zhu W., Homoud M.K., Estes N.A.M., Paul D.L., Wang P.J. 2000. Connexin40-defecient mice exhibit atrioventricular nodal and infra-hisian conduction abnormalities. *J. Cardiovasc. Electrophysiol.* 11:1270-1276.

van Kempen M.J., Jongsma H.J. 1999. Distribution of connexin37, connexin40 and connexin43 in the aorta and coronary artery of several mammals. *Histochem. Cell Biol.* 112(6):479-486.

van Rijen H.V., van Veen T.A., Hermans M.M., Jongsma H.J. 2000. Human connexin40 gap junction channels are modulated by cAMP. *Cardiovasc. Res.* 45(4):941-951.

van Veen T.A., van Rijen H.V., Jongsma H.J. 2000. Electrical conductance of mouse connexin45 gap junction channels is modulated by phosphorylation. *Cardiovasc. Res.* 46(3):496-510.

Warren K.S., Fishman M.C. 1998. "Physiological genomics": mutant screens in zebrafish. *Heart Circ. Phys.* 275(1):H1-7.

Westerfield M. 1995. The zebrafish book. a guide for the laboratory use of zebrafish (*Danio rerio*). 3rd Edition. Eugene, OR. University of Oregon Press. 385 pp.

White T.W., Bruzzone R., Paul D. 1995. The connexin family of intercellular channel forming proteins. *Kidney Int.* 48:1148-1157.

White T.W., Paul D.L. 1999. Genetic diseases and gene knockouts reveal diverse connexin functions. *Annu. Rev. Physiol.* 61:283-310.

Willecke K., Jungbluth S., Dahl E., Hennemann H., Heynkes R., Grzeschik K.H. 1990. Six genes of the human connexin gene family coding for gap junctional proteins are assigned to four different human chromosomes. *Eur. J. Cell Biol.* 53(2):275-280.

Willecke K., Heynkes R., Dahl E., Stutenkemper R., Hennemann H., Jungbluth S., Suchyna T., Nicholson B.J. 1991. Mouse connexin37: cloning and functional expression of a gap junction gene highly expressed in lung. *J. Cell Biol.* 114(5):1049-1057.

Willecke K., Eiberger J., Degen J., Eckardt D., Romualdi A., Guldenagel M., Deutsch U., Sohl G. 2002. Structural and functional diversity of connexin genes in the mouse and human genome. *Biol. Chem.* 383(5):725-737.

Yamanaka I., Kuraoka A., Inai T., Ishibashi T., Shibata Y. 2001. Differential expression of major gap junction proteins, connexin26 and 32, in rat mammary glands during pregnancy and lactation. *Histochem. Cell Biol.* 115(4):277-284.

Yeager M., Unger V.M., Matthias M.F. 1998. Synthesis, assembly and structure of gap junction intercellular channels. *Curr. Opin. Struct. Biol.* 8:517-524.

Yeh H.I., Dupont E., Coppen S., Rothery S., Severs N.J. 1997. Gap junction localization and connexin expression in cytochemically identified endothelial cells of arterial tissue. *J. Histochem. Cytochem.* 45(4):539-550.

Yelon D., Horne S.A., Stainier D.Y. 1999. Restricted expression of cardiac myosin genes reveals regulated aspects of heart tube assembly in zebrafish. *Dev. Biol.* 214(1):23-37.

Yelon D., Tocho B., Halpern M.E., Ruvinsky I., Ho R.K., Silver L.M., Stanier D.Y. 2000. The bHLH transcription factor hand2 plays parallel role in the zebrafish heart and pectoral fin development. *Development.* 127:2573-2582.

Zhongan Y., Ningai L., Shuo L. 2001. A zebrafish forebrain-specific zinc finger gene can induce ectopic *dlx2* and *dlx6* expression. *Dev. Biol.* 231(1):138-148.